Reducing Water Demands with Innovative Fire Protection Solutions

FM Global®

Reducing Water Demands with Innovative Fire Protection Solutions

Prepared by

Stephanie Thomas
Yogish Gopala
Dong Han
Stanislav Kostka
Xiangyang Zhou

FM Global
1151 Boston-Providence Turnpike
Norwood, MA 02062

April 2020

Project ID RW000206

Disclaimer

The research presented in this report, including any findings and conclusions, is for informational purposes only. Any references to specific products, manufacturers, or contractors do not constitute a recommendation, evaluation or endorsement by Factory Mutual Insurance Company (FM Global) of such products, manufacturers or contractors. FM Global does not address life, safety, or health issues. The recipient of this report must make the decision whether to take any action. FM Global undertakes no duty to any party by providing this report or performing the activities on which it is based. FM Global makes no warranty, express or implied, with respect to any product or process referenced in this report. FM Global assumes no liability by or through the use of any information in this report.

Executive Summary

Innovative technologies for fire protection are increasingly in demand due to the limited water resources in some areas around the world. When it comes to fire protection, many businesses use traditional wet-pipe sprinkler systems to protect the value of their business. The water for these systems is provided by either the municipal water supply or on-site storage. With the rising hazard of stored goods due largely to an increased plastics content, the water demand for adequate protection has increased. FM Global Property Loss Prevention Data Sheets provide protection guidance for traditional ceiling sprinklers that is feasible for locations that have plenty of water available. FM Global has initiated research into emerging technologies that could be used as alternatives to traditional sprinklers. In 2018, multiple research projects investigated two potential fire protection options that targeted low water usage designs for plastics, specifically using Simultaneous Monitoring, Assessment and Response Technology (SMART) sprinklers or an Automated Water Cannon (AWC).

The SMART sprinkler concept revolves around a sprinkler system that uses advanced technology to identify the point of fire ignition and activate a set number of ceiling-level sprinklers over the ignition area to achieve fire control. Fire detection is achieved using either smoke, heat, optical or a combination of these various detection systems. A calculation method provides the real-time fire location, which then allows the system to activate a set number of sprinklers closest to the fire. The calculation method employed relies on a temperature threshold of 5°C (9°F) over a period of one minute or a single thermocouple reaching a temperature of 57°C (135°F). Typically, two types of detection are used to activate the system to avoid false alarms and ensure a faster response when the fire is small. Fire location accuracy and the elimination of sprinkler skipping are also key benefits which contribute to reducing the total water demand to control a fire.

In contrast to the SMART sprinkler, the AWC avoids the use of ceiling sprinklers altogether. A typical AWC system consists of a fixed-in-place water cannon with a detection method, usually fast image-based flame detection, a fire scanner and a control unit. During operation, the detection method sends a signal that a fire has been detected to the control unit which activates the water cannon so the fire scanner can locate the fire. When the fire is located, water is discharged from the cannon to suppress the fire. The fast response of the image detection along with the targeted water delivery reduce the water demand when compared to traditional ceiling-only protection.

To evaluate these technologies, several fire hazards were selected, including low-piled plastics storage, high-bay rack storage and open-top combustible containers (OTCCs). For SMART sprinklers, large-scale fire tests were carried out to determine if simultaneous activation of a minimum set of sprinklers around the fire location could control the fire of low-piled storage. The protection was evaluated for two ignition scenarios with 4 or 5 sprinklers activating simultaneously when one of the ceiling thermocouples reached a temperature of 57 °C (135 °F). The storage tested was either uncartoned unexpanded plastic (UUP) or cartoned unexpanded plastic (CUP) commodity stored to a height of 1.5 m (5 ft) or 1.7 m (5.6 ft) respectively with a storage area of approximately 19 m^2 (200 ft^2). Protection options were evaluated for ceiling heights of 9.1 m (30 ft) and 18.3 m (60 ft). The protection was considered successful if the fire was controlled and the target arrays did not ignite. Fourteen full-scale fire tests

were conducted. The results for CUP commodity showed water reduction up to 80% under a 9.1 m (30 ft) ceiling and up to 88% under an 18.3 m (60 ft) ceiling when compared to traditional sprinkler system designs. While the water reduction results for UUP commodity were less than those of CUP, a significant benefit was still found. The UUP results showed up to 74% reduction under a 9.1 m (30 ft) ceiling and up to 69% under an 18.3 m (60 ft) when compared to traditional sprinkler designs.

For protection of low-piled CUP storage to 1.5 m (5 ft) high, the AWC was able to achieve even greater efficiency due to the targeted water delivery and 230 lpm (60 gpm) required flow, resulting in an overall reduction of 92%. During testing the water cannon was operated in a simulated automatic mode so that the fire response time, fire targeting accuracy, spray pattern, narrow angle sweeping, flow rate and delivery distance could be adjusted to evaluate the protection performance. The stream trajectory of the water cannon was measured in cold flow under various conditions and a parabolic path equation with an empirical coefficient was developed to predict the stream trajectory. Water flux distribution measurements for the water cannon were also made for different spray patterns using collection containers. Based on the trajectory and water flux measurements, nine fire suppression tests were conducted on low-piled CUP storage to 1.5 m (5 ft) high to evaluate the performance of the water cannon in a simulated automatic mode to protect this kind of occupancy. The results showed that the fire was well controlled when the water flux delivered to the fire zone was equal to or higher than the critical delivered flux (CDF) for the commodity.

The SMART sprinkler technology was also examined to determine if water reduction was possible for high-bay rack-storage of cartoned unexpanded plastics (CUP). A full-scale fire test was conducted using 12.2 m (40 ft) CUP commodity storage with 1.2 m (4 ft) aisles under a 13.7 m (45 ft) ceiling to compare the required water demand to the current FM Global guidance for ceiling-only protection. Ceiling-only protection was provided by six simulated SMART K200 (K14.0) pendent sprinklers delivering a water density of 33 mm/min (0.8 gpm/ft^2). The SMART system used linear heat detectors (LHDs) installed in the rack at half the height of the array. The results showed that SMART sprinklers in combination with linear heat detectors in the rack could reduce the water demand by 77% when compared to traditional ceiling-only protection, even when using a K200 (K14.0) pendent sprinkler that is not applicable in Data Sheet 8-9, *Storage of Class 1, 2, 3, 4 and Plastic Commodities*[i], for a 13.7 m (45 ft) ceiling height when protecting rack storage of CUP.

Lastly, the feasibility of using ceiling-only SMART sprinkler protection for the high hazard of OTCCs was examined. Six large-scale fire tests using the commodity classification protocol were conducted to determine the hazard of OTCCs with respect to FM Global standard commodities. The evaluation of OTCC focused on commodity classification style testing due to a lack of existing large-scale test data. The commodity used consisted of a commercially available open-top plastic bulk container. The test setup consisted of a 3-tier rack-storage arrangement with water applied at varying densities when a theoretical sprinkler reached a pre-determined temperature, either the standard commodity

---

[i] FM Global, Property Loss Prevention Data Sheet 8-9, Storage of Class 1, 2, 3, 4 and Plastic Commodities, January 2020.

classification sprinkler response or a simulated SMART sprinkler response. Each test was evaluated on the control of the fire. The test results showed that the CDF for OTCC using the standard WAA activation protocol is higher than 73 mm/min (1.8 gpm/ft^2), while that for a simulated SMART sprinkler response is approximately 32 mm/min (0.79 gpm/ft^2). Even though the results indicate water reduction is feasible for rack storage of OTCCs using a SMART system, the overall water requirement would still be greater than that used for standard commodities due to the water collection. Despite an observed reduction in the CDF, fire protection for OTCCs with a SMART system would still likely require water demands in excess of any current protection guidance for standard commodities.

As demonstrated in all the tests conducted, a key element to success in controlling any fire is through early detection. Early detection is particularly important if less water is available to control or suppress the fire. The SMART sprinkler activation criterion used was reasonably conservative. Future commercial systems are likely to have much earlier activation times, leading to greater reductions in water demand. On the other hand, negative factors like crossflowing air over the storage, if not properly arranged in accordance with Data Sheet 2-0, *Installation Guidelines for Automatic Sprinklers*[ii], may need to be compensated with a greater number of sprinkler activations in the design. Early activation can also be achieved by the AWC system, which, together with its localized penetration, provides an even greater reduction in water demand.

Future certified commercial systems using these innovative technologies may differ in fire detection and water delivery characteristics. Therefore, further exploration is expected to study what alternative protection systems can offer when it comes to water reduction and system reliability. The present work shows promising results and offers potential protection solutions for those facilities that exist in areas where water shortages challenge fire protection or as alternative solutions at a potentially lower cost.

[ii] FM Global, Property Loss Prevention Data Sheet 2-0, Installation Guidelines for Automatic Sprinklers, January 2019.

Abstract

Innovative technologies that can protect property from fire using less water are increasingly in demand due to the limited water resources available for fire protection in some areas around the world. FM Global has initiated research into emerging technologies that could be used as alternatives to traditional sprinklers, specifically Simultaneous Monitoring, Assessment and Response Technology (SMART) sprinklers and Automatic Water Cannons (AWCs). SMART sprinklers use detectors (smoke, heat and/or optical) to detect a fire, identify its location and open sprinklers simultaneously to surround and control it. AWCs generally utilize imaging-based detection to locate a fire source and direct a water stream to control it. Both these technologies were examined in large-scale fire tests for low-piled plastics storage. The SMART sprinkler technology was also examined for high-bay rack-storage of plastics as well as limited open-top combustible container (OTCC) applications. Large-scale tests demonstrated that SMART sprinklers can reduce the water demand by more than 50% for both low-pile storage and high-bay rack-storage, while the AWC showed an even greater reduction of 92% for low-pile storage. For the challenging fire hazard of OTCCs, which currently have very limited protection guidance, SMART sprinklers were shown to be a potential viable protection option that could provide achievable water demands.

Acknowledgements

Table of Contents

List of Figures

List of Tables

PAGE LEFT INTENTIONALLY BLANK

1.   Introduction

When it comes to fire protection, many businesses use traditional wet-pipe sprinklers to protect their facilities. The water supply for these systems is provided by either the municipal network or on-site storage. With the rising hazard of stored goods due largely to an increased plastics content, the water demand for adequate protection has increased. FM Global Property Loss Prevention Data Sheets provide protection guidance that is feasible for locations that have access to plenty of water. However, in locations where water is not easily accessible, the required demands limit the feasibility of sprinklers or simply make them cost prohibitive. A reduction in water demand for fire protection systems can help make protection options feasible in these locations and more cost-effective in locations with plenty of water available. Where ceiling sprinklers alone cannot provide adequate protection or meet the water demand requirements, in-rack sprinklers are often recommended. In-rack sprinklers can be more cost effective in terms of water demand and offer additional benefits, by containing fire size, such as limiting smoke damage and business interruption. However, in-rack sprinklers can reduce the storage flexibility and are often not compatible with the logistical needs of a facility. In order to reduce the fire protection water demand and allow for storage flexibility, innovative fire protection solutions are needed that maintain the same high level of protection offered by traditional ceiling systems and at the same time reduce the costs and logistical constraints placed on facilities.

In 2018, multiple research projects were initiated to investigate potential fire protection options that targeted low water usage designs for cartoned plastics, specifically using Simultaneous Monitoring, Assessment and Response Technology (SMART) sprinklers or an Automatic Water Cannon (AWC). The SMART sprinkler protection option was examined for low-pile storage, high-bay storage, as well as open-top containers, while the water cannon work focused on low-pile storage scenarios with high ceiling clearances. All testing, however, pointed to the need for early fire detection to control the fires with a limited water supply. The tests conducted are summarized in this report along with the results and water reduction potential. Testing of emerging technologies is expected to continue and explore fire protection solutions that offer low water demands or alternatives to water in general.

1.1   SMART Sprinkler

The concept of a SMART sprinkler protection system was first reported in 2017 [1, 2]. The SMART concept revolves around a sprinkler system that uses simultaneous monitoring, assessment and response technology. The system uses multi-sensor detection and a calculation method to provide a real-time fire location that allows the system to activate a set number of sprinklers closest to the fire. The type of detection systems used with a SMART system can vary and can include thermal heat detectors, smoke detectors or linear heat detection located at the ceiling or even in storage racks for earlier activation. The key point is that two types of detection are used to activate the system to avoid false alarms and ensure a faster response when the fire is small. Fire location accuracy and the

elimination of sprinkler skipping[iii] are additional benefits which contribute to reducing the total water demand to control a fire.

In large-scale fire testing of the SMART concept [1, 2], the system was simulated by providing simultaneous sprinkler operations controlled by a separate detection method for early activation. The FM Global algorithm utilized the combination of a smoke detector and sprinkler event to trigger the SMART sprinkler system. The sprinklers were activated when a smoke detector was triggered and a temperature threshold of 5°C (9°F) was reached in a heat detector over a period of one minute. To determine which sprinklers to operate, a thermal-based centroid algorithm using temperatures at the ceiling was applied. The six closest sprinklers to the thermal centroid were activated. Simulation of a SMART system provided a means for evaluating protection options without relying on a specific manufacturer's system. During tests, the water supply to the open sprinklers was provided manually upon system activation. The number of open sprinklers tested provided the minimum requirement for any protection design. The FM Global SMART system algorithm activated the protection before the fire reached the ceiling and was only halfway up the storage array for cartoned commodity. By detecting the fire before it reached the ceiling, the system was able to reduce the water requirements. As evident through the test results in the following sections, SMART sprinkler protection can offer a low water demand option for both low-pile storage and high-bay rack storage. It can also help with high hazards such as open-top containers which currently have very limited protection options available.

1.2   Water Cannon

An automatic water cannon (AWC) system consists of a fixed-in-place or mounted water cannon with a detection method, usually fast image-based flame detection, a fire scanner and a control unit. During typical operation, the detection method sends a signal that a fire has been detected to the control unit, which activates the water cannon so the fire scanner can locate the fire. When the fire is located, water is discharged from the cannon to suppress the fire. The fast response of the image detection along with the targeted water delivery reduce the water demand when compared to traditional ceiling-only protection as was shown in previous work [3]. The tests conducted aimed to characterize the response time, water distribution and protection effectiveness of the specific AWC used. Results showed that the AWC can respond to fire events in large open spaces much faster than sprinklers and, under certain conditions, can control and/or suppress the fire with a water flow rate of 1,200 lpm (320 gpm), which is about 20% of the sprinkler water demand for the same occupancy [3].

The current work builds upon the previous work by using the water cannon in a simulated automatic mode to evaluate its protection effectiveness. AWC systems can have different fire scanning times to respond and to target a fire automatically depending on the particular flame scanner and computer algorithm used. Using a predetermined response time and targeting accuracy allowed the AWC technology to be evaluated in general terms. The simulated mode conservatively set the fire response time to 40 s and the accuracy of the fire targeting parameters to follow that which is allowed in

---

[iii] Sprinkler skipping occurs when water spray from one sprinkler prevents or delays the activation of a nearby sprinkler.

FM Approval Standard 1421, *Fire Protection Monitor Assemblies* [4]. The water cannon was tested for low solid-pile storage in high-clearance scenarios using both a wide fog and narrow angle sweeping mode for water application. Water cannon protection was found to greatly reduce the water demand.

The use of AWCs is gaining momentum in countries where the number of facilities with high ceiling clearance is becoming more prevalent and have been increasingly used in facilities such as stadiums, exhibition halls, convention centers, railroad stations, airports and even warehouses. The technology is still relatively new with room for optimization of certain factors such as fire response time, targeting accuracy, water flux distribution with narrow angle sweeping and the reliability of the moving parts. One major drawback is that one mechanical-electrical failure in the AWC system can cause a complete malfunction, unlike the more reliable sprinkler protection system. Another issue to consider is the strength of the water stream from an AWC can also scatter lighter burning materials which can spread the fire further.

1.3 Test Commodity

Five different commodities were used in the tests presented in this report and included Class 2, Cartoned Unexpanded Plastic (CUP), Cartoned Expanded Plastic (CEP), Uncartoned Unexpanded Plastic (UUP) and open-top combustible containers (OTCC). A description of each commodity is provided in the following sections.

1.3.1 Class 2

The FM Global standard Class 2 test commodity consists of a five-faced steel liner in three double-wall corrugated paper cartons. The dimensions for the inner, middle, and outer box are 1.0 × 1.0 × 0.97 m (3.3 × 3.3 × 3.2 ft), 1.0 × 1.0 × 0.99 m (3.4 × 3.4 × 3.3 ft), and 1.1 × 1.1 × 1.1 m (3.5 × 3.5 × 3.5 ft), respectively. Inside the cartons is a five-sided sheet metal liner, which represents non-combustible contents. The sheet metal liner weighs approximately 21 kg (46 lb). The entire assembly is supported on an ordinary, two-way, slatted deck, hardwood pallet resulting in an overall dimension of 1.1 × 1.1 × 1.2 m (3.5 × 3.5 × 3.8 ft). The total combustible weight of the commodity is approximately 57.8 kg (127 lb); the corrugated containerboard weighs approximately 35.4 kg (78.0 lb), and the hardwood pallet weighs approximately 22.4 kg (49.4 lb). A photo of Class 2 commodity including the pallet is provided in Figure 1-1.

1.3.2 Cartoned Unexpanded Plastic (CUP)

The FM Global standard Cartoned Unexpanded Plastic commodity consists of rigid crystalline polystyrene cups (empty, 0.46L (16 oz)) packaged, facing down, in a single-wall corrugated containerboard carton measuring 0.53 × 0.53 × 0.53 m (1.8 × 1.8 × 1.8 ft). The cups are individually compartmentalized with single-layer corrugated board partitions, arranged in five layers of 25 cups per layer, yielding a total of 125 cups per box. Each cup is separated by corrugated containerboard partitions, and each layer rests on a corrugated containerboard pad. Eight cartons are arranged in a 2 × 2 × 2 arrangement on an ordinary, two-way, slatted deck, hardwood pallet resulting in a total dimension of 1.1 × 1.1 × 1.2 m (3.5 × 3.5 × 3.9 ft). The total combustible weight of one pallet load is approximately 73.9 kg (163 lb); the corrugated containerboard weighs approximately 19.8 kg (43.7 lb), the plastic cups

weigh approximately 31.6 kg (69.7 lb), and the hardwood pallet that supports the commodity weighs approximately 22.4 kg (49.4 lb). A photo of the CUP commodity including the pallet is provided in Figure 1-1.

1.3.3   Cartoned Expanded Plastic (CEP)

The FM Global standard Cartoned Expanded Plastic test commodity consists of expanded polystyrene trays packaged in a single-wall corrugated containerboard carton measuring 0.53 × 0.53 × 0.53 m (1.8 × 1.8 × 1.8 ft). Each tray measures 250 × 200 × 28 mm (10 × 8.0 × 1.1 in.) and weighs approximately 10 g (0.35 oz). There are 280 trays arranged in four, 60-tray stacks in each corner of the carton and four, 10-tray stacks placed vertically in the center of the carton. The trays stack to a nominal height of 420 mm (16.5 in.) leaving a 114 mm (4.5 in.) air gap at the top of the carton. Eight cartons are arranged in a 2 × 2 × 2 setup on an ordinary, two-way, slatted deck, hardwood pallet resulting in a total dimension of 1.1 × 1.1 × 1.2 m (3.5 × 3.5 × 3.9 ft). The total combustible weight of a single pallet load is approximately 52.6 kg (116 lb); the corrugated cartons weigh approximately 8.2 kg (18 lb), the expanded plastic weighs approximately 22.4 kg (49.4 lb), and the hardwood pallet weighs approximately 22.4 kg (49.4 lb). A photo of the CEP commodity including the pallet is provided in Figure 1-1.

1.3.4   Uncartoned Unexpanded Plastic (UUP)

The FM Global standard Uncartoned Unexpanded Plastic commodity consists of seven plastic pallets stacked on top of an ordinary, two-way, slatted deck, hardwood pallet resulting in an overall dimension of 1.1 × 1.2 × 1.1 m (3.5 × 4.0 × 3.7 ft). The plastic pallets are four-way entry pallets constructed of high-density polyethylene. Each pallet has the dimensions of 1.0 m × 1.2 m × 140 mm (3.3 ft × 4.0 ft × 5.6 in.) and weighs approximately 25.4 kg (56.0 lb). The total combustible weight of one standard UUP pallet load is 200 kg (441 lb); the plastic pallets weigh approximately 178 kg (392 lb), and the hardwood pallet that supports the commodity weighs approximately 22.4 kg (49.4 lb). A photo of the standard UUP commodity including the pallet is provided in Figure 1-1.

1.3.5   Open-Top Combustible Container

The commercially available open-top plastic bulk container has overall dimensions of 1.1 × 1.2 × 1.1 m (3.8 × 4.0 × 3.5 ft). The container is constructed of high-density polyethylene and is collapsible with a built-in pallet. Each container has four solid walls and a solid bottom. The hinges that allow the container to be collapsible are located 51 mm (2 in.) above the bottom on the 1.2 m (4.0 ft) sides and 150 mm (6 in.) above the bottom on the 1.1 m (3.8 ft) sides. The hinges and small vent holes located in the bottom surface provide a path for water to drain from the container. In some cases, a plastic bag liner was placed inside each container to create the effect of a fully sealed container. A photo of the OTCC commodity is provided in Figure 1-1. Commercially available OTCCs have different venting configurations, sizes and customizable options such as gridded bottoms and knock-down doors. The project scope focused on the containers described and did not include variations such as gridded bottoms.

Class 2
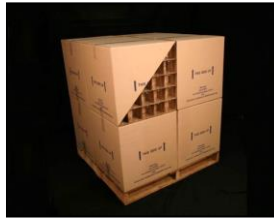
Cartoned Unexpanded Plastic (CUP)

Cartoned Expanded Plastic (CEP)

Uncartoned Unexpanded Plastic (UUP)

Open-Top Container with Plastic Liner

Figure 1-1: FM Global standard commodities and open-top container commodity.

1.4 Test Facility

All testing was performed in the Large Burn Laboratory (LBL) at the FM Global Research Campus (RC) located in West Glocester, RI. The LBL has two movable ceilings (North and South Ceilings) and a 20-Megawatt (MW) Fire Products Collector located between the two ceilings as shown in Figure 1-2. Both movable ceilings are 24.4 m (80 ft) long by 24.4 m (80 ft) wide and can be placed between 3.0 m (10 ft) to 18.3 m (60 ft) above the floor. The fire products collector has a diameter of 10.7 m (35 ft) with the inlet is located 11.3 m (37 ft) above the floor. Gas concentration, velocity, temperature and moisture measurements are made in the exhaust ductwork. Beyond the measurement location, the exhaust duct connects to a wet electrostatic precipitator (WESP) prior to the scrubbed gases venting to the atmosphere. All tests under the movable ceilings were conducted as described in Section 2.1 and 0 at a nominal exhaust rate of 94.4 m^3/s (200,000 ft^3/min) and all tests under the 20-MW fire products collector described in Section 4 at 70.8 m^3/s (150,000 ft^3/min).

The LBL has a humidity control system which is used to manage pre-test laboratory temperature and humidity. The laboratory ambient temperature is typically held in the range of 10 to 27°C (50 to 80°F) with 35% humidity. Managing the lab temperature and humidity allows the commodity moisture content to be maintained within required limits prior to ignition for each test. For hygroscopic materials, like corrugated cardboard cartoned products, the moisture content requirement is 6% ± 2% on a dry basis [5].

(a)   (b)
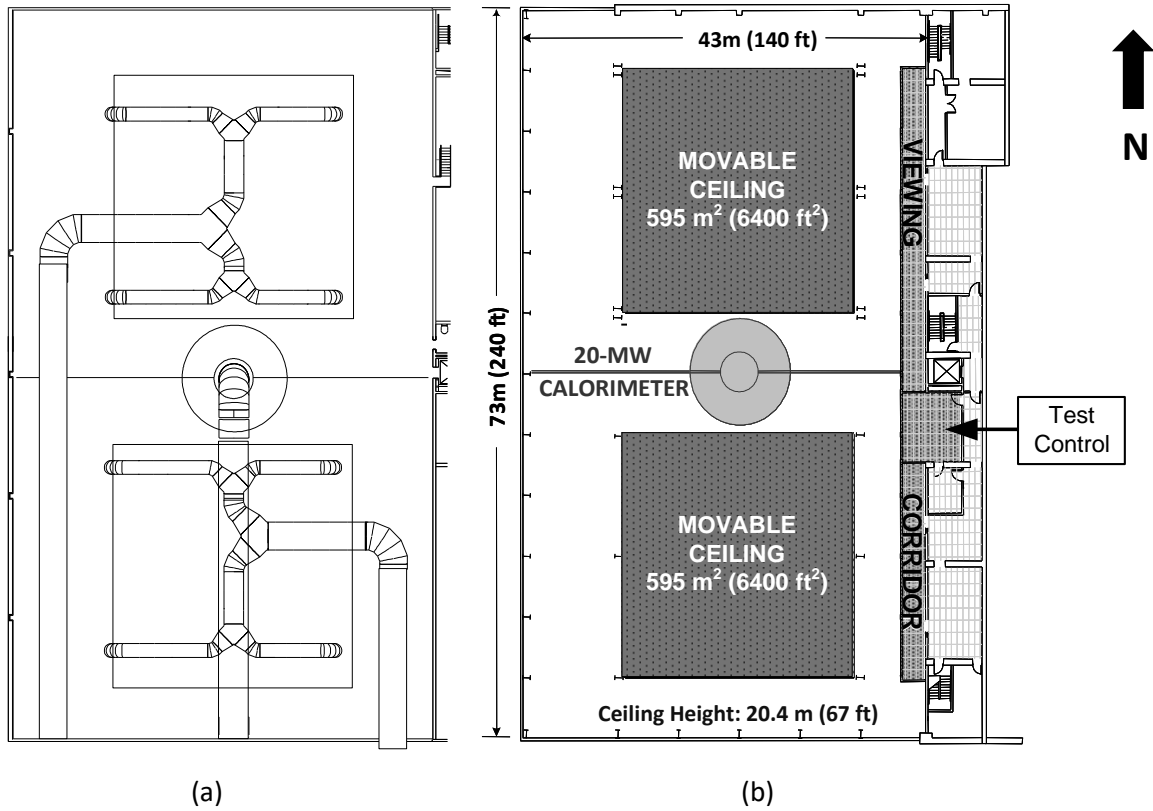
Figure   1-2 :   Layout of Large Burn Laboratory, plan view of (a) exhaust ductwork located at building roofline and (b) testing areas.

2. **Low-Pile Storage**

Low-pile storage is typically used in manufacturing areas and work in progress storage areas. The protection guidance for these types of storage is ceiling-only as there are usually no racks available to support in-rack sprinklers. Typical storage areas have high clearances which often lead to high water demands that can quickly become out of reach for areas without sufficient water supplies. Low-piled storage of plastics to a height of 1.8 m (6 ft) is classified as Hazard Category 3 (HC-3) occupancy in FM Global Property Loss Prevention Data Sheet 3-26, *Fire Protection for Nonstorage Occupancies* (DS 3-26) [6]. In the National Fire Protection Association Standard 13, *Standard for the Installation of Sprinkler Systems* (NFPA 13) [7], cartoned and uncartoned low-piled storage of plastics to a height of 1.8 m (6 ft) is categorized as either Extra Hazard (EH) Group 1 or EH Group 2 occupancies. The protection recommendations in both these standards require a minimum water density over a demand area with any sprinkler approved for use in non-storage occupancies. The protection guidance is summarized in Table 2-1. One common guideline in all these protection recommendations is the large design area, which drives up the water demand. Some of the large-scale fire tests supporting the guidance show sprinkler skipping is the primary reason for the large demand area. Several sprinklers farther away from the ignition location operated sooner than nearby sprinklers and contributed little or no water to control the fire. In these cases, the fire was controlled either through commodity burnout or the subsequent operation of sprinklers closer to ignition.

Table   2-1:   Protection guidance for low-piled storage of plastics.

	FM Global DS 3-26 [6]	NFPA 13 [7]
Cartoned Plastics under 9.1 m (30 ft) ceiling	HC-3 12 mm/min (0.3 gpm/ft^2) over 232 m^2 (2,500 ft^2)	EH Group 1 or 2 12-16 mm/min (0.3-0.4 gpm/ft^2) over 232 m^2 (2,500 ft^2)
Uncartoned Plastics under 9.1 m (30 ft) ceiling	Low-piled storage of UUP* 33 mm/min (0.8 gpm/ft^2) over 232 m^2 (2,500 ft^2)	EH Group 1 or 2 12-16 mm/min (0.3-0.4 gpm/ft^2) over 232 m^2 (2,500 ft^2)
Cartoned Plastics under 18 m (60 ft) ceiling	HC-3 20 mm/min (0.5 gpm/ft^2) over an area of 280 m^2 (3,000 ft^2)	NA
* HC-3 protection listed in DS 3-26 (Table 2). † UUP sprinkler design listed in DS 3-26 (Table 3) as number of K160 (K11.2) sprinklers at a pressure of 3.4 bar (50 psi).		

Both the SMART sprinkler system and the AWC were tested to see if the water demand requirements could be reduced for low-pile storage with high ceiling clearances. SMART systems provide very early and simultaneous activation of multiple sprinklers that surround the fire and by design, avoid sprinkler skipping, while AWCs have shown promise to work well for large open spaces [3]. The recent testing results were very positive with the SMART sprinklers showing water demand reductions up to 88% and AWC up to 92%.

2.1 SMART Sprinkler Experimental Setup and Results

Large-scale fire tests were carried out to determine if a fire can be controlled by the simultaneous activation of four to five sprinklers in a SMART system and to what extent the water demand can be reduced when compared to the requirements for traditional ceiling sprinkler protection. The details of SMART sprinkler design and performance can be found in [1] and [2]. These past studies have shown that the water demand can be reduced significantly for rack-storage protection with SMART sprinklers. To explore the potential of using this type of protection to reduce the water demand for low-piled storage of plastics, tests were conducted with three different commodities, CUP, CEP and UUP under two different ceiling heights, 9.1 m (30 ft) and 18.3 m (60 ft), and in two ignition scenarios, fire located under 1 or among 4 ceiling sprinklers. The operation of the SMART system was simulated using temperature measurements at the ceiling together with open sprinklers and a controlled water supply. The water was supplied to four or five sprinklers when the activation criterion was reached. These large-scale fire tests were carried out in the Large Burn Laboratory (LBL) under a movable ceiling.

For low-piled storage, the fuel in an HC-3 occupancy was represented by CUP at a nominal height of 1.5 m (5 ft). Therefore, the commodity used in this test was a slight modification of CUP. In order to increase the height of storage, twelve boxes were stored on a wooden pallet instead of eight. This brought the storage height to 1.7 m (5.6 ft). Figure 2-1 shows a photograph of the test array and Figure 2-2 shows its plan view along with the sprinklers. The CUP boxes were stacked in a solid pile array, simulating an in-process manufacturing arrangement consisting of several rows. The main array comprised of three rows of piled storage running North-South. Each row consisted of six piles with 7.5 cm (3 in.) flue space between them. The three rows were separated by 15 cm (6 in.) flues. Three target arrays were used, each made of the same commodity used in the main array. They were placed to the West, East and North of the main array. The target arrays on the West and East had four pallet loads and the array to the North had three. All of them were separated from the main array by 2.4 m (8 ft) aisles. For all the tests, ignition was achieved using one standard FM Global full igniter, which is a 150 mm (6 in.) cylinder of rolled cellucotton, soaked with 240 ml (8 oz) of gasoline. The igniter was placed at floor level at the center of the wooden pallet of the second pile from the North in the center row of the main array as shown in Figure 2-2. The ignition location with respect to the ceiling sprinklers was under 1. This scenario usually results in the strong fire plume being located beneath the first sprinkler to operate and tests the ability of the water discharged to penetrate the fire plume, provide adequate protection and overcome sprinkler skipping.

The test array using UUP commodity is shown in Figure 2-3. Each pallet load consisted of 11 plastic pallets stored to a nominal height of 1.5 m (5 ft). The main array had three rows of piled storage running North-South. Each row had five piles butted against each other bringing the total length of the row to 5 m (16.7 ft). The three rows were separated by 150 mm (6 in.) flues. Three target arrays were used, each of them made of four pallets of Class 2 commodity butted against each other. They were placed to the West, East and North of the main array with 2.4 m (8 ft) aisles separating them from the main array. For all the tests, ignition was achieved using one standard FM Global full igniter. The igniter was placed at the floor level at the center of the pallet in the second pile from the North in the center row of the main array as shown in Figure 2-2.

Figure 2-1: SMART sprinkler test setup with low-piled storage of CUP or CEP.

(a)   (b)
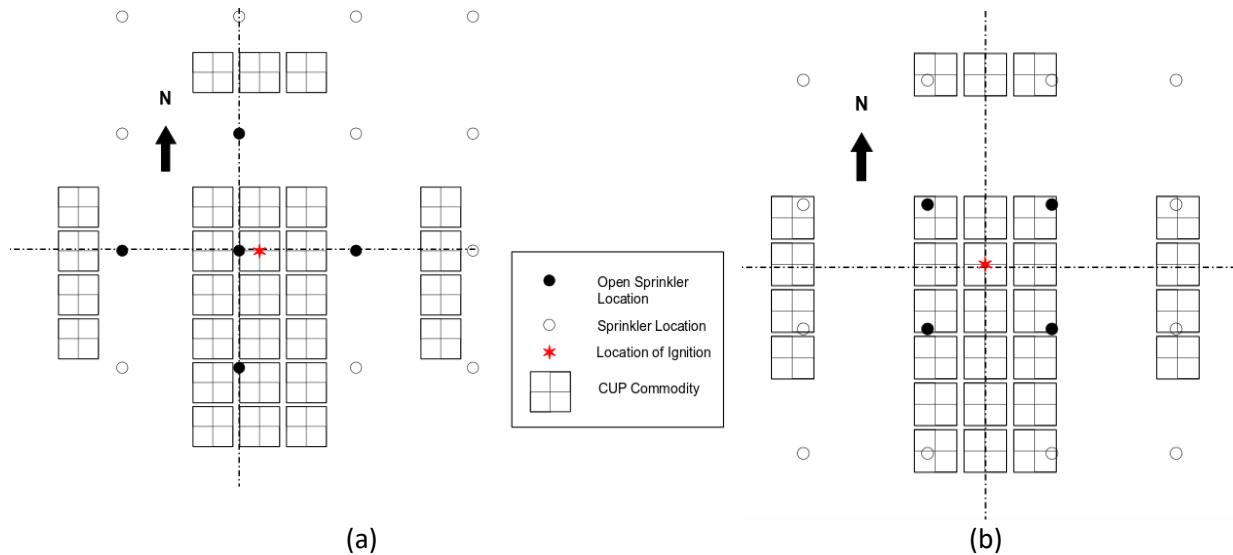
Figure 2-2: Plan view of SMART sprinkler test layout showing sprinkler locations for (a) under-1 and (b) among-4 ignition scenarios.

Two ignition scenarios: under 1 and among 4 were considered in this series of tests. The sprinklers that operate in a SMART sprinkler system are usually dependent on where the thermal centroid is located at the ceiling level at the time of sprinkler activation. Figure 2-4 shows examples of the location of the thermal centroid around the times when a SMART sprinkler system is likely to operate during three tests with different ceiling heights carried out with low-piled storage of UUP. The activation times plotted encompass a wide variety of activation criteria that a SMART sprinkler system can use: from one thermocouple directly over ignition reaching a rise in temperature of 10°C (18°F) to one thermocouple at a distance of 3 m (10 ft) away from ignition reaching a rise in temperature of 25°C (45°F). These data show that the thermal centroid for low-piled storage does not usually move more than 1.2 m (4 ft) radially from the ignition location. It should be noted that, in a client application scenario, there could be

air movement that can affect the location of the thermal centroid, which may require a larger number of sprinkler operations than determined in tests conducted under laboratory conditions.

Figure   2-3:   SMART sprinkler test setup with low-piled storage of UUP.

Consider a SMART sprinkler system design with six simultaneous sprinkler operations. For an under-1 ignition scenario, the five closest sprinklers to the ignition location would operate, plus an additional one that cannot be pre-determined. Therefore, to verify the feasibility of the protection scheme, the tests were conducted with four or five open sprinklers as shown in Figure 2-2. Since, the thermal centroid is not expected to move more than 1.2 m (4 ft), the sprinklers expected to operate will be very close to the ignition location. Figure 2-2a shows the under-1 ignition scenario with five open sprinklers and Figure 2-2b shows the among-4 ignition scenario with only four open sprinklers. The two additional sprinklers that could operate cannot be determined prior to the test and therefore, only four sprinklers were opened for among-4 ignition scenario and five sprinklers were opened for under-1 scenario. For simplicity, it was decided to conduct tests with under-1 and among-4 ignition locations to gain confidence in the effectiveness of the fire protection scheme.
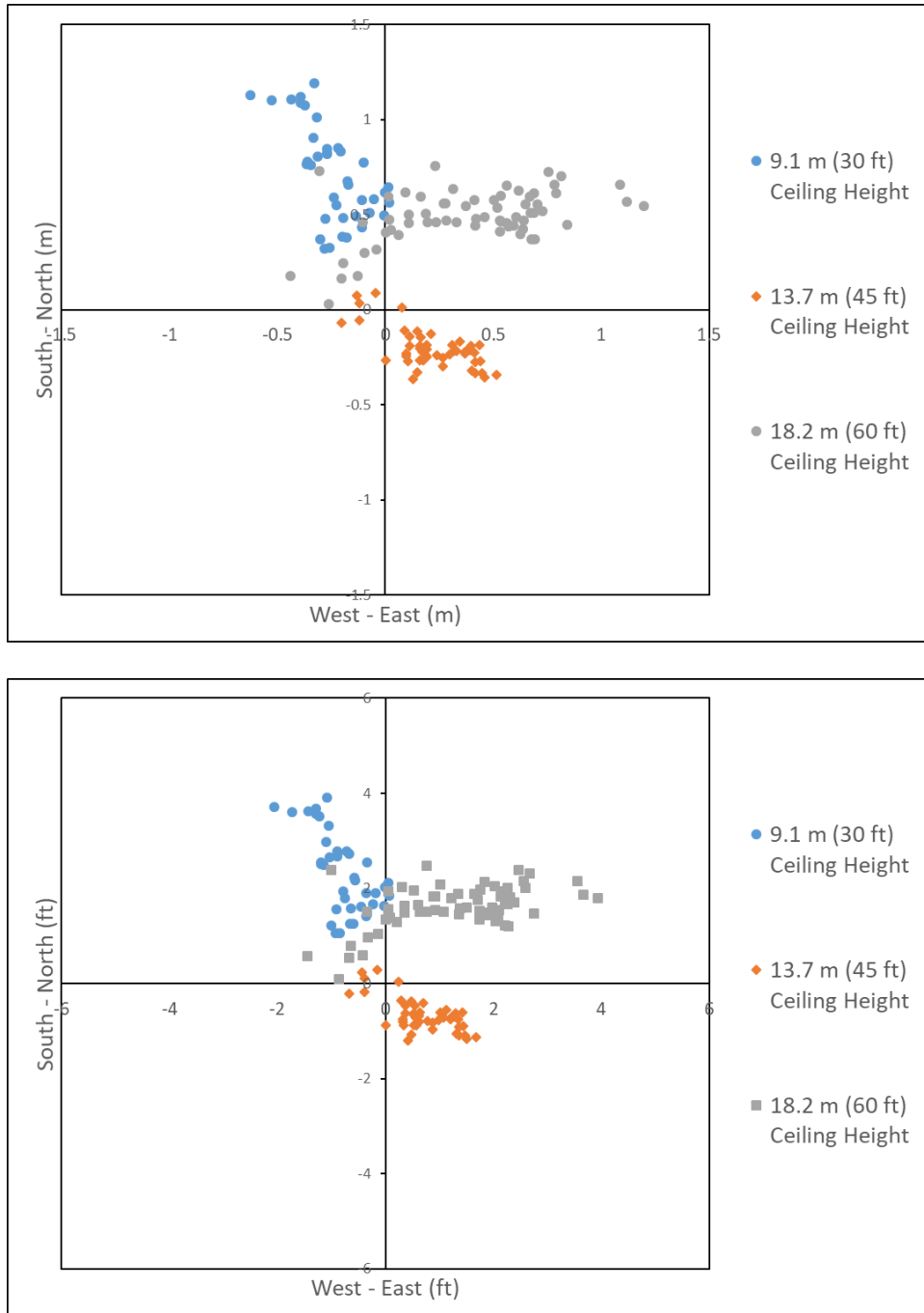
Figure   2-4:   Location of thermal centroid at instances when a SMART system can be expected to activate for low-piled storage of UUP at different ceiling heights.

During testing, ceiling thermocouples at a spacing of 1.5 × 1.5 m (5 × 5 ft) near the relevant sprinklers were used as inputs to determine the activation time based on one of the two criteria defined below.

1. One thermocouple showing an increase in temperature of 5°C (9°F) within one minute. The thermal centroid is calculated based on thermocouple data which tell the system what sprinklers to activate. This criterion matches the FM Global SMART sprinklers [1, 2] since the

smoke detector almost always gets triggered before the threshold for temperature is reached. This criterion provides a very early activation.

2. One thermocouple reaching a temperature of 57°C (135°F). This absolute value is close to, but lower, than the sprinkler activation temperature. It is expected that most versions of SMART sprinklers will activate before this threshold is reached. The results obtained with this activation criterion will, therefore, be applicable to most systems when they become commercially available. In a similar manner to the first algorithm, the thermal centroid is calculated based on thermocouple data which tell the system what sprinklers are closest to the centroid to activate.

The two different algorithms' activation times are illustrated in Figure 2-5 using a test with low-piled storage of UUP. The third photograph was taken at the time when the first quick-response (QR) sprinkler with an activation temperature of 74°C (165°F) would have operated. Both algorithms provide earlier sprinkler activation than QR sprinklers. The heat release rate at the time when these photographs were taken was estimated using the flame volume method [8]. They were estimated at 270 kW, 2500 kW and 3800 kW, respectively. The second algorithm was used in fire tests to activate sprinklers except in Test 7 which used a variation of the first algorithm.
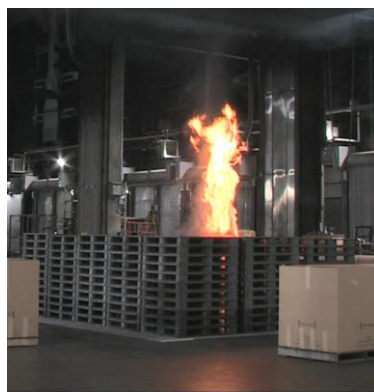
| Algorithm 1 | Algorithm 2 | First QR Sprinkler Activation |
| (143 s) | (182 s) | (214 s) |

Figure 2-5: Sample UUP fire at times when the activation thresholds were reached for SMART sprinkler Algorithm 1 and 2. Also shown is the fire size when the first quick-response (QR) sprinkler would have activated.

The activation mechanisms of SMART sprinklers can also be distinguished by their reliance on the sprinkler thermal element. In a single-activation case, like the FM Global SMART sprinkler model, sprinkler activations are triggered only by a control system relying on temperature and/or other measurements, without involving any sprinkler thermal element. In a dual-activation case, activations are allowed, including both triggered by a controller algorithm and by sprinkler thermal elements. An example is described in [9], where the protection is activated either by a conventional thermal element or by the use of an external heater acting on the thermal element.

During fire testing, the protection provided was considered adequate when the following three conditions were met.

1. The fire was controlled, i.e., contained within the main fuel array.
2. The target arrays did not ignite. The fire could reach the ends of the main array since the storage was restricted to an area of 19 m^2 (200 ft^2).
3. For a dual-activation system, the highest ceiling temperature beyond the open sprinklers at locations where neighboring sprinklers would be installed could not exceed the activation temperature of a typical sprinkler, i.e., 74°C (165°F). The rationale behind this criterion is to avoid additional sprinkler operations beyond the first few sprinklers activated by the algorithm. If the fire is not controlled by the first sprinklers activated by the SMART algorithm, sprinkler activations beyond the initial six could be triggered by their thermal elements. These additional activations would lead to an increase in water demand. This criterion is used to limit the activations to the number specified by the algorithm. For a single-activation system, the number of sprinkler activations is limited by the algorithm and, therefore, this restriction does not apply.

2.1.1   CUP and CEP Protection Under a 9.1 m (30 ft) Ceiling

FM Global guidance for HC-3 occupancy under a 9.1 m (30 ft) high ceiling is a density of 12 mm/min (0.3 gpm/ft^2) over 232 m^2 (2500 ft^2). Table 2-2 summarizes the parameters and results of Tests 1, 2, 6 and 15 that were carried out to simulate HC-3 occupancy under a 9.1 m (30 ft) ceiling.

Tests 1 and 2 used a sprinkler density of 12 mm/min (0.3 gpm/ft^2) provided by K200 (K11.2) pendent sprinklers at 0.5 bar (7 psi). The ignition scenarios were under 1 in Test 1 with five open sprinklers and among 4 in Test 2 with four open sprinklers. The water was applied when any one of the ceiling thermocouples close to the open sprinklers reached a value of 57°C (135°F) following Algorithm 2.

In Test 1, the threshold ceiling temperature was reached at 3 min 25 s after ignition and the water was supplied to the five open sprinklers. Following the water delivery, the fire decreased in intensity gradually over several minutes but was not extinguished. Flames were limited to a few pallets around ignition and were visible occasionally on top of the main array until the test was terminated at 30 min. No additional fire spread was expected. Figure 2-6 shows the damage to the test array. The highest ceiling temperature at locations of sprinklers neighboring those that activated was 52°C (125°F). Therefore, additional sprinklers with a thermal element would not have operated if they had been installed. The peak steel temperature was within acceptable limits at 33°C (92°F). Therefore, all evaluation criteria were satisfied in this test.

Test 2 was conducted with four open sprinklers in the among-4 ignition scenario with results similar to Test 1. Figure 2-7 shows the damage to the test array. The fire was limited to the pallets around ignition and did not spread to the target arrays. The peak ceiling and steel temperatures were within acceptable limits and all test evaluation criteria were satisfied. In both Tests 1 and 2, the fire was controlled with less sprinklers (five and four respectively) compared to the large number of sprinklers called for in the current guidance (25 sprinklers) operating at the same density. These results show SMART sprinklers have the potential to significantly reduce the water demand.

Table   2-2:   Summary of test parameters and results for SMART sprinkler protection of low-piled storage of CUP and CEP under a 9.1 m (30 ft) ceiling.

<table>
<tr><td rowspan="17">TEST PARAMETERS</td><td>Test ID</td><td>1</td><td>2</td><td>6</td><td>15</td></tr>
<tr><td>Test Date</td><td>2/14/2018</td><td>2/16/2018</td><td>3/2/2018</td><td>5/1/2018</td></tr>
<tr><td>Movable Ceiling Test Site</td><td>South</td><td>South</td><td>North</td><td>South</td></tr>
<tr><td>Ceiling Height, m (ft)</td><td colspan="4">9.1 (30)</td></tr>
<tr><td>Test Commodity / Fuel</td><td colspan="3">CUP</td><td>CEP</td></tr>
<tr><td>Storage Arrangement</td><td colspan="4">Solid piled storage on floor</td></tr>
<tr><td>Main Array Size, pallet loads</td><td colspan="4">3 x 5</td></tr>
<tr><td>Targets (3), pallet loads</td><td colspan="4">1 x 4 x 1</td></tr>
<tr><td>Nominal Storage Height, m (ft)</td><td colspan="4">1.7 (5.6)</td></tr>
<tr><td>Aisle Width, m (ft)</td><td colspan="4">2.4 (8)</td></tr>
<tr><td>Ignition Location</td><td>Under 1</td><td colspan="3">Among 4</td></tr>
<tr><td>Sprinkler Orientation</td><td colspan="4">Pendent (QR deflector)</td></tr>
<tr><td>Sprinkler K-factor,
L/min/bar^½ (gpm/psi^½)</td><td>160 (11.2)</td><td>160 (11.2)</td><td>115 (8.0)</td><td>160 (11.2)</td></tr>
<tr><td>Sprinkler Spacing,
m x m (ft x ft)</td><td>3.0 x 3.0 (10 x 10)</td><td>3.0 x 3.0 (10 x 10)</td><td>3.0 x 3.0 (10 x 10)</td><td>3.0 x 3.0 (10 x 10)</td></tr>
<tr><td>Discharge Pressure, bar (psi)</td><td>0.5 (7)</td><td>0.5 (7)</td><td>0.5 (7)</td><td>0.5 (7)</td></tr>
<tr><td>Discharge Density,
mm/min (gpm/ft²)</td><td>12 (0.3)</td><td>12 (0.3)</td><td>8 (0.2)</td><td>12 (0.3)</td></tr>
<tr><td rowspan="5">TEST RESULTS</td><td>Time of Water Delivery to Open Sprinklers, min:s</td><td>3:25</td><td>4:50</td><td>4:17</td><td>4:31</td></tr>
<tr><td>Highest Ceiling Temperature beyond Open Sprinklers at Locations of Neighboring Sprinklers, °C (°F)</td><td>52 (125)</td><td>56 (133)</td><td>89 (192)</td><td>64 (147)</td></tr>
<tr><td>Peak Steel Temperature, °C (°F)</td><td>33 (92)</td><td>32 (89)</td><td>40 (104)</td><td>30 (86)</td></tr>
<tr><td>Target Array Ignited</td><td>No</td><td>No</td><td>No</td><td>No</td></tr>
<tr><td>Test Duration, min</td><td>30</td><td>30</td><td>30</td><td>30</td></tr>
</table>
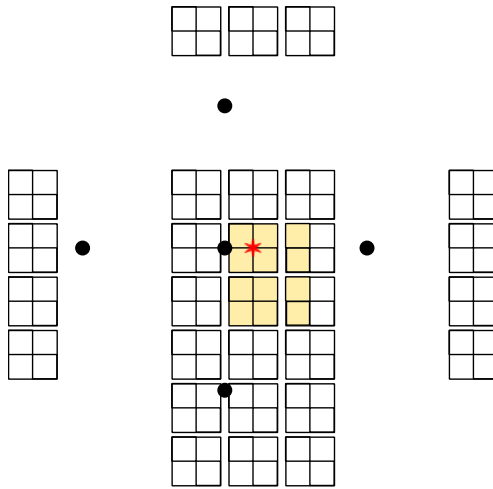
Figure   2-6:   SMART sprinkler Test 1 fire damage.
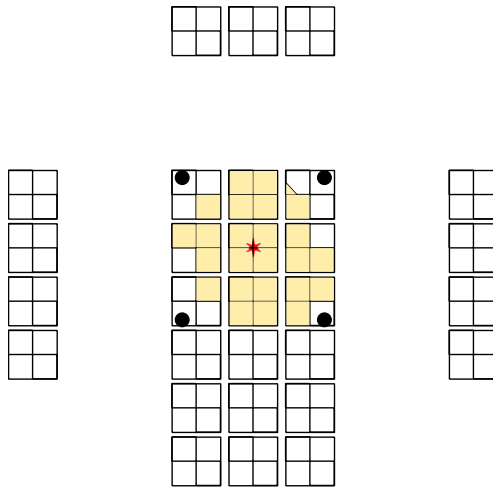
Figure   2-7:   SMART sprinkler Test 2 fire damage.
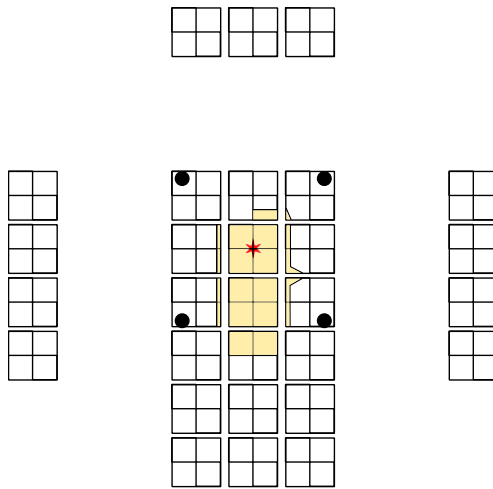
Figure   2-8:   SMART sprinkler Test 6 fire damage.

Test 6 used a lower density of 8 mm/min (0.2 gpm/ft²) with simulated SMART sprinklers to evaluate if less water could provide adequate protection to low-piled storage of CUP. Between Tests 1 and 2, Test 2 had a larger area of fire damage and, therefore, Test 6 was conducted with the same configuration as Test 2 using an among-4 ignition. After ignition, the threshold for water activation (Algorithm 2) was reached at 4 min 17 s. When the water was delivered to the sprinklers the fire reduced in size gradually. However, the flames intensified at about 11 min causing the ceiling temperatures to rise. The peak ceiling temperature at locations of sprinklers neighboring the open sprinklers was 89°C (192°F). Six sprinkler locations reached a temperature greater than the 74°C (165°F) activation temperature for QR sprinklers. All other test evaluation criteria were satisfied. The fire was limited to the main array and did not involve the target arrays as shown in Figure 2-8. The peak steel temperature was within acceptable limits and the fire was controlled. The results of Test 6 showed that a lower density of 8 mm/min (0.2 gpm/ft²) with single-activation SMART sprinklers may provide adequate protection to HC-3 occupancies. However, because of the higher ceiling gas temperatures, the thermal elements in a dual-activation SMART sprinkler system are expected to open an unknown number (less than six) of additional sprinklers.

An HC-3 occupancy has a hazard that can also be represented by nominal 1.5 m (5 ft) high in-process storage of CEP commodity. One test was conducted to verify that the protection recommended for CUP can provide adequate protection for CEP stored under the same configuration. Since, the among-4 ignition scenario in Test 2 had a greater fire damage, the test with CEP was conducted in the same configuration. Table 2-2 summarizes the parameters and results of the test and Figure 2-9 shows the fire damage. As seen in the table and figure, all the test evaluation criteria were satisfied, and the protection was deemed adequate for an HC-3 occupancy represented by low-piled storage of CEP commodity.
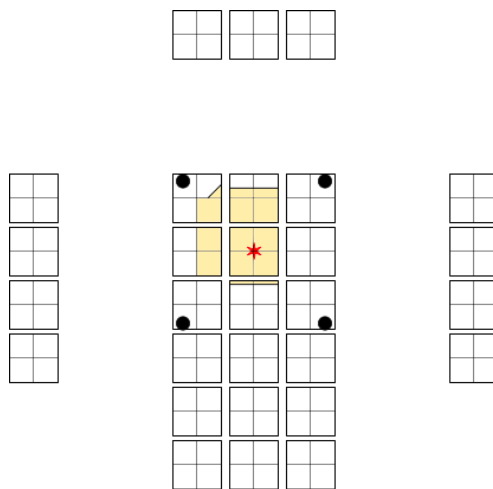
Figure   2-9:   SMART sprinkler Test 15 fire damage.

2.1.2   CUP Protection Under an 18.3 m (60 ft) Ceiling

FM Global guidance for HC-3 occupancy under an 18.3 m (60 ft) high ceiling is a density of 20 mm/min (0.5 gpm/ft²) over 280 m² (3000 ft²). Table 2-3 summarizes the parameters and results of Tests 8, 9 and 10 that were conducted to simulate HC-3 storage under an 18.3 m (60 ft) ceiling.

Test 8 used a density of 20 mm/min (0.5 gpm/ft^2) in the under-1 ignition scenario with K200 (K14) pendent sprinklers. Four min after ignition, water was applied as the criterion for Algorithm 2 had been reached (temperature of 57°C (135°F) at one location). Within 40 s, the flames were no longer visible on top of the main array and conditions remained that way until test termination at 30 min. All evaluation criteria were satisfied. Figure 2-10 shows the fire damage to the array.

Since Test 8 was overwhelmingly successful, Tests 9 and 10 were conducted at a lower density of 15 mm/min (0.37 gpm/ft^2). These two tests used the same sprinkler as Test 8 but changed the operating pressure to 0.5 bar (7 psi), which is the lowest pressure for which a sprinkler is approved. Ignition scenarios varied between the two tests, with Test 9 using an under-1 and Test 10 an among-4 scenario. The sprinkler protection controlled the fire in both tests and satisfied all evaluation criteria as summarized in Table 2-3. These results showed a potential for significant reduction in water demand for the protection of HC-3 occupancies under an 18.3 m (60 ft) ceiling.

Table   2-3:   Summary of test parameters and results for SMART sprinkler protection of low-piled storage of CUP under an 18.3 m (60 ft) ceiling.

		8	9	10
TEST PARAMETERS	**Test ID**	8	9	10
	Test Date	3/22/2018	4/4/2018	4/6/2018
	Movable Ceiling Test Site	North	North	North
	Ceiling Height, m (ft)	18.3 (60)		
	Test Commodity / Fuel	CUP		
	Storage Arrangement	Solid piled storage on floor		
	Main Array Size, pallet loads	3 x 5		
	Targets (3), pallet loads	1 x 4 x 1		
	Nominal Storage Height, m (ft)	1.7 (5.6)		
	Aisle Width, m (ft)	2.4 (8)		
	Ignition Location	Under 1	Under 1	Among 4
	Sprinkler Orientation	Pendent (QR deflector)		
	Sprinkler K-factor, L/min/bar$^{\frac{1}{2}}$ (gpm/psi$^{\frac{1}{2}}$)	200 (14.0)	200 (14.0)	200 (14.0)
	Sprinkler Spacing, m x m (ft x ft)	3.0 x 3.0 (10 x 10)	3.0 x 3.0 (10 x 10)	3.0 x 3.0 (10 x 10)
	Discharge Pressure, bar (psi)	0.9 (13)	0.5 (7)	0.5 (7)
	Discharge Density, mm/min (gpm/ft^2)	20 (0.5)	15 (0.37)	15 (0.37)
TEST RESULTS	**Time of Water Delivery to Open Sprinklers, min:s**	4:00	4:48	4:05
	Highest Ceiling Temperature beyond Open Sprinklers at Locations of Neighboring Sprinklers, ºC (ºF)	56 (133)	58 (136)	54 (130)
	Peak Steel Temperature, ºC (ºF)	26 (78)	28 (83)	27 (81)
	Target Array Ignited	No	No	No
	Test Duration, min	30	30	30
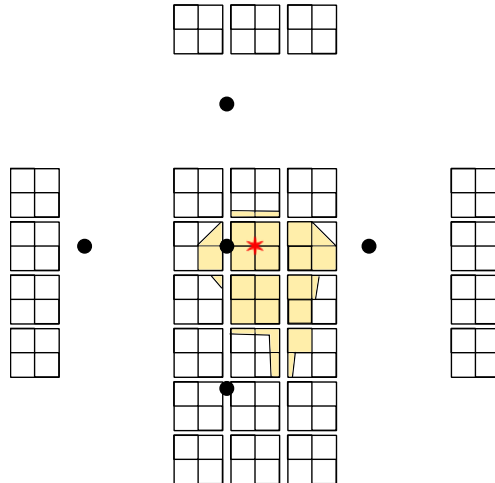
Figure   2-10: SMART sprinkler Test 8 fire damage.
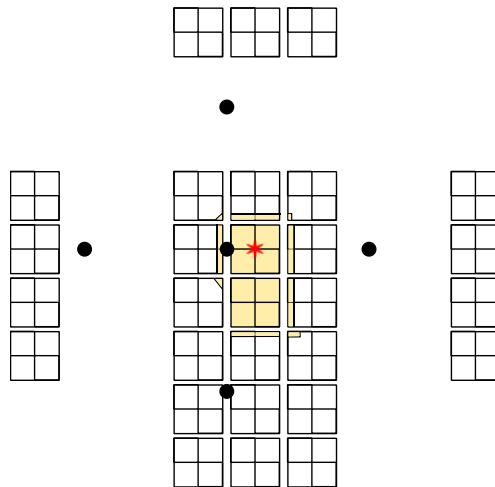
Figure   2-11: SMART sprinkler Test 9 fire damage.
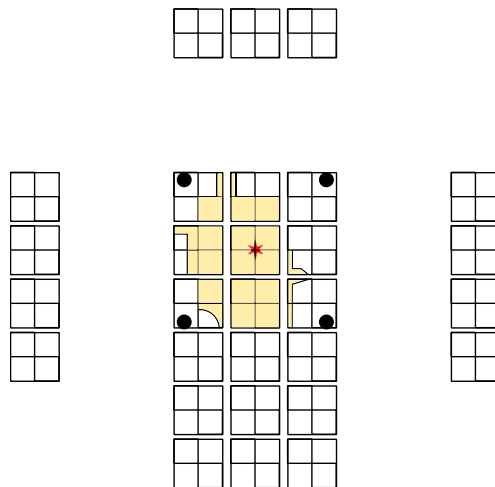
Figure   2-12: SMART sprinkler Test 10 fire damage.

2.1.3   UUP Protection Under a 9.1 m (30 ft) Ceiling

FM Global guidance for low-piled UUP storage under a 9.1 m (30 ft) ceiling with the least water demand is a density of 45 mm/min (1.1 gpm/ft^2) over 93 m^2 (1000 ft^2). Tables 2-4 and 2-5 summarize the parameters and results of Tests 3, 4, 5, 7 and 11 conducted to explore options with SMART sprinklers. The protection was activated using Algorithm 2 – temperature of 57°C (135°F) at one location, with the exception of Test 7 which used a modified version of Algorithm 1 - one location reaching a temperature rise of 8.3°C (15°F).

Test 3 was conducted with a density of 18 mm/min (0.44 gpm/ft^2). After ignition, the sprinkler activation criterion was reached at 3 min 32 s and the water was delivered to the five open sprinklers. The application of water did not control the fire, which grew gradually. By 10 min, the flames were reaching the ceiling. The intensity of the fire kept increasing and the test was terminated at 24 min. Figure 2-13 shows the fire damage revealing the extent of fire spread beyond the ignition pallet. The peak ceiling temperature at locations of sprinklers adjacent to those activated was 272°C (522°F), showing that additional sprinklers would have operated if they had been installed and their thermal elements used as a secondary mechanism of sprinkler activation. This protection is therefore not adequate.

Tests 4 and 5 were conducted at a density of 33 mm/min (0.8 gpm/ft^2), which is the current FM Global guidance for traditional sprinklers. In both tests, the fire was controlled within 1 min after water was applied. Figures 2-14 and 2-15 show the fire damage which in both tests did not spread much beyond the ignition pallet. All test evaluation criteria were satisfied as summarized in Table 2-4. The results indicate SMART sprinklers at this density are effective and can reduce the water demand significantly.

Additional efforts were made to further reduce the water demand for the UUP hazard. Test 7 aimed to investigate if an earlier activation could help reduce the water demand by lowering the density to 18 mm/min (0.44 gpm/ft^2). A modified version of Algorithm 1 was used for the earlier activation criterion. Instead of activating the system when one thermocouple reached a specified temperature rise over a minute, the system was activated and water delivered to the sprinklers when one thermocouple reached an 8.3°C (15°F) rise. This strategy, however, did not improve the results. The fire was not controlled, and the test was terminated at 12 min. Figure 2-16 shows the fire damage. The peak ceiling temperature at nearby sprinkler locations was 308°C (586°F), much higher than the threshold set.

Test 11 was conducted with a density of 24 mm/min (0.6 gpm/ft^2) in the under-1 ignition scenario. The water was delivered at 3 min 30 s after ignition. After water application, the fire increased in intensity very slowly over the next 25 min. The sprinkler protection prevented the fire from spreading beyond the pallets surrounding ignition as seen in Figure 2-17. Eventually the commodity in the ignition pallet burned out and the fire was controlled at about 30 min, just before the test was terminated. The peak ceiling temperature at nearby sprinkler locations was 207°C (405°F). The perimeter of the ceiling reached temperatures over the typical activation temperature of a sprinkler, indicating further sprinkler activations could have occurred. Since all other test evaluation criteria were satisfied, similar to Test 6, the results of Test 11 show that the protection is adequate for a single-activation SMART sprinkler system but will open a large number of additional sprinklers when a dual-activation SMART sprinkler

system is used. Since the results of Tests 4 and 5 with under-1 and among-4 ignition scenarios were very similar to each other, another test with among-4 ignition was deemed unnecessary.

Table   2-4:   Summary of test parameters and results for SMART sprinkler protection of low-piled storage of UUP under a 9.1 m (30 ft) ceiling.

	Test ID	3	4	5
	Test Date	2/21/2018	2/23/2018	2/26/2018
	Movable Ceiling Test Site	North	North	North
	Ceiling Height, m (ft)	9.1 (30)		
	Test Commodity / Fuel	UUP		
TEST PARAMETERS	**Storage Arrangement**	Solid piled storage on floor		
	Main Array Size, pallet loads	3 x 5		
	Targets (3), pallet loads	1 x 4 x 1 of Class 2 commodity		
	Nominal Storage Height, m (ft)	1.5 (5)		
	Aisle Width, m (ft)	2.4 (8)		
	Ignition Location	Under 1	Under 1	Among 4
	Sprinkler Orientation	Pendent (QR deflector)		
	Sprinkler K-factor, L/min/bar$^{\frac{1}{2}}$ (gpm/psi$^{\frac{1}{2}}$)	200 (14.0)	200 (14.0)	200 (14.0)
	Sprinkler Spacing, m x m (ft x ft)	3.0 x 3.0 (10 x 10)	3.0 x 3.0 (10 x 10)	3.0 x 3.0 (10 x 10)
	Discharge Pressure, bar (psi)	0.7 (10)	2.2 (32)	2.2 (32)
	Discharge Density, mm/min (gpm/ft^2)	18 (0.44)	33 (0.8)	33 (0.8)
TEST RESULTS	**Time of Water Delivery to Open Sprinklers, min:s**	3:32	3:20	3:25
	Highest Ceiling Temperature beyond Open Sprinklers at Locations of Neighboring Sprinklers, ºC (ºF)	272 (522)	54 (129)	52 (126)
	Peak Steel Temperature, ºC (ºF)	153 (308)	24 (76)	23 (73)
	Target Array Ignited	No	No	No
	Test Duration, min	24	24	25

Table   2-5:   Summary of test parameters and results for SMART sprinkler protection of low-piled storage of UUP under a 9.1 m (30 ft) ceiling.

	Test ID	7[iv]	11
TEST PARAMETERS	**Test Date**	3/20/2018	4/10/2018
	Movable Ceiling Test Site	North	North
	Ceiling Height, m (ft)	9.1 (30)	
	Test Commodity / Fuel	UUP	
	Storage Arrangement	Solid piled storage on floor	
	Main Array Size, pallet loads	3 x 5	
	Targets (3), pallet loads	1 x 4 x 1 of Class 2 commodity	
	Nominal Storage Height, m (ft)	1.5 (5)	
	Aisle Width, m (ft)	2.4 (8)	
	Ignition Location	Under 1	Under 1
	Sprinkler Orientation	Pendent (QR deflector)	
	Sprinkler K-factor, L/min/bar^{½} (gpm/psi^{½})	200 (14.0)	200 (14.0)
	Sprinkler Spacing, m x m (ft x ft)	3.0 x 3.0 (10 x 10)	3.0 x 3.0 (10 x 10)
	Discharge Pressure, bar (psi)	0.7 (10)	1.2 (18)
	Discharge Density, mm/min (gpm/ft^2)	18 (0.44)	24 (0.6)
TEST RESULTS	**Time of Water Delivery to Open Sprinklers, min:s**	3:29	3:30
	Highest Ceiling Temperature beyond Open Sprinklers at Locations of Neighboring Sprinklers, ℃ (℉)	308 (586)	207 (405)
	Peak Steel Temperature, ℃ (℉)	204 (400)	111 (231)
	Target Array Ignited	No	No
	Test Duration, min	12	30

[iv] The strategy used in this test for sprinkler operation was a modified version of Algorithm 1 to provide an earlier activation. The water was delivered to the open sprinklers when one thermocouple reached 8.3℃ (15℉) above ambient temperature.
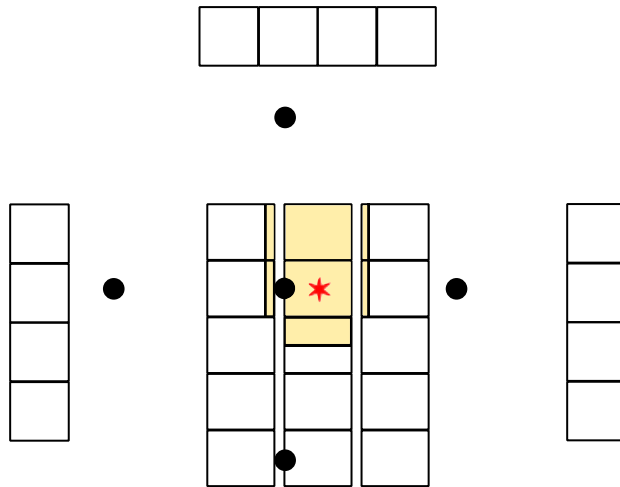
Figure   2-13: Smart sprinkler Test 3 fire damage.
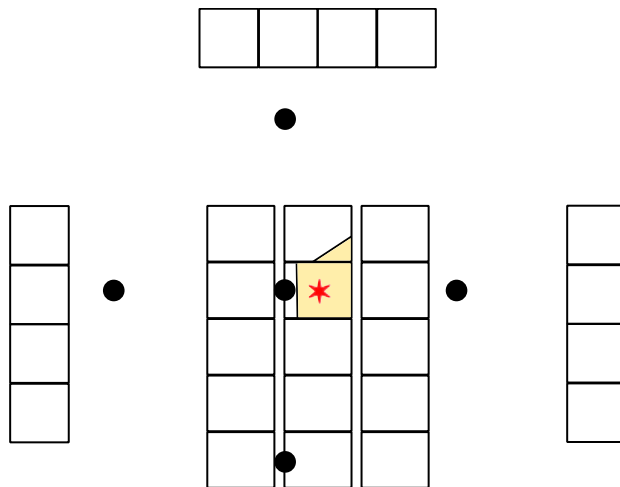
Figure   2-14: Smart sprinkler Test 4 fire damage.
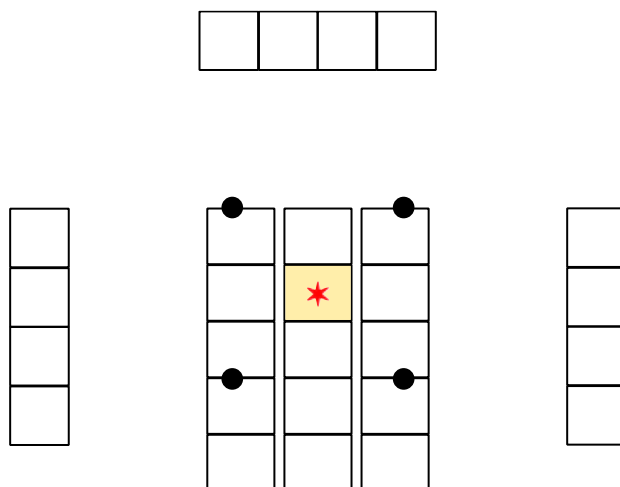
Figure   2-15: Smart sprinkler Test 5 fire damage.
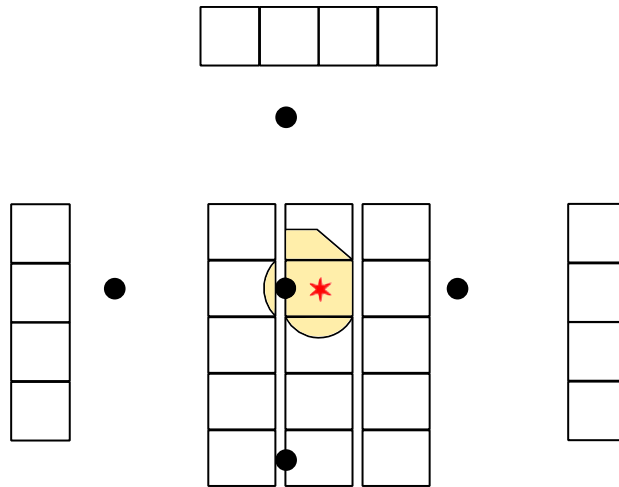
Figure   2-16: SMART sprinkler Test 7 fire damage.
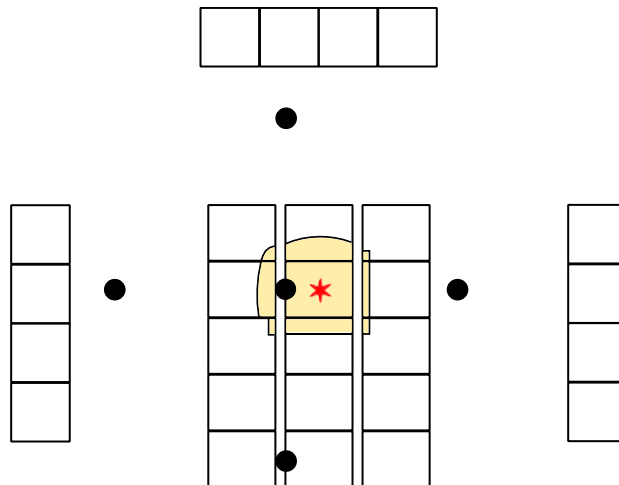
Figure   2-17: SMART sprinkler Test 11 fire damage.

2.1.4   UUP Protection Under an 18.3 m (60 ft) Ceiling

For low-piled storage of UUP under an 18.3 m (60 ft) ceiling, the current FM Global guidance is a design of ten sprinklers at a density of 65 mm/min (1.6 gpm/ft^2). Tests 12 and 13 were conducted at a density of 41 mm/min (1.0 gpm/ft^2) in an under-1 ignition scenario using K200 (K14.0) and K360 (K25.2) sprinklers. The protection was activated using Algorithm 2 – temperature of 57°C (135°F) at one location. The change in the sprinkler K-factor was to verify if the pressure difference from the two sprinklers at the same density would not negatively impact their performance. In both tests, the fire was controlled within 30 s after water was delivered. Flames were not seen on top of the main array until test termination at 15 min. Table 2-6 summarizes the parameters and test results showing that all test evaluation criteria were satisfied.

Table   2-6:   Summary of test parameters and results for SMART sprinkler protection of low-piled storage of UUP under an 18.3 m (60 ft) ceiling.

		12	13
TEST PARAMETERS	**Test ID**	12	13
	Test Date	4/12/2018	4/16/2018
	Movable Ceiling Test Site	North	North
	Ceiling Height, m (ft)	18.3 (60)	
	Test Commodity / Fuel	UUP	
	Storage Arrangement	Solid piled storage on floor	
	Main Array Size, pallet loads	3 x 5	
	Targets (3), pallet loads	1 x 4 x 1 of Class 2 commodity	
	Nominal Storage Height, m (ft)	1.5 (5)	
	Aisle Width, m (ft)	2.4 (8)	
	Ignition Location	Under 1	Under 1
	Sprinkler Orientation	Pendent (QR deflector)	
	Sprinkler K-factor, L/min/bar$^{\frac{1}{2}}$ (gpm/psi$^{\frac{1}{2}}$)	200 (14.0)	360 (25.2)
	Sprinkler Spacing, m x m (ft x ft)	3.0 x 3.0 (10 x 10)	3.0 x 3.0 (10 x 10)
	Discharge Pressure, bar (psi)	3.5 (50)	1.1 (16)
	Discharge Density, mm/min (gpm/ft^2)	41 (1.0)	41 (1.0)
TEST RESULTS	**Time of Water Delivery to Open Sprinklers, min:s**	4:29	4:15
	Highest Ceiling Temperature beyond Open Sprinklers at Locations of Neighboring Sprinklers, °C (°F)	58 (137)	47 (116)
	Peak Steel Temperature, °C (°F)	27 (80)	26 (78)
	Target Array Ignited	No	No
	Test Duration, min	15	15

2.1.5   Fire Suppression Performance

Traditional protection options for HC-3 occupancies with any sprinkler (standard or quick-response; pendent or upright) require a large water demand area. The results of the tests presented here have shown that fewer sprinklers are required with SMART sprinkler systems and in some cases the water density can also be reduced when compared to traditional sprinkler guidance. These factors lead to a significant reduction in water demand. For a dual-activation SMART sprinkler system, with a standard thermal element alongside the "SMART" mechanism to operate the sprinklers, additional sprinklers can operate if the ceiling temperatures beyond the region of initial sprinkler operations exceed the sprinkler activation temperature. However, for a single-activation system, it is sufficient that the steel temperatures at the ceiling do not exceed 538°C (1,000°F). Therefore, a single-activation system can provide adequate protection at a lower density.

The number of SMART sprinkler operations will depend on the activation algorithm and any safety factors included in the system design. Therefore, the reduction in water demand from standard sprinkler design was estimated for two scenarios, a five or nine sprinkler design; the results are tabulated in Table 2-7 for a single-activation system. The reduction in water demand for all the test conditions investigated is due to both reduction in demand area and required density. It should be noted that the activation criterion used in this study is very conservative and is designed to include most SMART sprinkler systems that are likely to be available in the future. An algorithm that offers earlier activation can further reduce the required density and, therefore, offer additional reductions in water demand.

Table 2-7: Reduction in water demand for single-activation SMART sprinklers compared to traditional ceiling sprinkler protection.

Commodity	Ceiling Height m (ft)	DS 3-26 Design* mm/min over m^2 (gpm/ft^2 over ft^2)	SMART Sprinkler System Density mm/min (gpm/ft^2)	Reduction in Water Demand	
				5-Sprinkler Design	9-Sprinkler Design
CUP	9.1 (30)	12/232 (0.3/2,500)	8 (0.2)	87 %	76 %
	18.3 (60)	20/280 (0.5/3,000)	15 (0.37)	88 %	78 %
UUP[†]	9.1 (30)	45/93 (1.1/1,000)	24 (0.6)	73 %	51 %
	18.3 (60)	65/93 (1.6/1,000)	41 (1.0)	69 %	44 %
* Assuming 9.3 m^2 (100 ft^2) coverage area per sprinkler.					
[†] UUP sprinkler design listed in DS 3-26 (Table 3) [6] as number of K360 (K25.2) sprinklers at a specified pressure.					

For a dual-activation system, the required density is higher in some cases to limit the number of sprinkler operations. The design densities for such systems and their potential to reduce water demand under a ceiling height of 9.1 m (30 ft) is listed in Table 2-8. The reduction in water demand is attributed to reduced demand area alone. For a ceiling height of 18.3 m (60 ft), the reduction is attributed to both reduced design density and demand area.

Table 2-8: Reduction in water demand for dual-activation SMART sprinklers compared to traditional ceiling sprinkler protection.

Commodity	Ceiling Height m (ft)	DS 3-26 Design* mm/min over m² (gpm/ft² over ft²)	SMART Sprinkler System Density mm/min (gpm/ft²)	Reduction in Water Demand	
				5-Sprinklers Design	9-Sprinkler Design
CUP	9.1 (30)	12/232 (0.3/2,500)	8 (0.3)	80 %	64 %
	18.3 (60)	20/280 (0.5/3,000)	15 (0.37)	88 %	78 %
UUP†	9.1 (30)	45/93 (1.1/1,000)	33 (0.8)	63 %	35 %
	18.3 (60)	65/93 (1.6/1,000)	41 (1.0)	69 %	44 %
* Assuming 9.3 m² (100 ft²) coverage area per sprinkler.					
† UUP sprinkler design listed in DS 3-26 (Table 3) [6] as number of K360 (K25.2) sprinklers at a specified pressure.					

2.2 Water Cannon Experimental Setup and Results

Two different types of tests were conducted with the water cannon: the first setup was designed to measure the stream trajectory and water flux without a fire and the second to evaluate the suppression performance with a fire under different operating conditions.

2.2.1 Background

A typical water cannon system installed under a ceiling to protect a low-piled fuel array is illustrated in Figure 2-18. After detecting and targeting the fire, the AWC discharges a stream at a height (H_0) above the floor, a launch angle (θ, or elevation angle) relative to the floor, a horizontal reach radius (R) measured from the cannon, and a flow rate ($\dot{Q}$) with a water coverage area (*A*) on the fire. Using the concept of the critical delivered flux (CDF) developed in commodity classification testing [10], the effective water flux $\dot{q}_e^{"}$ [mm/min (gpm/ft²)] delivered to the fuel surface by the AWC should be higher than the CDF, $\dot{q}_c^{"}$, as

$$\dot{q}_e^{"} > \beta \dot{q}_c^{"},$$

2-1

where $\beta > 1$ is a factor that accounts for possible reduction in spray penetration through the fire. Theoretically, the effective water flux, $\dot{q}_e^{"}$, can be defined as

$$\dot{q}_e^{"} = \frac{\dot{Q}_e}{A_e},$$

2-2

where $\dot{Q}_e$ is the water flow rate actually delivered to the protected area, A_e. The value of $\dot{q}_e^{"}$ can be measured by using collection containers placed in a pre-defined area. When determining the protected area, it is important to note that the AWC solid stream usually exhibits a parabolic trajectory. Due to air resistance and force of gravity on the water droplets, the distribution pattern on the ground is generally

elliptical with a spray head and a tail as will be discussed below with reference to Figure 2-20. The water flux distribution is also nonuniform, where the spray head has the highest flux. The coverage area changes with the AWC operating conditions such as pressure (P), elevation angle (θ), initial cone angle (α), and the stream trajectory described by height (H_0) and horizontal reach radius (R). For example, the coverage area can increase with the cone angle (α) when the spray is changed from solid stream to wide fog. A comparison of the solid stream and wide fog sprays is shown in Figure 2-19. A longer horizontal reach can also enlarge the area due to spray dispersion.
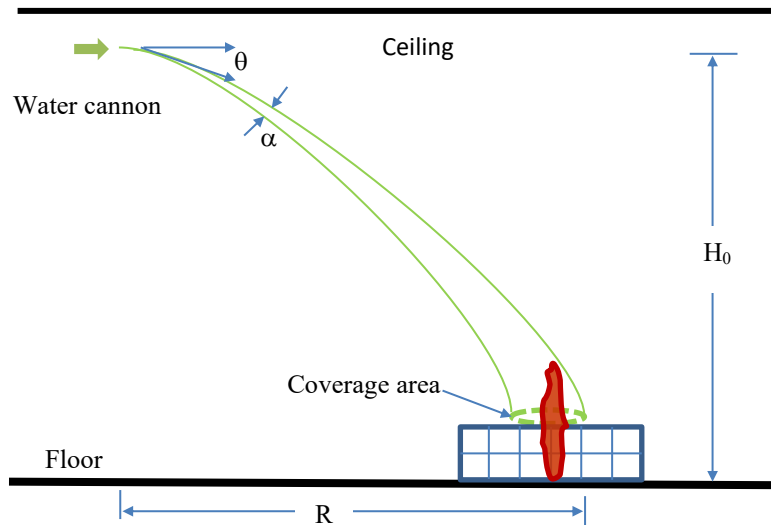
Figure   2-18: Elevation view of a typical water cannon system installed under a ceiling to protect low-piled storage.
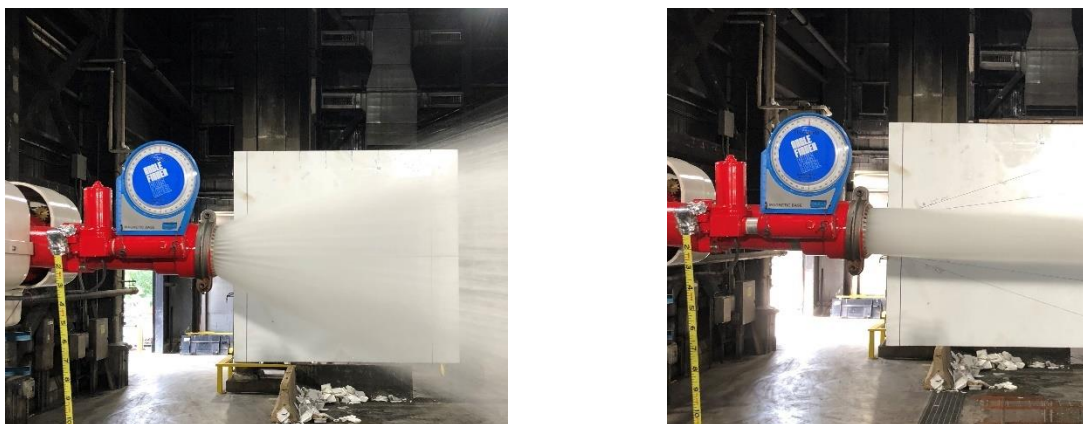
Figure   2-19: The nozzle of the water cannon and spray pattern as it changes from a wide fog (left) to a solid stream (right).

The CDF values, $\dot{q}_c''$, have been measured for standard commodities in rack storage for sprinkler protection conditions [10]. However, the AWC is different from ceiling-level sprinklers in three respects:

1. different water distribution pattern and stream angle interacting with the fire plume,
2. variation in system response time to detect and target a fire, and
3. fire targeting accuracy.

The water distribution pattern of the cannon is generally elliptical as shown in Figure 2-20 which is different from the axisymmetric pattern of a ceiling-level sprinkler. There is also a large interaction angle between the stream and the fire due to the launch angle (θ). The large interaction angle can cause a strong stream to push burning objects away from the fire origin, resulting in additional fire spread. Furthermore, an AWC can deliver water to the fire through streams or wide-angle sprays. A water stream provides a longer delivery distance and higher penetration ratio through the fire, while the latter generates a larger coverage area. These differences may affect the fire protection results and were examined during the fire suppression tests.

The variation of response time (detection and targeting) is another important issue for the AWC system. Previous work [3] showed that a range of response times (11 to 39 s) was possible in four fire suppression tests. Generally, the fast response had an advantage in fire protection and a very late response led to an uncontrolled fire. Given these results, a reasonably long response time of 40 s was considered as a conservative condition during the AWC tests.

The last major difference between an AWC and ceiling sprinklers is the accuracy of fire targeting. For example, Figure 2-20 shows three cases of fire targeting accuracy for an AWC: (a) the fire is accurately targeted and fully covered by water, (b) the fire is not well targeted and only partially covered by water and (c) the fire is not targeted accurately and not covered by water.

Stream

Tail   Head

Water Contour on Floor

(a)   (b)   (c)

Water Contour on Fire Zone
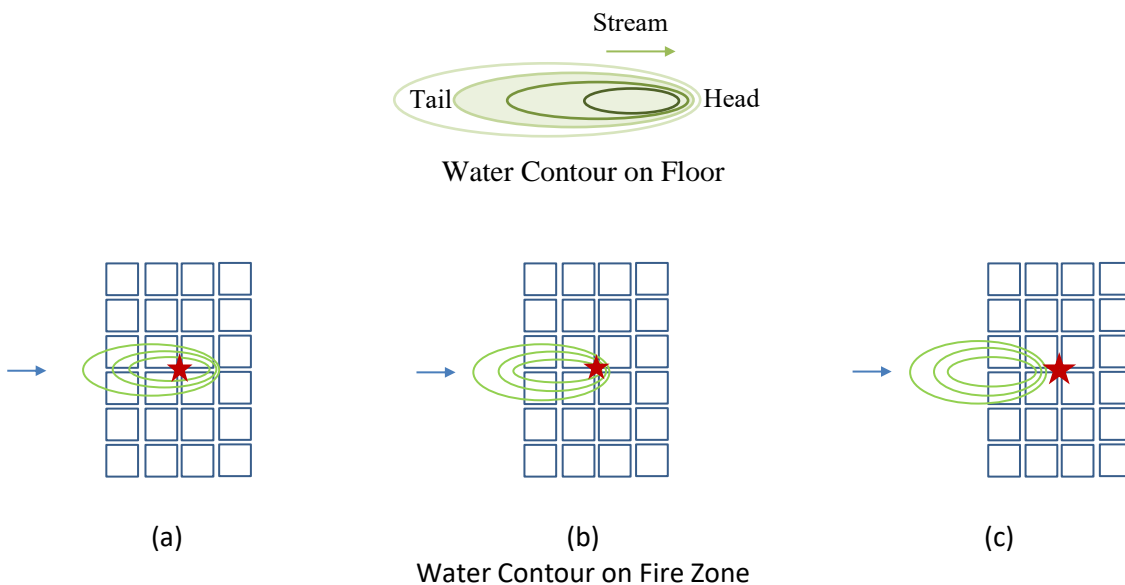
Figure   2-20: Plan view of water distribution contours on the floor and on a fire zone: (a) fully covered, (b) partially covered, and (c) not covered.

The best performance is the case shown in Figure 2-20 (a) where the fire zone is fully covered by water. The fire may be controlled/suppressed if the water discharge is sufficient. In contrast, Figure 2-20 (c) depicts the worst case where no water is delivered to the fire and suppression is not possible. For the case shown in Figure 2-20 (b), the fire region is partially covered by water and the fire may be controlled

To relax the fire targeting accuracy and increase the water coverage area, narrow-angle sweeping is often utilized by AWC systems [3]. For example, Figure 2-21 shows a sweeping pattern where the cannon is moved along the azimuthal angles ($\phi_1 - \phi_2$) in the horizontal (left-right) direction, elevation angles ($\theta_1 - \theta_2$) in the vertical (up-down) direction, or the combined sequence of both left-right and up-down directions. The increased water coverage area due to sweeping will change the water flux distribution as the speed (sweeping degrees per second), the intermittency (the fraction of time that water is delivered to one location) and the range of the sweeping angle can be varied. If the sweeping speed is too slow, the fire at one location may not have water applied for a longer time. The fire is thus in a free-burning condition that can lead to propagation. If the sweeping speed is changed, the water delivery to a location may be much higher than that to another location due to different time spent at each location. Because of this uneven water distribution, the fire may continue to propagate in areas with a low water flux. A large sweeping angle, while increasing the coverage area, can significantly reduce the average water flux. The equivalent water flux produced by the AWC sweeping motion was examined in the water distribution tests and compared to direct water application.
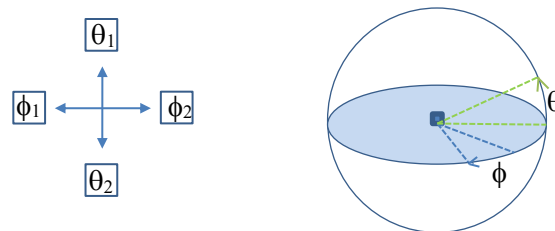
Figure   2-21: AWC sweep motion with azimuthal angles ($\phi_1 - \phi_2$) in the horizontal (left-right) or elevation angles ($\theta_1 - \theta_2$) in the vertical (up-down) directions.

2.2.2   Water Stream Trajectory and Flux

The water stream trajectory and water flux were measured using flow tests without a fire. The trajectory testing used the AWC installed at an elevation of 15 m (50 ft) with a horizontal ruler marked on the floor measuring the distance away from the cannon. Figure 2-18 shows a schematic of a water cannon installation under a ceiling with important parameters labeled and Figure 2-22 shows the actual test layout for the trajectory measurements. The trajectory was measured for various elevation angles (0°, -15°, -30° and -45° - negative values for nozzle pointing down) at three flow rates 230, 450 and 680 lpm (60, 120 and 180 gpm) as shown in Table 2-9 along with the horizontal reach results. The table shows both the measured and calculated horizontal reach results. The measured results are reported as the average value and standard deviation of the location of the front head of the stream on the floor as determined by ten snapshots that were randomly selected from the test videos. The calculated results use the parabolic path equation, Equation 2-3, assuming negligible air resistance. In the equation, H is

the final height of the water stream, H_0 is the initial height of the water stream, g is the gravitational acceleration, R is the horizontal reach, θ is the elevation angle and U_0 is the initial stream velocity.

$$H = H_0 - \frac{g}{2U_0^2 \cos^2 \theta} \cdot R^2 + \tan \theta \cdot R$$
2-3

The initial stream velocity is estimated using the Bernoulli's principle expressed as Equation 2-4 with an empirical coefficient for a nozzle represented by c_0 which was set to 0.8 based on calibration with the actual measurements for the pressure, P, and for the water density, ρ. Equation 2-3 was developed for solid stream conditions. When the solid stream is switched to a wide fog by changing the cone angle α, Equation 2-3 may not be appropriate for describing the spray trajectory because dispersed water droplets have different initial θ angles and are more affected by air friction than the solid jet.

$$U_0 = c_0 \left(\frac{2P}{\rho} \right)^{0.5}$$
2-4

Figure   2-22: AWC test layout used to measure stream trajectory.

The results showed that, under the same conditions, a greater reach was achieved with increasing flow rate or discharge pressure. Based on flow rate and discharge pressure from the measurements, the AWC used has an equivalent sprinkler K-factor of 360 lpm/bar$^{0.5}$ (25 gpm/psi$^{0.5}$). The calculated horizontal reach was also found to be in good agreement with the measurements with an average relative difference of 3% as shown in Figure 2-23. The entire stream trajectory was calculated for the three flow rates and is illustrated in Figure 2-24. The impingement angles shown in Figure 2-24 also agree well with those observed during testing. Figure 2-25 presents the AWC solid stream trajectory at two flow rates, 230 lpm (60 gpm) and 450 lpm (120 gpm). Based on the floor markers, the horizontal reach of the stream front head was approximately 13.1 m (43 ft) for the flow rate of 230 lpm (60 gpm), and 25.9 m

(85 ft) for 450 lpm (120 gpm). Figure 2-25 also shows that the impingement angle of the stream to the floor was approximately 75° for 230 lpm (60 gpm), and 45° for 450 lpm (120 gpm).

Table 2-9: Horizontal reach measurements of solid stream trajectory with water cannon installed at elevation of 15 m (50 ft).

Test ID	Elevation Angle degree	Flow Rate lpm (gpm)	Measured Horizontal Reach m (ft)	Calculated Horizontal Reach m (ft)
1	0	230 (60)	13.4 ± 0.1 (44.0 ± 0.3)	12.6 (41.3)
2	0	450 (120)	25.8 ± 0.1 (84.6 ± 0.4)	25.2 (82.5)
3	0	680 (180)	36.3 ± 0.2 (119.2 ± 0.6)	37.7 (123.8)
4	-15	230 (60)	11.1 ± 0.1 (36.5 ± 0.3)	10.9 (35.8)
5	-15	450 (120)	20.0 ± 0.1 (65.4 ± 0.3)	19.7 (64.5)
6	-30	230 (60)	9.0 ± 0.1 (29.4 ± 0.2)	8.9 (29.1)
7	-30	450 (120)	14.2 ± 0.1 (46.4 ± 0.3)	14.6 (47.8)
8	-45	230 (60)	6.7 ± 0.1 (21.8 ± 0.2)	6.9 (22.6)
9	-45	450 (120)	9.9 ± 0.1 (32.4 ± 0.2)	10.2 (33.5)
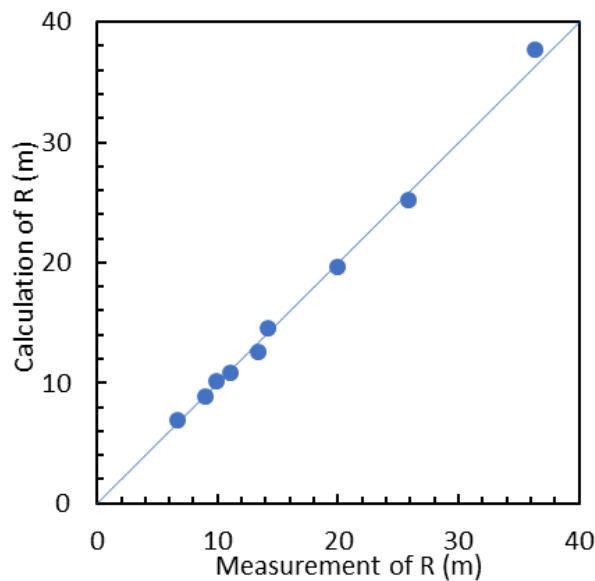
Figure 2-23: Comparison of measured and calculated horizontal reach (R) for the results presented in Table 2-9.
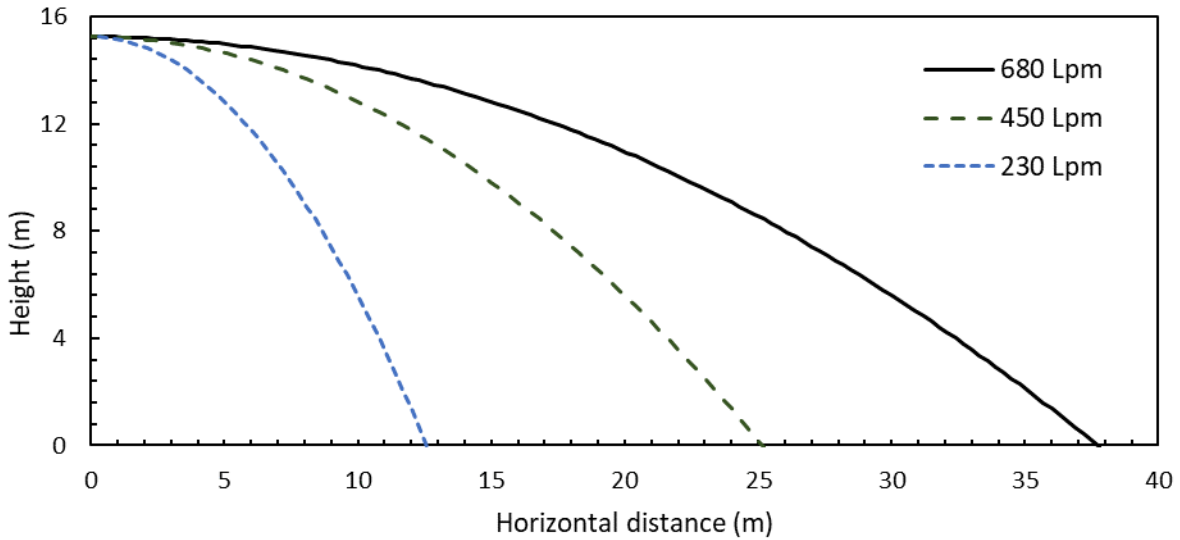
Figure   2-24: AWC solid stream trajectory calculated from Equations 2-3 and 2-4 for three water flows at the same conditions (c_0 = 0.8, H_0 = 15 m (50 ft), θ = 0°, α = 0°).

| (a) | (b) |

Figure   2-25: AWC stream trajectory at (a) 230 lpm (60 gpm), and (b) 450 lpm (120 gpm) with H_0 = 15 m (50 ft), θ = 0°, and α = 0°.

After the stream trajectory was quantified, the applied water flux from the water cannon was measured. The water flux measurements used a similar setup as the trajectory measurements except collection containers were positioned under the spray stream to collect the water and calculate the flux distributions. The number and configuration of the containers varied depending on the spray parameters being tested. The containers measured 0.74 × 0.70 × 0.48 m (29 × 28 × 19 in.) and the water volume in each container was determined by using the area and measuring the water depth. The water volume was then divided by the collection time and the container surface area to calculate the water flux. To verify this method, the water volume was also calculated from the mass measured by a scale. The deviation was between 1.2% and 10.8 % depending on the water depth, with higher accuracy for deeper water. All water flux measurements were collected at a 0° elevation angle with either no sweep,

horizontal sweep or vertical sweep and with the same three flow rates used in the trajectory tests (see Table 2-10 for complete list of water flux tests conducted). The solid stream no sweeping tests used a straight line of five containers for low flow, seven containers for medium flow and 24 containers for high flow scenarios. The sweeping tests as well as the wide fog setting tests used 15 to 24 containers positioned evenly in three rows side by side, with the number of containers in each row increasing with increased flow see Figure 2-26 for the various test layouts. Water was collected until any one container was full. The total water collection time was generally several minutes depending on the maximum water flux collected by the container.

Table   2-10: AWC water flux distribution tests at a height of 15 m (50 ft) above the floor.

Test ID	Initial elevation angle θ	Initial spray cone angle, α stream or fog	Water flow rate lpm (gpm)
1	0°	0°	230 (60)
2	0°	0°	450 (120)
3	0°	0°	680 (180)
4	0°	30° (fog)	230 (60)
5	0° (horizontal sweeping 0° < ϕ < 9°)	0°	230 (60)
6	0° (horizontal sweeping 0° < ϕ < 5°)	0°	450 (120)
7	0° (horizontal sweeping 0° < ϕ < 2°)	0°	680 (180)
8	Vertical sweeping 0° < θ < 9°	0°	230 (60)
9	Vertical sweeping 0° < θ < 18°	0°	230 (60)

The initial elevation angle was 0° for all tests and was not changed except in the tests that examined the effects of sweeping. Two sweeping cycles of horizontal (left-right) and vertical (up-down) were examined, and the range of the sweeping angle was adjusted so that the water containers were covered by the stream. In the original water cannon design, the sweeping was manually controlled by a handle that sends electrical signals to change the nozzle orientation. To improve the control stability, the manual control was replaced by computer programmed electrical signals to rotate the nozzle. For different sweeping angles, the time of a sweeping cycle was in the range of 6 to 15 seconds. The initial spray cone angle was 0° for all solid stream tests and 30° for wide fog tests. The wide fog angle was estimated from the spray pattern as shown in Figure 2-19.

During testing, a peak water flux was observed at the stream head for the solid stream tests and the peak value decreased with increasing horizontal reach. The tail was also observed to become longer with increasing horizontal reach or flow rate. Figure 2-27 presents the water flux measurements for three solid stream flow rates under the same conditions [H_0 = 15 m (50 ft), θ = 0°, and α = 0°]. Due to spray dispersion along the travel distance, not all the water exiting the AWC was collected by the containers. At the low flow rate only 200 lpm (53 gpm) was collected or 88% of the initial discharge rate. At the medium flow with a longer travel distance, the total collection was 370 lpm (98 gpm) or 82% of the initial discharge rate and at the highest flow 510 lpm (135 gpm) was collected or 75% of the initial discharge rate.

Solid Stream

| 5 containers
low flow | 7 containers
medium flow | 24 containers
high flow |

Wide Fog or Sweeping

Up to 24 containers
all flows
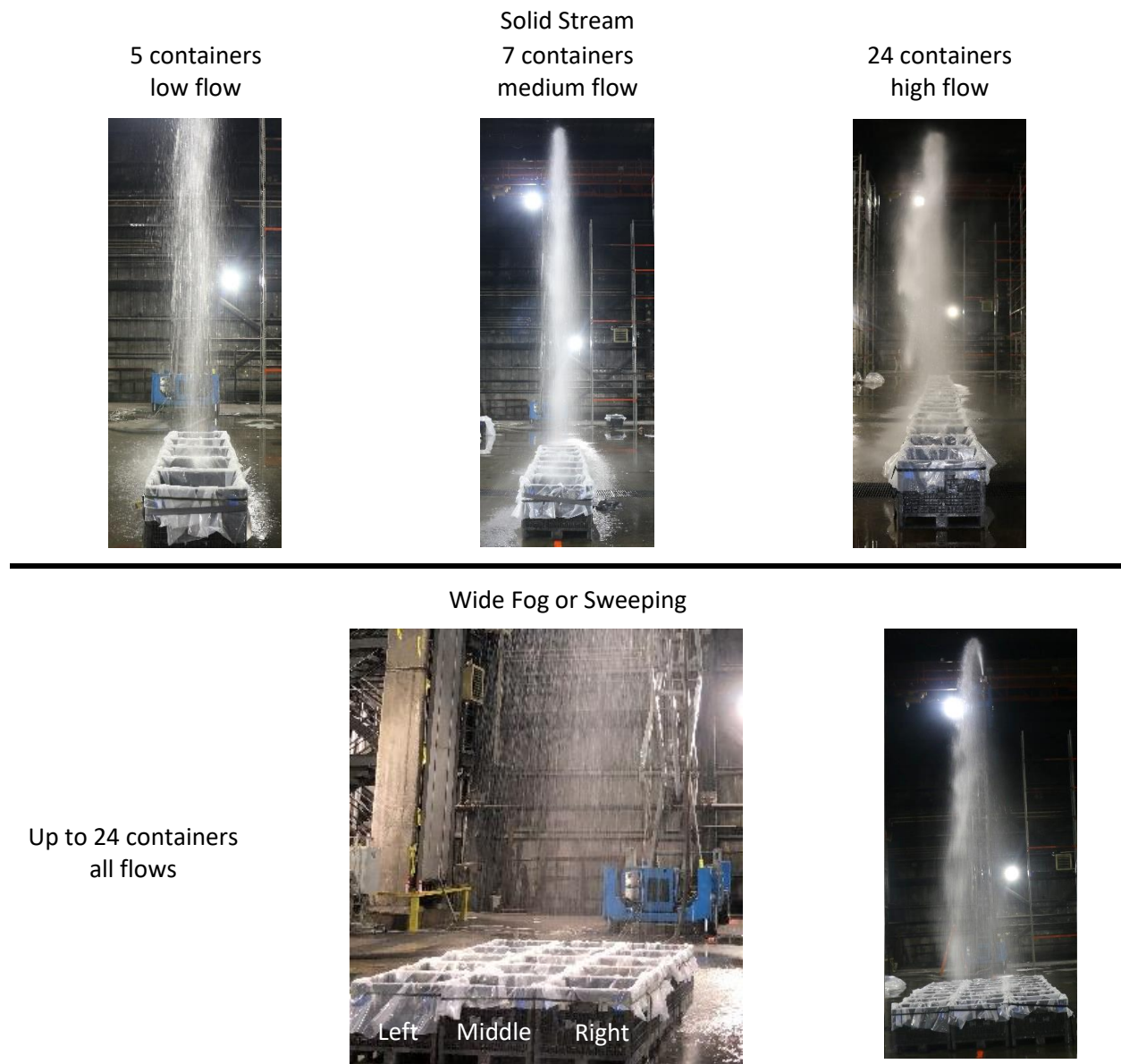
Figure   2-26: AWC water flux distribution test layouts.

When the spray pattern was changed from a solid stream to a wide fog, the coverage area increased at the expense of a reduction in the horizontal reach. The overall water flux was less than for the solid stream and was found to reach values similar to those obtained with sprinklers. The water flux distribution measured for the wide fog AWC with flow rate of 230 lpm (60 gpm) is shown in Figure 2-28. The collection for the wide fog tests was accomplished with three rows of containers that were five containers long for the lowest flow rate and increased up to eight long for the highest flow rate. For the data shown in Figure 2-28, 15 containers were used in a 3 × 5 array covering an area of 9.2 m^2 (100 ft^2). Facing the water cannon, the three rows were labeled left, middle and right as shown in Figure 2-26. The total collection rate of the 15 containers was 182 lpm (48 gpm), which is 80% of the initial discharge rate. The water flux distribution of the wide fog spray was more dispersed than that of the solid stream

(compare to the results presented in Figure 2-27). The maximum water flux for the wide fog spray of 39 mm/min (0.96 gpm/ft^2) was also much less than the 220 mm/min (5.4 gpm/ft^2) observed for the solid stream. The horizontal reach from the wide fog AWC was determined to be 9.7 m (32 ft) using the water flux profile of the middle row, which was again less than the 13.4 m (44 ft) the solid stream achieved under the same conditions.

Another way to increase the coverage area but maintain a long horizontal reach is to operate the AWC with narrow angle sweeping and a solid stream spray. The sweeping action creates an intermittent delivery of water because of the mechanical gear switching mechanism. Therefore, the water flux when using sweeping depends on how the water cannon moves. Like a windshield wiper, the stream from the cannon was rotated left to right and back left to cover the three rows of collection containers. Figure 2-29 shows the horizontal sweeping and water distribution measurements. The coordinate R denotes the streamwise direction and y denotes the spanwise direction. The difference between the sweeping and wide fog pattern is that the water delivery of the wide-fog spray is continuous and steady, while the narrow-angle sweeping delivery is intermittent. A container at a location (y, R) collects water at discrete times such as t_1, t_2, t_3, etc., due to intermittent delivery. The time difference between t_1 and t_2 depends on the sweeping speed. Except for the total discharge flow rate, the volume of water collected also depends on the sweeping intermittency or the time fraction of the water delivery on the container in a sweeping cycle. Figure 2-29 also shows the water flux distribution for three flow rates with horizontal sweeping. In the sweeping cycle tested from left to right and then back to left, the middle row had two chances per cycle to collect water. However, the gear system paused at the two sides when the rotating direction was forced to change. Therefore, the average time fraction of the water delivery on the left, middle and right rows was similar. The three collection rows had the same distribution profiles. During the high flow rate test, the water cannon did not target accurately on the containers leaving the right row only partially covered by the spray, which accounts for the lower peak seen in the results. With horizontal sweeping, the total water flow was shared by the three collection rows in space and time, therefore the magnitude of the water flux was approximately one-third of that observed without sweeping (see Figure 2-27).

AWC can also be operated with a vertical sweep (up-down) motion as shown in Figure 2-30. Two ranges ($-9° < \theta < 0°$ and $-18° < \theta < 0°$) of vertical motion were tested at the low flow rate of 230 lpm (60 gpm) using one row of collection containers. The water flux distribution results are presented in Figure 2-30, which shows that vertical sweeping can extend the water distribution along the streamwise direction. For the wider range of $-18° < \theta < 0°$ two peaks exist in the data along the horizontal distance R due to the mechanical stop at each programmed angle. The sweeping speed was not smooth along the elevation angle; the cannon paused at each of the three angles of 0°, -9°, and -18°. As a result, the cannon stayed a relatively longer time (or delivered more water) at the three angles than at the angles in-between. While the first peak was generated in the sweeping range of $-9° < \theta < 0°$, the second peak (at the shorter distance) was generated due to the third angle of -18° added to the sweeping range for $-18° < \theta < -9°$.
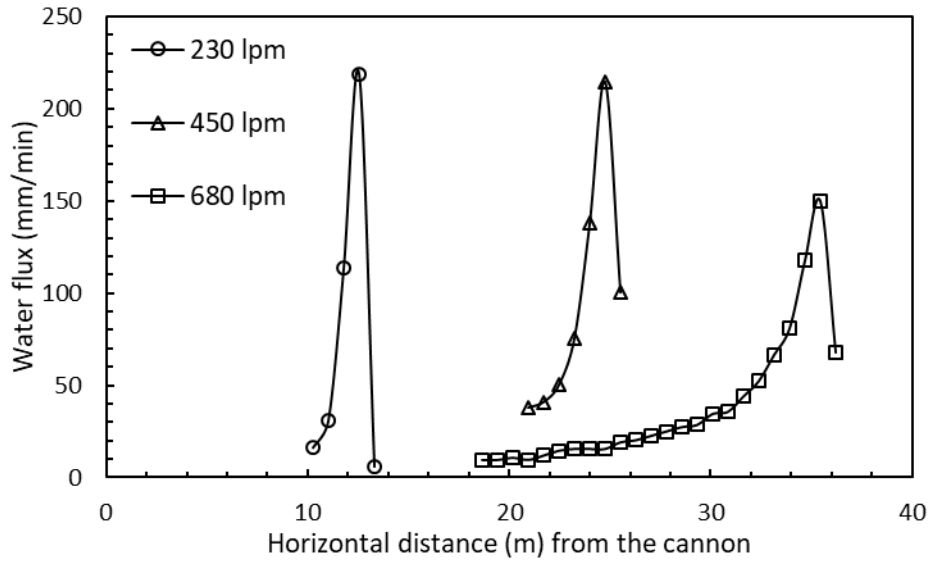
Figure 2-27: AWC water flux distribution for solid stream AWC at H_0 = 15 m (50 ft), θ = 0° and α = 0°.
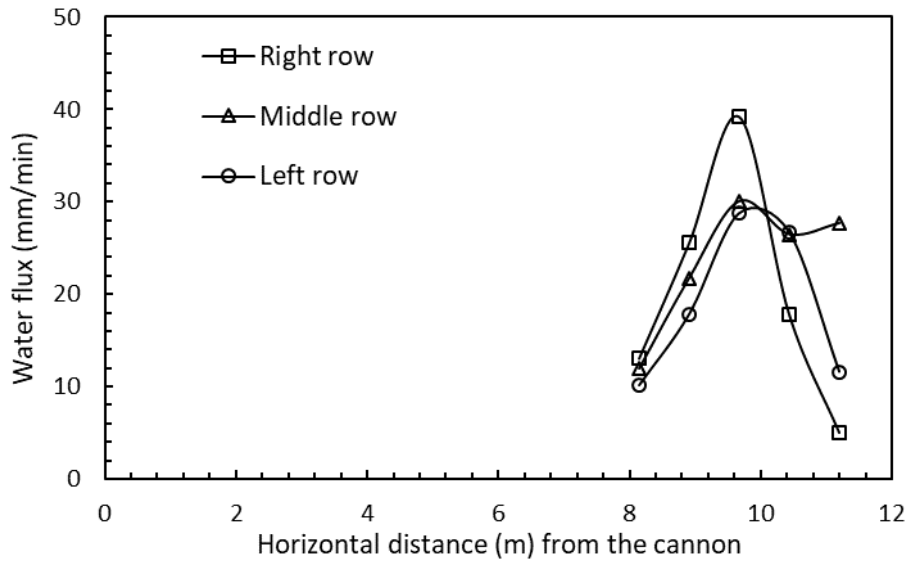
Figure 2-28: AWC water flux distribution for wide fog AWC at 230 lpm (60 gpm), H_0 = 15 m (50 ft), θ = 0° and α = 30°.
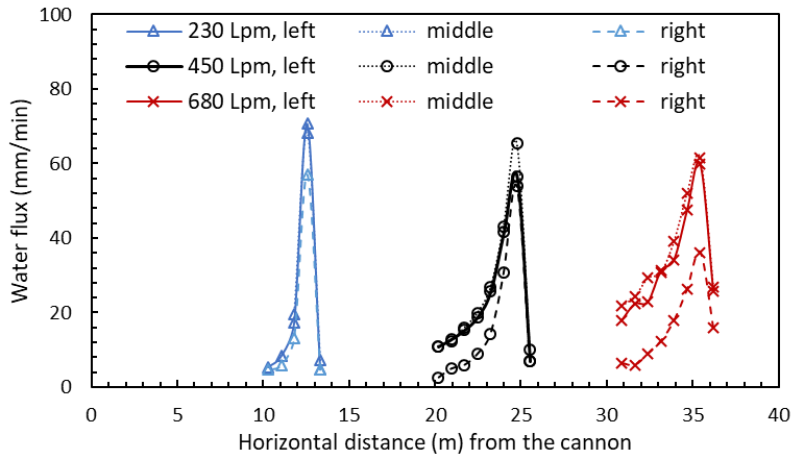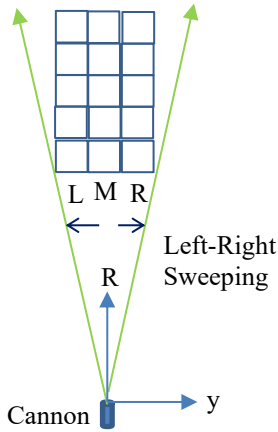
Figure 2-29: AWC horizontal sweeping motion and water flux distribution for solid stream with horizontal sweeping at H_0 = 15 m (50 ft), $\theta = 0°$, and $\alpha = 0°$.
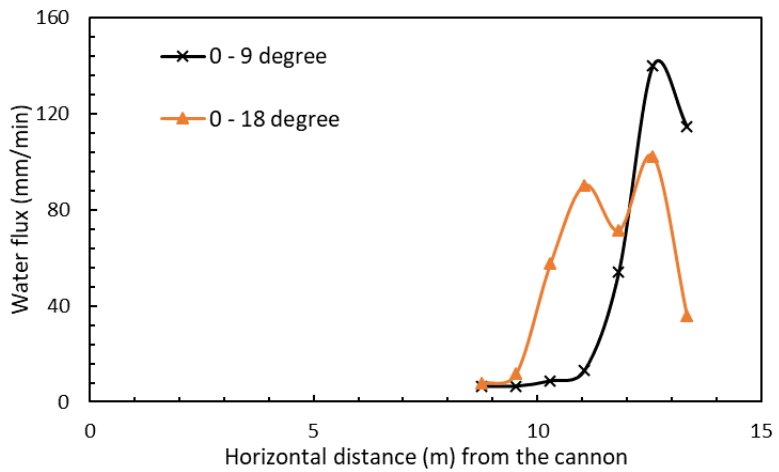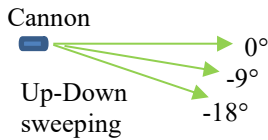
Figure 2-30: AWC vertical sweeping motion and water flux distribution over two ranges $(-9° < \theta < 0°$ and $-18° < \theta < 0°)$ for a flow rate of 230 lpm (60 gpm) at H_0 = 15 m (50 ft) and $\alpha = 0°$.

2.2.3 Fire Suppression Performance

The fire suppression tests used the information obtained regarding trajectory and flux to test the water cannon's ability to control a low-piled HC-3 occupancy fire. Nine fire tests were conducted to evaluate the water cannon targeting accuracy, water flux distribution and response time on firefighting effectiveness; eight tests were conducted under the 20-MW calorimeter and one under a movable ceiling due to the long delivery distance required (Test 8). The test parameters and results are summarized in Table 2-11. The parameters that were changed during testing included the spray pattern (wide fog or solid stream), sweeping pattern, flow rate, and reaching distance.

Table   2-11: AWC low-pile storage fire test summary.

Test ID	Water Flow lpm (gpm)	Sweeping type, points	Coverage Area m² (ft²)	R$_{c-i}$ m (ft)	Response Time s	Fire Outcome
0	0	Free Burn				
1	230 (60)	None (Wide Fog)	9.3 (100)	8.2 (27)	40	Controlled
2	230 (60)	H, 2	9.3 (100)	10.7 (35)	40	Uncontrolled
3	230 (60)	H, 2	9.3 (100)	9.8 (32)	40	Controlled
4	230 (60)	H + V, 6	11.4 (120)	9.8 (32)	40	Controlled
5	450 (120)	H + V, 6	15.0 (160)	9.8 (32)	40	Controlled
6	450 (160)	H + V, 6	26.6 (290)	16.5 (54)	40	Controlled
7	450 (160)	H + V, 9	26.6 (290)	16.5 (54)	40	Controlled
8	680 (180)	H + V, 9	74.3 (800)	27.4 (90)	40	Uncontrolled
9	230 (60)	H + V, 9	12.0 (130)	9.8 (32)	60	Controlled
H = Horizontal V = Vertical						

Each test used a low-pile storage array consisting of modified CUP commodity arranged in three rows, four pallet loads long and one pallet load high under the 20-MW calorimeter. The modification to the CUP commodity consisted of adding one more layer of CUP boxes to the pallet load resulting in a total of 12 boxes on a pallet with nominal dimensions of 1.1 × 1.1 m (3.5 × 3.5 ft) by 1.7 m (5.6 ft) high. The array was set up with 75 mm (3 in.) transverse flues and 150 mm (6 in.) longitudinal flues. The water cannon was positioned away from the array at a distance based on the stream trajectory measurements as shown in Figures 2-31 and 2-32 and at an elevation of 10.7 m (35 ft). The water cannon height during fire tests differed from the flow testing because of the height restriction imposed by the 20-MW calorimeter. The water cannon flow rate was 230 lpm (60 gpm) for the first test resulting in an effective distribution area of approximately 9.3 m² (100 ft²) with an estimated average flux of 24 mm/min (0.6 gpm/ft²). The water cannon response time was set to 40 s with a pre-set targeting accuracy. As indicated in Section 2.2.1, the conservative response time was selected based on past testing of water cannons showing response times varying from 11 to 39 s [3]. The targeting accuracy of the spray was based upon the requirements in FM Approval standard 1421 [4]. The array was ignited using one standard FM Global ignitor placed under the center of the second pallet load in the middle row as shown in Figure 2-31. An FM Global standard ignitor is a 150 mm (6 in.) cylinder of rolled cellucotton, soaked in 240 ml (8 oz) of gasoline. This ignition location was selected to represent a challenging deep-seated fire scenario where the fire is shielded from the water spray by the storage above.
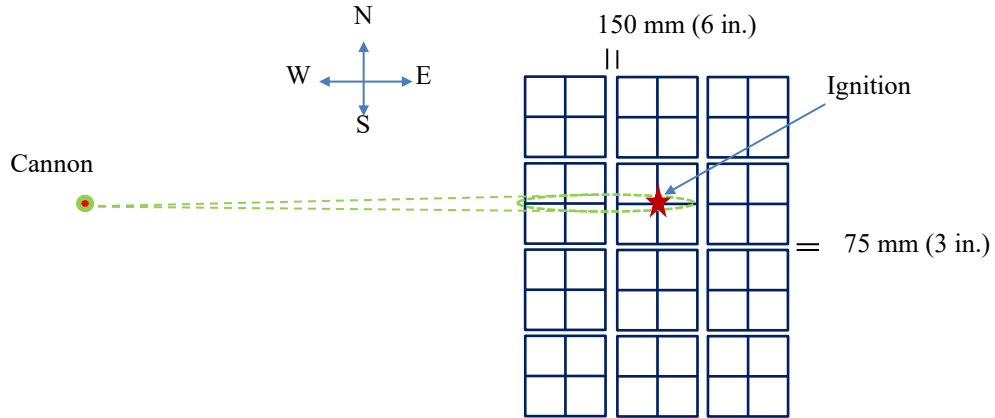
Figure   2-31: Plan view of the AWC fire suppression test layout.

For the case of control of a fire of low-piled storage in an HC-3 occupancy under a 9.1 m (30 ft) high ceiling, Table 2-12 presents the comparison of water demand between traditional ceiling-level sprinkler protection [6], the SMART sprinkler and the water cannon. The water demand of traditional ceiling-level sprinklers is defined in DS 3-26 [6] as 2,800 lpm (750 gpm) for standard sprinklers with a water flux of 12 mm/min (0.3 gpm/ft^2) to cover an area of 230 m^2 (2,500 ft^2) for adequate protection. The water demand of the SMART sprinklers was estimated from the number of sprinklers operations as 570 lpm (150 gpm) for five operations, or 1,000 lpm (270 gpm) for nine operations based on fire tests. Compared to traditional ceiling-level sprinklers, the water cannon used only 230 lpm (60 gpm) to control the fire of the HC-3 occupancy, for a water reduction of 92%. This suggests that the AWC system with targeted water delivery can be more efficient than SMART sprinklers in terms of water demand.
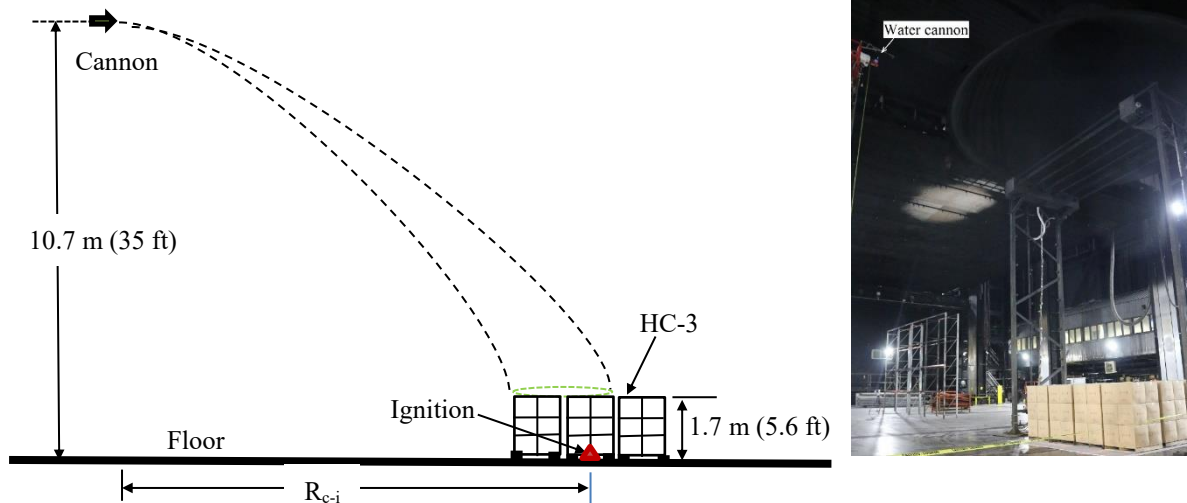
Figure   2-32: Elevation view of the AWC fire suppression test layout.

Table   2-12: Water demand for SMART sprinklers and AWC compared to traditional ceiling sprinkler protection for low-piled HC-3 occupancies under a 9.1 m (30 ft) high ceiling.

	Water demand lpm (gpm)	Reduction compared to DS 3-26
DS 3-26	2,800 (750)	NA
SMART	570 (150) for 5 sprinklers or 1,000 (270) for 9 sprinklers	80% or 64%
AWC	230 (60)	92%

As shown in Table 2-9 for the stream trajectory, the horizontal delivery distance of the stream was 13 m (43 ft) at the flow rate of 230 lpm (60 gpm). If the water cannon can be rotated 360° in azimuthal angle with 13 m (43 ft) as a radius, the theoretical coverage area of one water cannon placed at the center of a square space is 340 m^2 (3,700 ft^2). Assuming 9.3 m^2 (100 ft^2) coverage are per ceiling sprinkler, this suggests that in theory one water cannon can replace 37 ceiling sprinklers to protect the same area.

To cover a larger area, the water cannon flow rate (or water demand) can be increased to reach farther. Roughly, the delivery distance increases linearly with the flow rate, as shown in Table 2-9. At a high flow rate of 680 lpm (180 gpm), the horizontal delivery distance is 36 m (120 ft), which means that in theory a square area of 2,600 m^2 (28,000 ft^2) can be covered or 280 ceiling sprinklers can be replaced. When the water cannon is operated at 680 lpm (180 gpm) to cover a larger area, the water demand is reduced by 76% in comparison to traditional ceiling-level sprinklers.

To improve reliability, one more additional water cannon can be installed to protect the same area. This redundancy in design will increase the installation and maintenance costs but may not change the water demand. Generally, the system could be designed to operate only one water cannon for a given fire event. If two cannons are operated simultaneously, the water demand will be doubled with the same discharge time. At the flow rate of 230 lpm (60 gpm) per cannon, the water demand of two cannons would still be 84% less than that of traditional ceiling-level sprinklers.

2.2.3.1   Effect of Targeting Accuracy

Test 2 and Test 3 were conducted to target the fire on different locations so that the fire zone could be fully or partially covered by water. As shown in Figure 2-33, the stream head in Test 2 targeted the ignition location at the floor level with R_{c-i} = 10.7 m (35 ft), while Test 3 targeted the fire appeared on the top surface of the fuel array with a shorter R_{c-i} = 9.8 m (32 ft). Except for this difference in target location, the two tests had the same experimental conditions using a water flow rate of 230 lpm (60 gpm), height of 10.7 m (35 ft) above the floor, and elevation angle of 0°. Both tests used horizontal sweeping with a range of 12° in azimuthal angle and a cycle time of 15.9 s, see Figure 2-29.

Test 2	Test 3
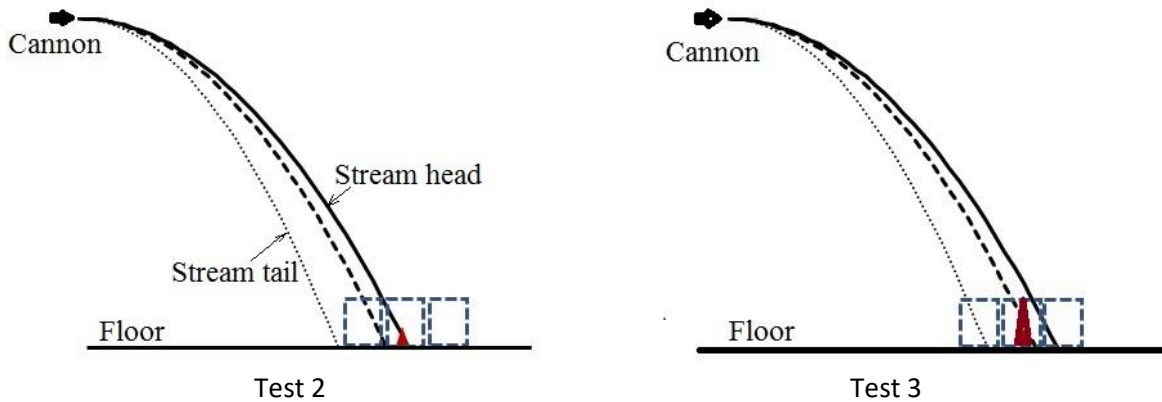
Figure   2-33: Elevation view of AWC fire Tests 2 and 3 showing the stream head targeting on the ignition zone.

The fire development for the two tests was similar during the incipient stage but differed after water application. After ignition, the flame was visible out the top of the fuel array at about 2 min; this time with the flame visible to the water cannon is denoted as t_f. Once the flame becomes visible, an AWC system would be triggered to detect, target and deliver water to the fire with a response time depending on the specific system. This automatic response process was simulated in this work by pre-setting the response time to 40 s such that water application occurred at t_f + 40 s or 3 min from ignition. In Test 2, the stream head impinged on the top-right corner of the middle fuel array with an inclined angle. The upward fire plume was pushed to the left side due to the air flow induced by the water stream. At 4 min from ignition, the fire was almost invisible under the water application. However, it was observed that most of the water discharge was blocked by the middle stack of the fuel array, except for the water splashing on the top surface. The fire zone was partially covered by water; therefore, the fire propagated slowly to the left side of the fuel array. At 11 min from ignition, the fire started to grow again. At 21 min, a large uncontrolled fire was visible, and fire spread to the other end of the fuel array. The test was terminated, and the fire was extinguished manually at 21 min. In Test 3, which moved the water cannon 0.9 m (3 ft) closer to the fuel array changing the targeting area, the fire was controlled after water application. Figure 2-34 shows the fire development in Test 2 that resulted in an uncontrolled fire.

3 min	4 min
11 min	21 min
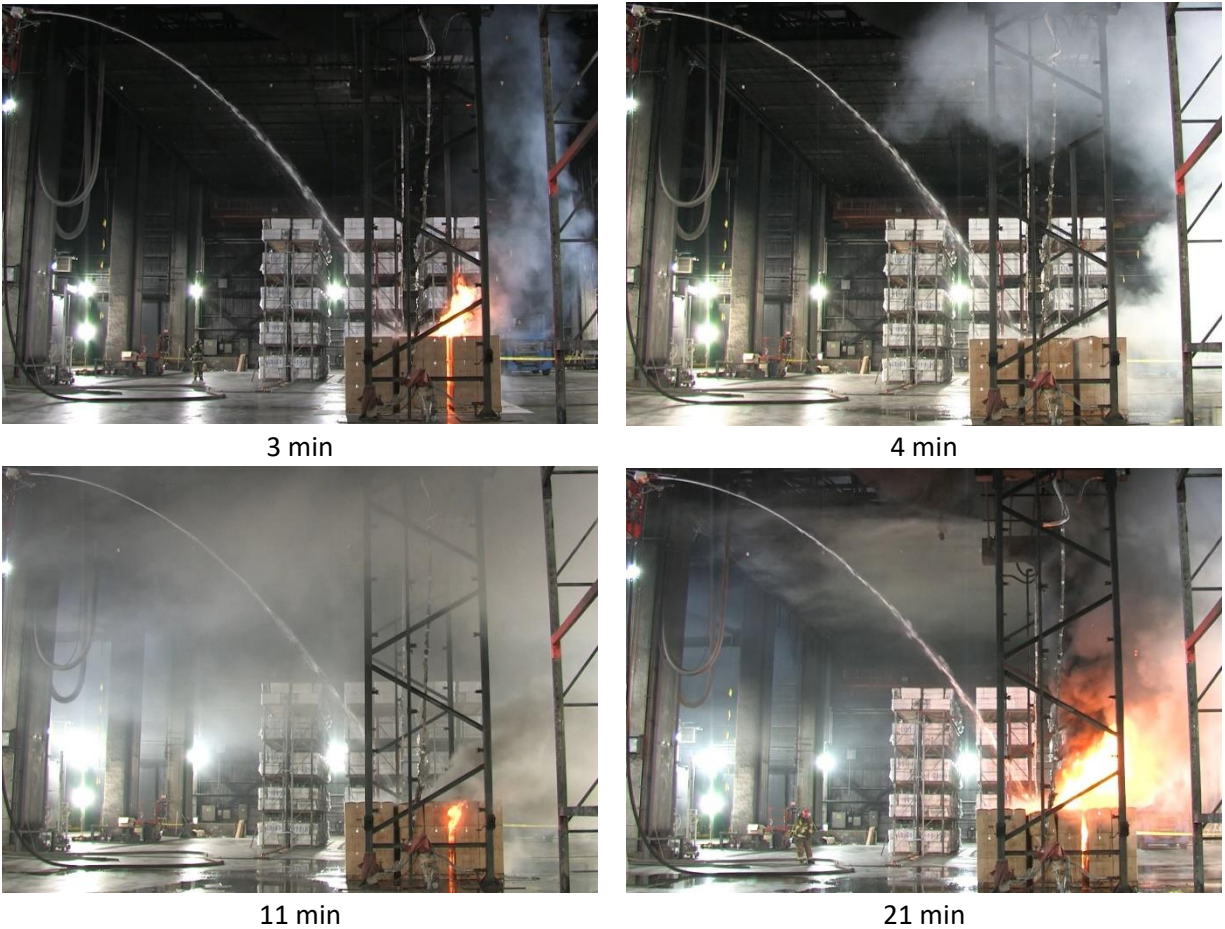
Figure   2-34: AWC Test 2 fire development at four instances from ignition.

The chemical heat release rates (HRR) based on CO_2/CO calorimeter measurements for Tests 2 and 3 are compared in Figure 2-35. The arrows in the figure mark the time of water application and test termination. After the water cannon was activated at about 3 minutes from ignition, the figure shows that the fast HRR growth in the two tests decreased rapidly. The low HRR values were maintained throughout Test 3 during the water application; however, in Test 2 the HRR started to increase again around 10 min from ignition. The fire in Test 2 continued to grow to 5 MW by 21 min at which point the test was terminated. The flame spread beyond the ignition location in Test 2 led to the increase in HRR observed later in the test. Test 2 resulted in an uncontrolled fire because the water cannon spray did not fully cover the initial fire zone and was not adjusted to respond to changes in its location. Test 3 resulted in a controlled fire due to the improved targeting accuracy which fully covered the fire zone with water.
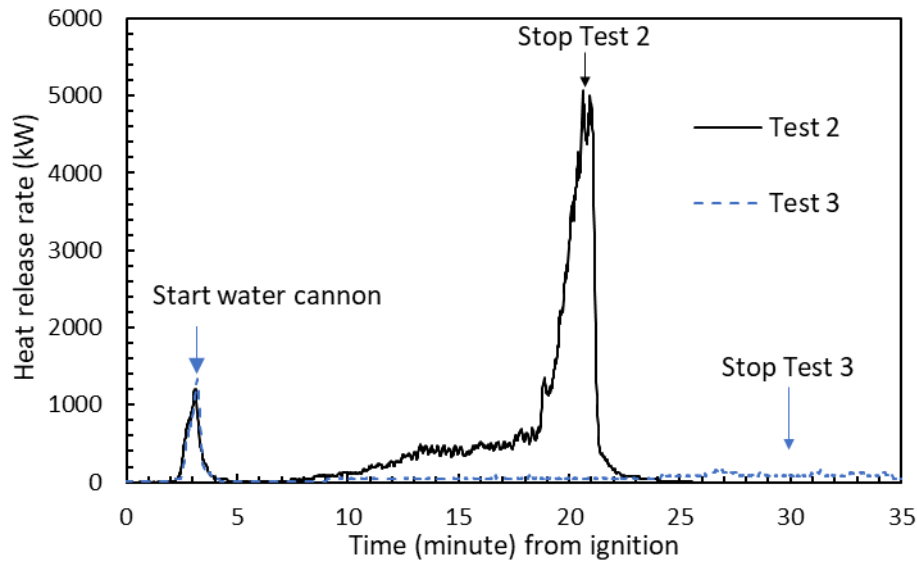
Figure   2-35: AWC fire Test 2 and 3 chemical heat release rates (HRR).

2.2.3.2   Effect of Water Flux on Fire

The effective water flux delivered to the fire zone is important to the final suppression result. Generally, as described in Eq. 2-1, the fire can be controlled if the effective water flux is higher than the CDF for the commodity protected. Test 1 used a wide fog spray pattern for the AWC which is similar to that of the ceiling sprinkler, except the interaction angle between the fire and the spray is different. The flow rate of 230 lpm (60 gpm) delivered over an area of 9.3 m^2 (100 ft^2) resulted in an effective density of 24 mm/min (0.6 gpm/ft^2). The targeting of the AWC resulted in the ignition location being in the center of the water coverage area. Figure 2-36 shows the chemical and convective HRRs measured in Test 1. Note that the calorimeter has a capacity of 20-MW in convective HRR; therefore, any measured convective HRRs (or corresponding chemical HRRs) below 200 kW (1% of the calorimeter capacity) are beyond the uncertainty range. The HRR curves show a fast growth during the freeburn period followed by a rapid drop after the water cannon was activated. The low HRR values were maintained during the water application, suggesting a controlled fire. However, after the water cannon was shut off approximately 30 min after ignition, the HRRs increased again as the fire had not been extinguished.

When the water cannon was changed from a wide fog to a solid stream, the water delivery distance had to be increased from 9.7 m (32 ft) to 13.4 m (44 ft). This suggests that the protection area of the water cannon increased. The penetration ability of the stream through the fire was also improved in comparison to the fog spray. However, it is difficult to target a solid stream accurately on a fire due to the narrow head. Therefore, narrow-angle sweeping is utilized to increase the water coverage area and to relax the fire targeting accuracy. As shown in Test 2, the horizontal sweeping alone does not make it easier to target the fire in the streamwise direction. Therefore, the water cannon design allows sweeping in both horizontal (spanwise) and vertical (streamwise) directions which was examined in other tests.
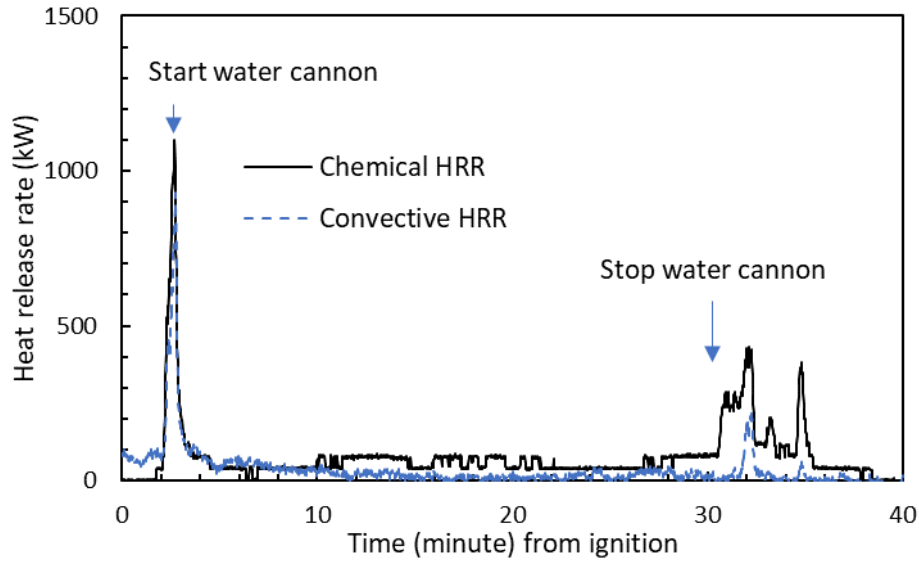
Figure 2-36: AWC Test 1 chemical and convective heat release rates (HRR).

Figure 2-37 shows the horizontal/vertical sweeping patterns employed for the fire tests using either six or nine points. As shown in Fig. 2-37(a) for six points, the sweeping cycle started from 1 to 2 and then rotated back to 1 in the horizontal direction. Afterwards, the cannon was rotated from 1 to 3 vertically, 3 to 4 horizontally, 4 to 5 vertically, 5 to 6 horizontally, and finally rotated back from 6 to 1 in the vertical direction. The total time of this sweeping cycle was 18.7 s. Due to limited control over the gear system, the sweeping speed was not uniform during the entire cycle. Figure 2-37(a) also shows the fraction of the sweeping time from one point to the others, and the pause duration on each point.

(a)

(b)
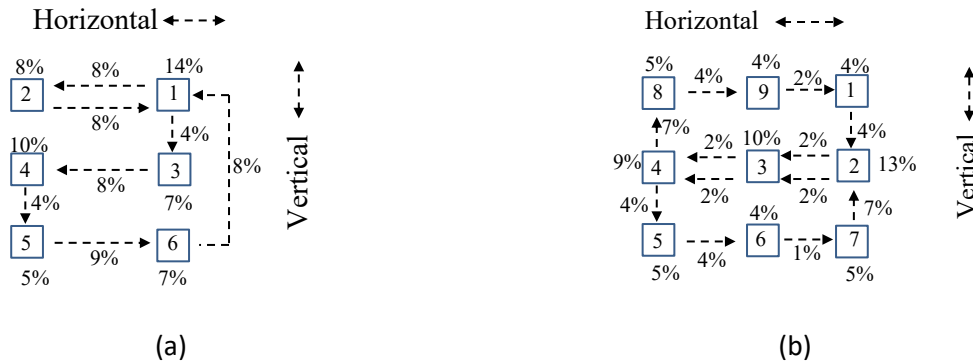
Figure 2-37: AWC horizontal and vertical sweeping patterns using 6 points (a) and 9 points (b) with the sweeping time fraction denoted for each subprocess.

To improve the uniformity of water flux distribution, additional points were added in the center of the horizontal sweep. Figure 2-37(b) shows the sweeping conducted through nine points. The sweeping cycle started from 1 to 2 in the vertical direction, and then rotated from 2 to 3 in the horizontal direction. The three points 3, 6 and 9 were added in the center of the horizontal sweeps. Afterwards, the cannon was rotated from 3 → 4 → 5 → 6 → 7, and then 7 → 2 → 3 → 4 → 8→ 9, and finally rotated

back from 9 to 1 in the horizontal direction. The total time of this sweeping cycle was 27.2 s. It should be noted that points 2, 3 and 4 were targeted two times in a sweeping cycle.

Six-point sweeping was used in Tests 4 to 6. Figure 2-38 shows the water flux distribution on the top surface of the fuel array for Test 4. These values were estimated from the water flux of a solid stream (see Figure 2-27) by calculating the sweeping time relative to different locations (or containers). The coordinate R in Figure 2-38 denotes the horizontal distance from the cannon in the streamwise direction, and y denotes the width of the water coverage area with horizontal sweeping in the spanwise direction. The sweeping range was 12° in azimuthal angle and -9° < θ < 6° in elevation angle. Test 4 used an R_{c-i} distance of 9.8 m (32 ft) and a water flow rate of 230 lpm (60 gpm). The total water flux averaged over the entire area as shown in Figure 2-38 was approximately 15 mm/min (0.37 gpm/ft^2). The star in the figure marks the ignition location.
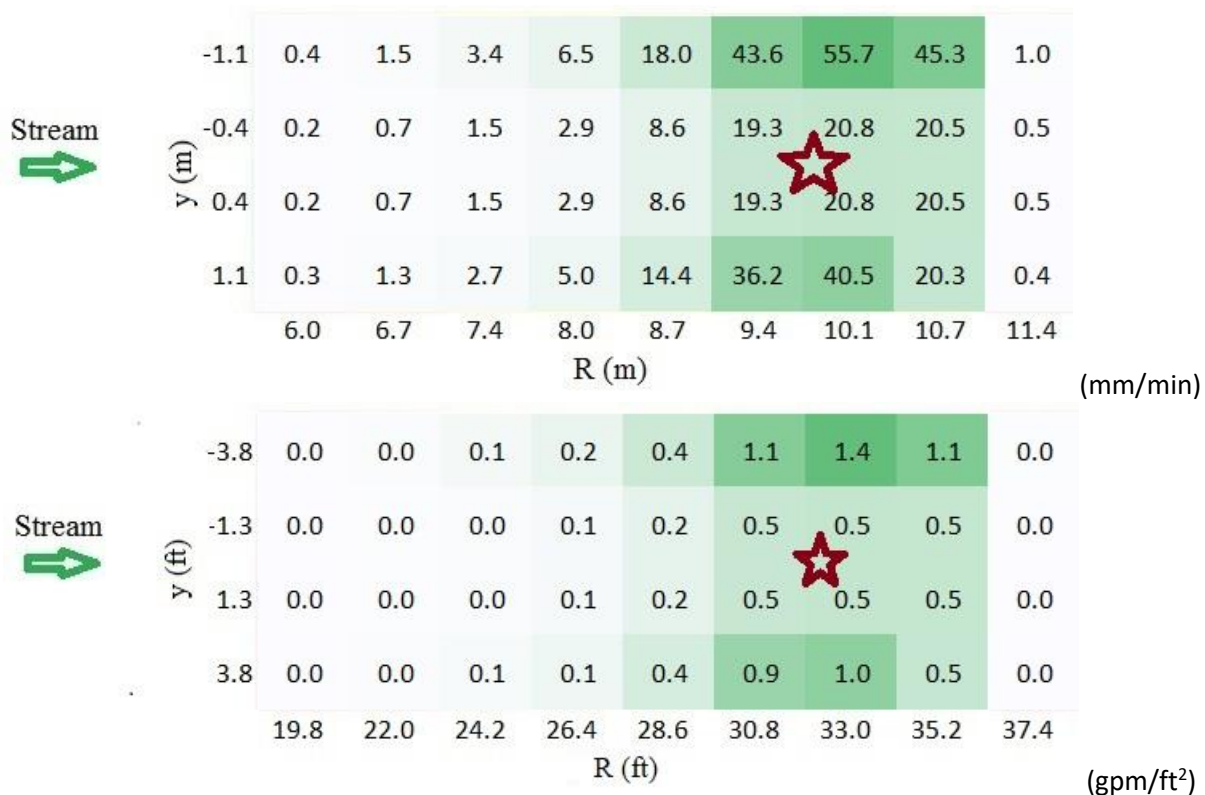
Figure 2-38: AWC Test 4 estimated water flux (mm/min [gpm/ft^2]) distribution on the top surface of the fuel array with six-point sweeping and water flow rate of 230 lpm (60 gpm).

Figure 2-38 shows that the ignition location was accurately targeted (or fully covered) by the water cannon in Test 4; however, the water delivery of a solid stream with sweeping was not uniform. The average flux on a localized spot (or a container) depends on the intermittent and unsteady water delivery imposed by the mechanical sweeping motion and the time fraction during which the sweeping stream is at a position. As shown in Figure 2-38, the water flux distribution was lower at the center, in the vicinity of the ignition zone, and highest on both sides along the spanwise direction. This is because

the cannon stayed a relatively longer time (or delivered more water) on the locations corresponding to the six sweeping points than the areas between the points.

To quantify the targeting accuracy and the water flux distribution around the fire, the method in FM Approval Standard 1421 [4] is used in this work to analyze the test results. The coordinate of the spray center (R_c, Y_c) is calculated as

$$R_c = \frac{\sum V_{i,j} R_i}{\sum V_{i,j}} \quad \text{and} \quad Y_c = \frac{\sum V_{i,j} y_j}{\sum V_{i,j}},$$

2-5

where V_{ij} is the water volume collected in the pan (i, j) with coordinate of (R_i, y_j). The spray area radius is calculated as

$$\text{spray area radius} = \left(\frac{1}{R_{max} - R_{min}} + \frac{1}{y_{max} - y_{min}} \right)^{-1},$$

2-6

where R_{max} and y_{max} are the maximum R or y coordinate of a pan with measurable and significant water flux, and R_{min} and y_{min} are the minimum R or y coordinate, respectively. The measurable and significant water flux is defined as 4.1 mm/min (0.1 gpm/ft^2).

For the water distribution shown in Figure 2-38, the spray center coordinate was calculated to be [9.7, -0.1 m (32, -0.4 ft)] and the spray area radius was 1.2 m (4 ft). The spray center was very close to the ignition location [9.8, 0 m (32, 0 ft)]. Therefore, Test 4 met the requirement for targeting accuracy that the distance from the calculated center of spray to the target location shall be no greater than half of the spray area radius. In the circle around the ignition location with a radius of 0.6 m (2 ft) the average flux was approximately 20 mm/min (0.5 gpm/ft^2) for Test 4, which is higher than the CDF value. Therefore, given the low HRRs shown in Figure 2-39, the fire of Test 4 was controlled by the water cannon with six-point sweeping at the flow rate of 230 lpm (60 gpm). After the water cannon was shut off at 30 min from ignition, the HRR increased again because the fire was not fully extinguished.
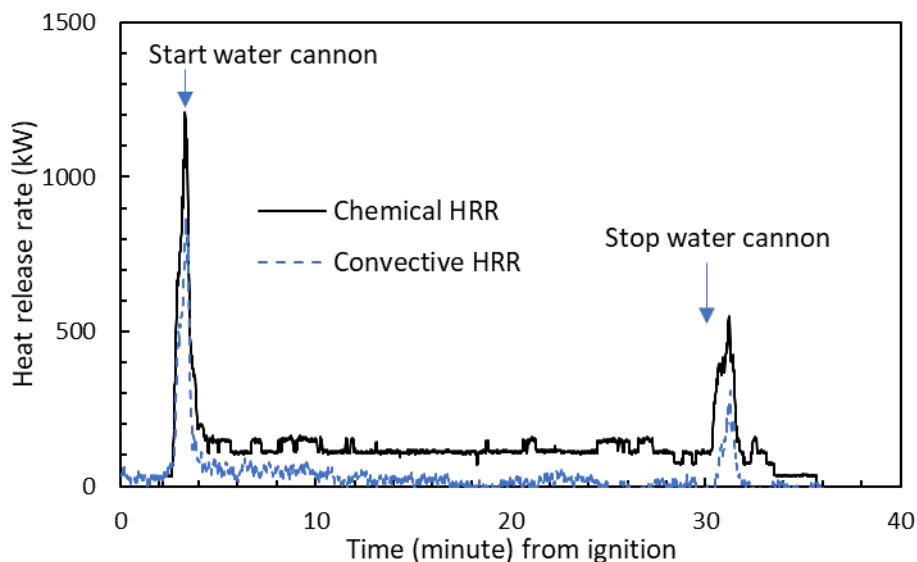
Figure   2-39: AWC Test 4 chemical and convective heat release rates (HRR).

A higher flow rate of 450 lpm (120 gpm) was applied in Tests 5 to 7 with varied delivery distance and sweeping patterns (Table 2-11). The fires of the three tests were all controlled by the water cannon due to the doubled flow rate. However, when Test 5 was conducted with a strong water stream at a close distance of R_{c-i} = 9.8 m (32 ft), the burning objects were pushed away from the fire origin, which did not, but could have, resulted in additional fire spread. Figure 2-40 shows two images of Test 5 recorded at different times from ignition. At 2 min and 48 s, the water cannon was activated to deliver water in a stream pattern and a low elevation angle on the fuel array. After 3 min, the fire was almost invisible, and about nine cartons stored on the front side of the fuel array were pushed to the floor by the water stream. Fortunately, these cartons had not ignited so that there was no additional fire spread.

| 2 min 48 s | 6 min |

Figure   2-40: AWC Test 5 fire development at 2 min and 48 s and at 6 min from ignition.

To reduce the impingement momentum of the stream on the cartons, Tests 6 and 7 were conducted after moving the cannon farther away to a horizontal distance of R_{c-i} = 16.5 m (54 ft). However, the water coverage area becomes larger with a longer R_{c-i} for the same six-point sweeping. A container located in the areas between two sweeping points may collect less water because the total time fraction allocated to the region does not change. Therefore, the uneven flux distribution as shown in Figure 2-38 was increased for the locations corresponding to the six sweeping points and those areas between the points. For Test 6, a low average flux of 8 mm/min (0.2 gpm/ft^2) was delivered to the ignition zone with a circular radius of 1.15 m (3.8 ft), which was in the center between the locations corresponding to the sweeping points. Therefore, a small fire was observed in Test 6 to continue for about 7 min in the ignition zone after the water cannon was activated. Because a higher water flux was delivered to the region outside the ignition zone, the fire in Test 6 was still ultimately controlled, and did not propagate to either end of the fuel array.

Nine-point sweeping as shown in Fig. 2-37(b) was used in Test 7 to improve the distribution uniformity, especially for the region between the sweeping points in the spanwise direction. Using the same flow rate of 450 lpm (120 gpm) as that in Test 6, Test 7 had a higher water flux of 12 mm/min (0.3 gpm/ft^2) delivered to the circle around the ignition location with a radius of 1.3 m (4.3 ft). This flux equaled the CDF value, which resulted in a controlled fire.

Test 8 was conducted at an increased flow rate of 680 lpm (180 gpm). The distance R_{c-i} between the cannon and the ignition zone was also increased to 27.4 m (90 ft). However, this long separation exceeded the distance between the 20-MW calorimeter and the west side wall of the LBL. To conduct the test, the fuel array of Test 8 was moved to the location under the center of the north movable ceiling. The ceiling height above the floor was 15 m (50 ft).

Test 8 was designed to use the same range of the sweeping angle as that of Test 7, which was 12° in azimuthal angle and -10° < θ < 0° in elevation angle for nine-point sweeping. Because the same angle range was used for a high value of the distance R_{c-i}, the water coverage area was increased. Figure 2-41 shows the water flux distribution estimated on the top surface of the fuel array. The total water flux averaged over the entire area is approximately 5.8 mm/min (0.14 gpm/ft^2).

Stream → y (m)	13.4	14.0	14.6	15.2	15.8	16.5	17.1	17.7	18.3	18.9	19.5	20.1	20.7	21.3	21.9	22.6	23.2	23.8	24.4	25.0	25.6	26.2	26.8	27.4	28.0	28.7	29.3	29.9	30.5	31.1
-3.0	2.9	3.4	3.8	4.1	4.9	5.8	6.5	7.2	8.0	9.1	10.1	11.7	13.2	15.2	17.6	22.5	27.5	25.0	22.6	23.9	25.6	31.4	35.4	19.5	8.9	8.9	9.0	10.5	10.9	4.1
-2.3	0.2	0.3	0.3	0.3	0.4	0.4	0.5	0.6	0.6	0.7	0.8	0.9	1.0	1.2	1.4	1.8	2.2	1.6	1.3	1.6	1.9	2.9	3.7	1.7	0.5	0.6	0.7	1.2	1.5	0.6
-1.5	0.2	0.3	0.3	0.3	0.4	0.4	0.5	0.6	0.6	0.7	0.8	0.9	1.0	1.2	1.4	1.8	2.2	1.6	1.3	1.6	1.9	2.9	3.7	1.7	0.5	0.6	0.7	1.2	1.5	0.6
-0.8	0.2	0.3	0.3	0.3	0.4	0.4	0.5	0.6	0.6	0.7	0.8	0.9	1.0	1.2	1.4	1.8	2.2	1.6	1.3	1.6	1.9	2.9	3.7	1.7	0.5	0.6	0.7	1.2	1.5	0.6
0.0	1.7	1.9	2.2	2.3	2.8	3.3	3.8	4.2	4.6	5.2	5.8	6.8	7.7	8.9	10.4	14.2	17.0	11.8	8.7	10.6	13.0	19.5	24.6	11.7	3.2	4.0	4.9	7.7	9.9	4.0
0.8	0.3	0.4	0.4	0.5	0.6	0.7	0.8	0.9	1.0	1.1	1.2	1.4	1.6	1.9	2.3	3.3	4.0	2.4	1.3	1.6	1.9	2.8	3.4	1.9	1.0	1.2	1.5	2.3	3.0	1.2
1.5	0.3	0.4	0.4	0.5	0.6	0.7	0.8	0.9	1.0	1.1	1.2	1.4	1.6	1.9	2.3	3.3	4.0	2.4	1.3	1.6	1.9	2.8	3.4	1.9	1.0	1.2	1.5	2.3	3.0	1.2
2.3	0.3	0.4	0.4	0.5	0.6	0.7	0.8	0.9	1.0	1.1	1.2	1.4	1.6	1.9	2.3	3.3	4.0	2.4	1.3	1.6	1.9	2.8	3.4	1.9	1.0	1.2	1.5	2.3	3.0	1.2
3.0	2.4	2.8	3.2	3.6	4.2	5.0	5.7	6.3	7.0	7.9	8.8	10.1	11.5	13.3	15.5	20.1	24.4	20.4	17.6	19.3	21.4	26.8	31.1	20.5	12.9	12.6	12.3	13.2	12.4	4.4

R (m)

(mm/min)

Stream → y (ft)	44	46	48	50	52	54	56	58	60	62	64	66	68	70	72	74	76	78	80	82	84	86	88	90	92	94	96	98	100	102
-10.0	0.07	0.08	0.09	0.10	0.12	0.14	0.16	0.18	0.20	0.22	0.25	0.29	0.32	0.37	0.43	0.55	0.67	0.61	0.55	0.59	0.63	0.77	0.87	0.48	0.22	0.22	0.22	0.26	0.27	0.10
-7.5	0.01	0.01	0.01	0.01	0.01	0.01	0.01	0.01	0.01	0.02	0.02	0.02	0.03	0.03	0.03	0.04	0.05	0.04	0.03	0.04	0.05	0.07	0.09	0.04	0.01	0.01	0.02	0.03	0.04	0.01
-5.0	0.01	0.01	0.01	0.01	0.01	0.01	0.01	0.01	0.01	0.02	0.02	0.02	0.03	0.03	0.03	0.04	0.05	0.04	0.03	0.04	0.05	0.07	0.09	0.04	0.01	0.01	0.02	0.03	0.04	0.01
-2.5	0.01	0.01	0.01	0.01	0.01	0.01	0.01	0.01	0.01	0.02	0.02	0.02	0.03	0.03	0.03	0.04	0.05	0.04	0.03	0.04	0.05	0.07	0.09	0.04	0.01	0.01	0.02	0.03	0.04	0.01
0.0	0.04	0.05	0.05	0.06	0.07	0.08	0.09	0.10	0.11	0.13	0.14	0.17	0.19	0.22	0.26	0.35	0.42	0.29	0.21	0.26	0.32	0.48	0.60	0.29	0.08	0.10	0.12	0.19	0.24	0.10
2.5	0.01	0.01	0.01	0.01	0.01	0.02	0.02	0.02	0.02	0.03	0.03	0.04	0.04	0.05	0.06	0.08	0.10	0.06	0.03	0.04	0.05	0.07	0.08	0.05	0.02	0.03	0.04	0.06	0.07	0.03
5.0	0.01	0.01	0.01	0.01	0.01	0.02	0.02	0.02	0.02	0.03	0.03	0.04	0.04	0.05	0.06	0.08	0.10	0.06	0.03	0.04	0.05	0.07	0.08	0.05	0.02	0.03	0.04	0.06	0.07	0.03
7.5	0.01	0.01	0.01	0.01	0.01	0.02	0.02	0.02	0.02	0.03	0.03	0.04	0.04	0.05	0.06	0.08	0.10	0.06	0.03	0.04	0.05	0.07	0.08	0.05	0.02	0.03	0.04	0.06	0.07	0.03
10.0	0.06	0.07	0.08	0.09	0.10	0.12	0.14	0.16	0.17	0.19	0.22	0.25	0.28	0.33	0.38	0.49	0.60	0.50	0.43	0.47	0.53	0.66	0.76	0.50	0.32	0.31	0.30	0.32	0.30	0.11

(gpm/ft^2)

Figure 2-41: Test 8 water flux (mm/min) distribution on the top surface of the fuel array with nine-point sweeping and water flow rate of 680 lpm (180 gpm).

Clearly, the water flux distribution was not uniform in this large coverage area even with nine-point sweeping. Figure 2-41 shows that the water flux at the locations corresponding to the nine sweeping points was higher than for the areas between the points due to the sweeping intermittency. The spray center coordinate was calculated to be [25, 0 m (82, 0 ft)] and the spray area radius was 5.1 m (16.6 ft). The distance between the spray center and the ignition location [27.4, 0 m (90, 0 ft)] was 2.4 m (8 ft), which is close to half of the spray area radius. The fire was reasonably targeted by the water cannon in Test 8. In a circle around the ignition location with a radius of 2.5 m (8.3 ft), the average flux was approximately 3.8 mm/min (0.09 gpm/ft^2). The overall average water flux was 5.8 mm/min (0.14 gpm/ft^2) which was also low. The fire in Test 8 is shown in Figure 2-42 at 6 min after ignition. Note that the HRR could not be measured accurately for the fire under the movable ceiling. The water cannon

with a flow rate of 680 lpm (180 gpm) was activated at 3 min 40 s from ignition. After 2 min and 20 s of water application, Figure 2-42 shows the fire size was not reduced by the water cannon with nine-point sweeping. This is because the applied water flux in the ignition zone was too low to control the fire. Several cartons were also found to be pushed out from the fuel array by the water stream. The fire continued to propagate to the far side of the fuel array and was ultimately extinguished by firefighters.

Figure   2-42: AWC Test 8 fire at 6 min from ignition.

Test 8 used the highest flow rate tested but resulted in a low water flux on the target due to a significantly increased coverage area. This low water flux can be increased by reducing the sweeping angle to narrow the coverage area. If the obtained water flux in the ignition zone had been higher than the CDF value, based on the above analysis of Tests 1 and 4 to 7, it is reasonable to expect that the fire of Test 8 would have been controlled by the water cannon with the high flow rate of 680 lpm (180 gpm).

2.2.3.3   Effect of Response Time

When the flame becomes visible, an AWC system needs a certain amount of time to detect, target and deliver water to the fire. As indicated, this response time was set at 40 s in fire suppression tests 1 to 8. To examine the impact of a slow response case, a longer time of 60 s was pre-set in Test 9. As listed in Table 2-11, Test 9 was conducted under the 20-MW calorimeter at a flow rate of 230 lpm (60 gpm) and a horizontal distance (R_{c-i}) of 9.8 m (32 ft) with nine-point sweeping. Test 9 was pre-set so the water cannon targeted the fire accurately. In a circle around the ignition location with a radius of 0.8 m (2.7 ft), the average flux was approximately 16 mm/min (0.4 gpm/ft^2), which is higher than the CDF value. Note that Test 9 was comparable to Test 4, except for the delayed activation and the different sweep pattern.

Figure 2-43 shows the chemical and convective HRRs measured in Test 9. Because of the slow response, the water cannon was activated at a higher chemical HRR value of 2 MW in comparison to the other tests. However, the HRR still decreased rapidly to a low value with water application. This is because the applied water flux is sufficient for fire control. As shown in Figure 2-43, the slow response with a longer

time of 60 s did not change the fire control results given that the applied water flux was sufficient to cover the fire zone.
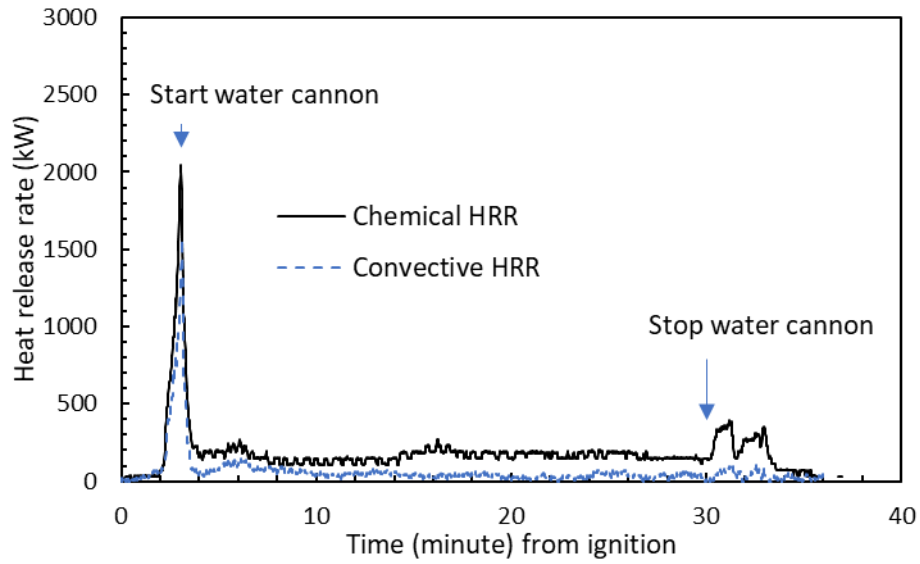
Figure   2-43: AWC Test 9 chemical and convective heat release rates (HRR).

3. **High-Bay Rack Storage**

The use of high rack-storage arrangements is increasing in commercial and warehouse facilities, a trend which places further strain on the water supply required to provide adequate fire protection with traditional ceiling-only automatic sprinkler systems. Depending on the storage configuration utilized at a facility, the protection guidance could call for systems consisting of ceiling-only sprinklers or a combination of ceiling and in-rack sprinkler systems. The ceiling-only option is typically preferred to avoid installations of in-rack systems which can complicate the overall system, increase installation costs and most importantly limit storage flexibility.

Table   3-1:   Summary of test parameters and results for SMART sprinkler protection of high-bay storage of CUP.

	Test ID	1
TEST PARAMETERS	**Test Date**	9/24/2018
	Movable Ceiling Test Site	South
	Ceiling Height, m (ft)	13.7 (45)
	Test Commodity / Fuel	CUP
	Storage Arrangement	Rack storage
	Main Array Size, pallet loads	2 × 8
	Targets (3), pallet loads	1 × 6 x 8
	Nominal Storage Height, m (ft)	11.9 (39)
	Aisle Width, m (ft)	1.2 (4)
	Ignition Location	Between 2
	Sprinkler Orientation	Pendent (QR deflector)
	Sprinkler K-factor, L/min/bar$^{\frac{1}{2}}$ (gpm/psi$^{\frac{1}{2}}$)	200 (14)
	Sprinkler Spacing, m x m (ft x ft)	3 × 3 (10 × 10)
	Discharge Pressure, bar (psi)	2.3 (33)
	Discharge Density, mm/min (gpm/ft^2)	32.6 (0.8)
TEST RESULTS	**Time of Water Delivery to Open Sprinklers, min:s**	1:02
	Highest Ceiling Temperature beyond Open Sprinklers at Locations of Neighboring Sprinklers, ºC (ºF)	57 (134)
	Peak Steel Temperature, ºC (ºF)	62 (144)
	Target Array Ignited	No
	Test Duration, min	40

When this project was initiated, the ceiling-only protection options provided within Data Sheet 8-9, *Storage of Class 1, 2, 3, 4 and Plastic Commodities* (DS 8-9) [11] for the storage of CUP were limited to maximum ceiling heights of 13.7 m (45 ft). At this ceiling height, protection guidance per DS 8-9 [11] states that the water demand should be a minimum of 72.5mm/min (1.78 gpm/ft^2) with 12 sprinkler operations, or 8,100 lpm, using either a K360 (K25.2) or K320 (K22.4) sprinkler. This water requirement

can be challenging for regions with limited water resources. Therefore, the use of SMART sprinklers in combination with in-rack linear heat detection was investigated to provide alternative protection guidance at ceiling heights of 13.7 m (45 ft) or greater.

A full-scale fire test was conducted to compare the required water demand to the current FM Global guidance for ceiling-only protection. The test parameters and results are summarized in Table 3-1. The results showed that, for ceiling protection under a 13.7 m (45 ft) ceiling in combination with linear LHDs in the rack, the water demand was reduced by 77% when compared to traditional ceiling-only protection.
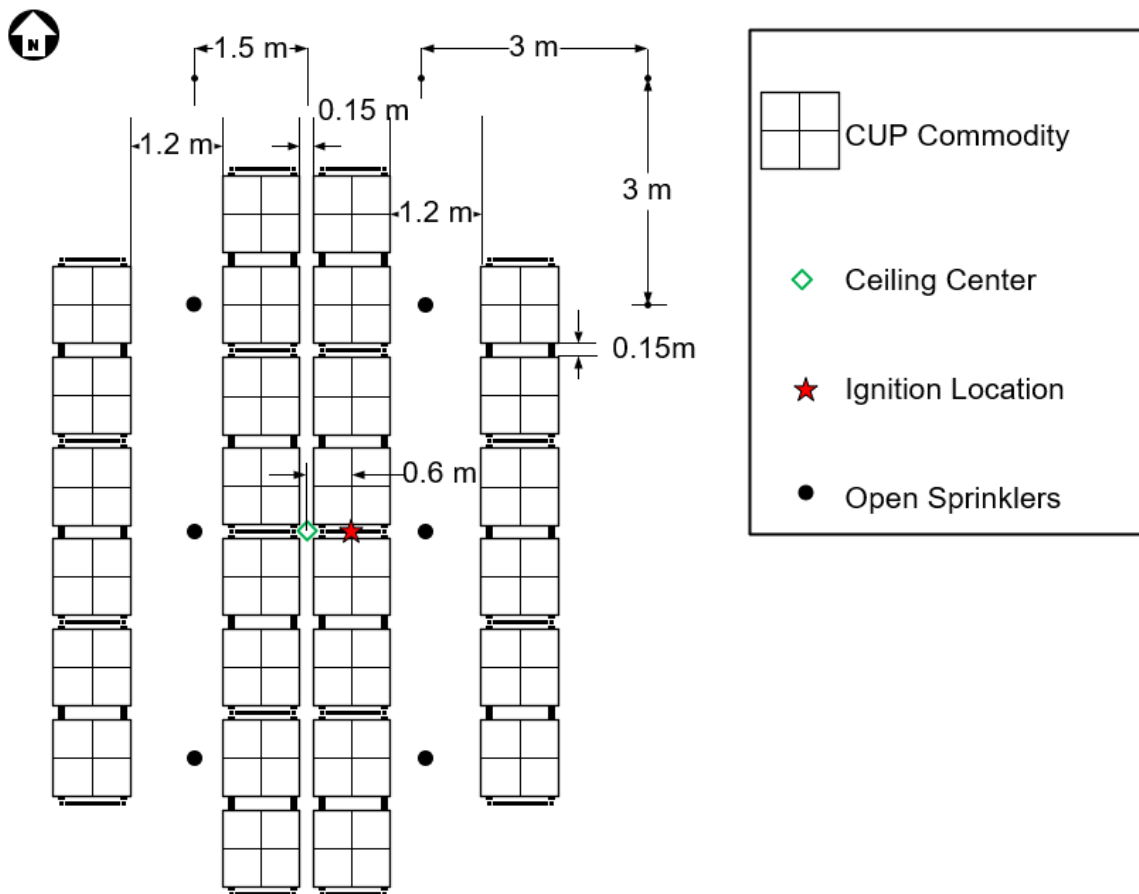
Figure   3-1:   Plan view of SMART sprinkler protection of high-bay rack-storage test.

3.1   Experimental Setup

The test array consisted of 12.2 m (40 ft) CUP commodity under a 13.7 m (45 ft) ceiling with a main array that was eight pallet loads long and two wide and two target arrays across 1.2 m (4 ft) aisles that were six pallet loads long and one wide. The flue spaces throughout the array were nominally 150 mm (6 in.) and the entire test array was centered under the ceiling with ignition offset to the east 0.6 m (2 ft). This resulted in a between 2 scenario for ignition with respect to the ceiling sprinklers. Ignition was achieved with two FM Global standard half ignitors that were placed on the floor to either side of the rack upright

between the rack support and the pallets. Elevation and plan views of the test setup are shown in Figures 3-1 and 3-2, respectively.

Ceiling-only protection was provided by simulated SMART sprinklers using linear heat detectors (LHDs) in the rack located at half the height of the array, fourth tier. The LHDs were used to determine if the activation time could be improved compared to the FM Global SMART algorithm while at the same time offering a higher threshold for detection to avoid false trips and ventilation effects. The SMART sprinkler activation was simulated with a localized deluge system as was done in the low-pile storage testing with six open sprinklers at pre-determined locations. The ceiling density for each test was determined by using the previous SMART sprinkler testing [1, 2] to extrapolate the required densities at the higher storage and ceiling heights and also accounting for the amount of damage that was observed and that which would be tolerable. The water density was set at 33 mm/min (0.8 gpm/ft^2) with a water supply pressure of 2.3 bar (33 psi) and was manually controlled. Six sprinklers were open to simulate the simultaneous activation of a SMART system as shown in Figure 3-1. The number and location of the active sprinklers can be modified for an actual system to incorporate safety factors.

To understand the performance and timing advantage of detectors placed within the racks of the commodity, LHDs were installed in a separate test conducted with CUP under a 15 m (50 ft) ceiling. Note that linear heat detectors (LHDs) have been tested and certified as FM Approved when installed directly under a ceiling; they have not been tested when installed within a rack structure. During the test, LHDs were placed above each of the first five tiers of CUP commodity, attached along the rails going north and south. Figure 3-3 shows the location of these LHDs with the dashed red lines. A side view of one tier shows the LHD placement, red circle, at each rail. Two detectors were placed above the ignition location, towards the east of the main array, while a single line was passed along the main array to the west. The goal of the test was to understand how well the LHDs could work when placed within the rack and to determine if detection was possible prior to the fire reaching the ceiling. The LHDs used had a 68°C (155°F) activation temperature and provided the activation location based on a current output from the control module.

The resultant activation times following ignition are shown in Figure 3-4 with each color representing a different LHD. Initial observations show two main activation groups: one group falls within a time window of approximately 45-60 s, while the second group is clustered around 100 s after ignition. These two groups represent the LHDs placed on the east and west portion of the main array respectively. The average activation time of LHDs placed along the east portion of the array, above the ignition location was 55 s after ignition, a similar time to that of using the low temperature rise threshold of the FM Global algorithm (Algorithm 1). Thus, LHD provides early activation while allowing for a higher temperature threshold, minimizing false detections. Furthermore, with similar activation times between the FM Global algorithm and the in-rack detectors, estimation of water flows to the higher tiers becomes more reasonable. The longest activation time of the detectors placed above the ignition location occurred at the fourth tier, at 62 s. The fifth tier activated slightly earlier but was within 5 s of the fourth tier.

Figure 3-2: Elevation view of SMART sprinkler protection of high-bay rack-storage Test 1 main array using eight tiers of CUP under a 13.7 m (45 ft) ceiling.
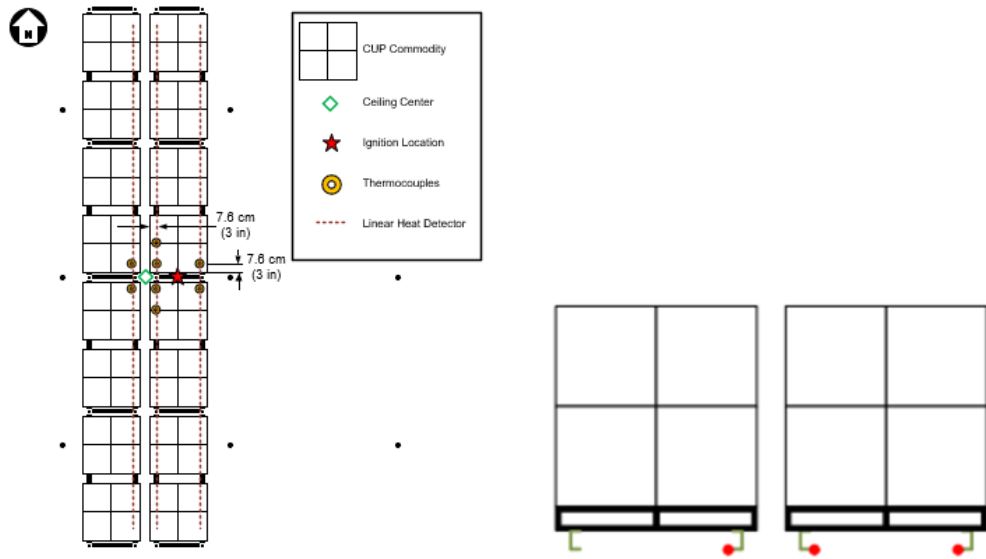
Figure   3-3:   In-rack LHD and thermocouple instrumentation placement (LHDs placed above first five tiers of CUP).
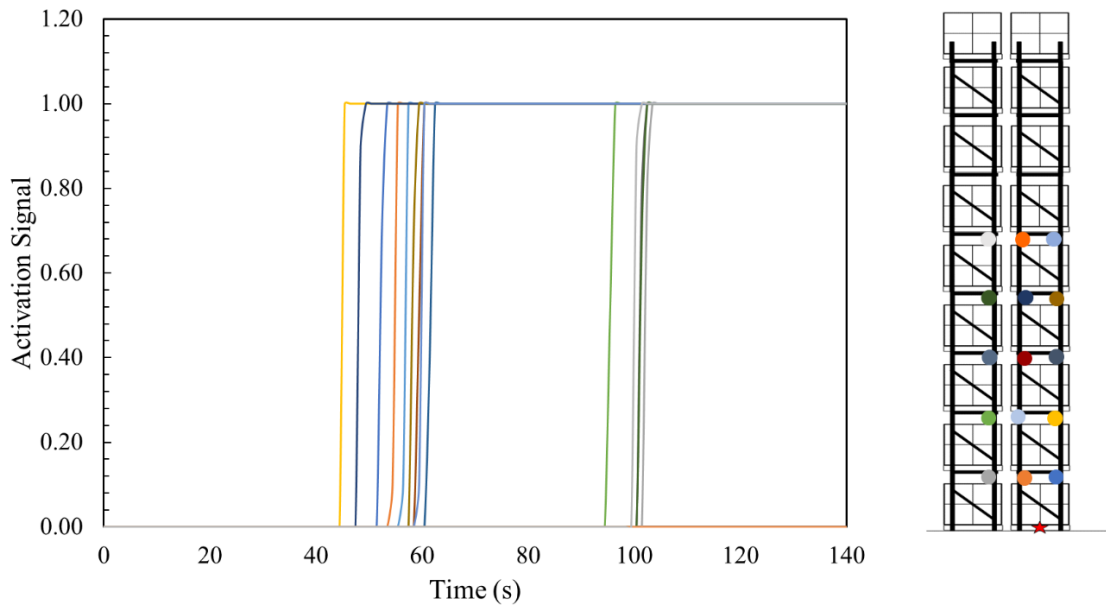
Figure   3-4:   Linear heat detector activation signals from multiple locations and tiers during a 15.2 m (50 ft) CUP test. Each color represents a different linear heat detector installed within the array as shown in the side view of the array on the left.

Examining sample CUP tests shows a significant reduction in fire size at detection when comparing the activation time of an LHD and that of a ceiling sprinkler. Figure 3-5 shows that the fire would have reached the sixth tier at activation and would not have reached the ceiling yet. This provides a window of opportunity for the sprinklers to begin pre-wetting the commodity prior to the fire reaching the ceiling, aiding in its control. The fire size would also be approximately one-third of the value at the first

sprinkler operation, see Figure 3-6. The estimated fire size of the test under a 15 m (50 ft) ceiling was similar at 62 s to that of an 8-tier legacy CUP test.

In addition to providing the activation signal, the LHDs can provide location information for where flame detection occurred. As the LHD is exposed to the fire, the wires within form a junction providing a difference in resistance along the wire, this resistance is related to the length of the wiring. The interface module stores the location of where the junction occurred and provides current output to the data acquisition system for active measurement. The module is calibrated based on the length of the wire; the wire is shorted at the control module and at the end of the installed wire to get minimum and maximum resistance readings for accurate stored distance measurements. The current output provided by the control module, however, is for a fixed range of 0 to 2,400 m (0 to 8,000 ft). The large distance unfortunately results in a reduction in dynamic range to the data acquisition system because the wire only spans 10 m (33 ft) length of the main array (less than 1% of the output range). The calibrated distance reading stored in the control module is most accurate; unfortunately, only the last activation which occurs closest to the unit is stored. Thus, the initial activation locations were lost as the fire progressed. For the purpose of this test, the activation signal is most important, the accuracy of fire location is secondary because the fire location is prescribed, and location detection can be improved upon in the future. The detection approach is suitable for our simulated system and for an actual SMART system, the module could directly communicate with the sprinklers providing the most accurate distance for the first activation prior to any further activations. This may be possible within the onboard module without the reliance on the output signal.

| (a) | (b) |
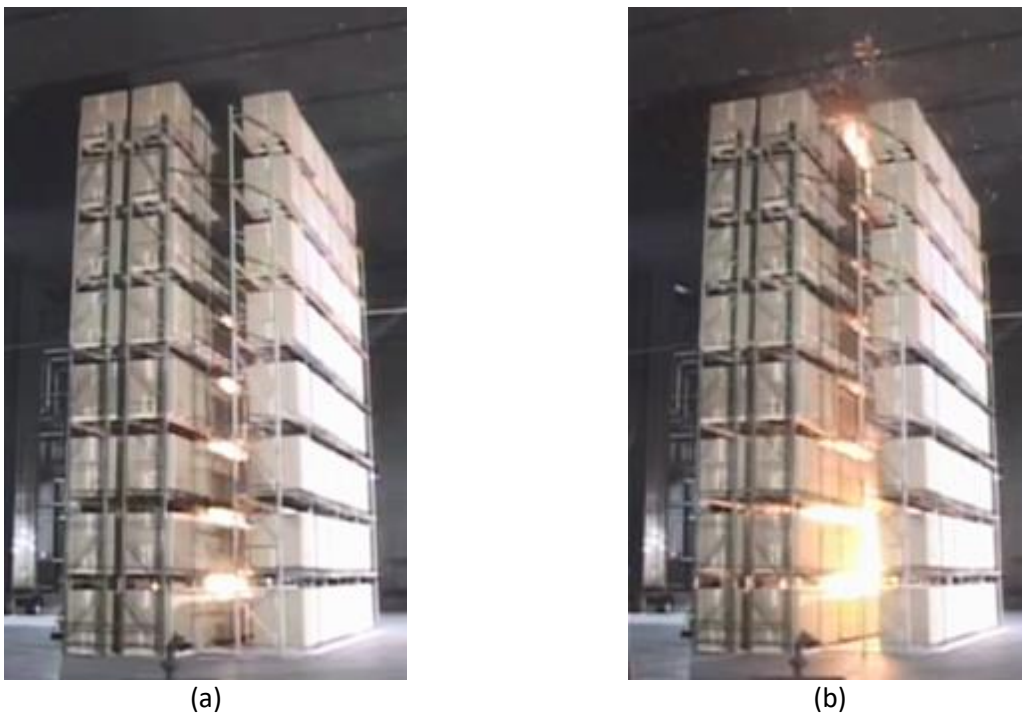
Figure   3-5:   Sample CUP test fire size (a) using LHD activation at 62 s and (b) at first sprinkler activation during the actual test.
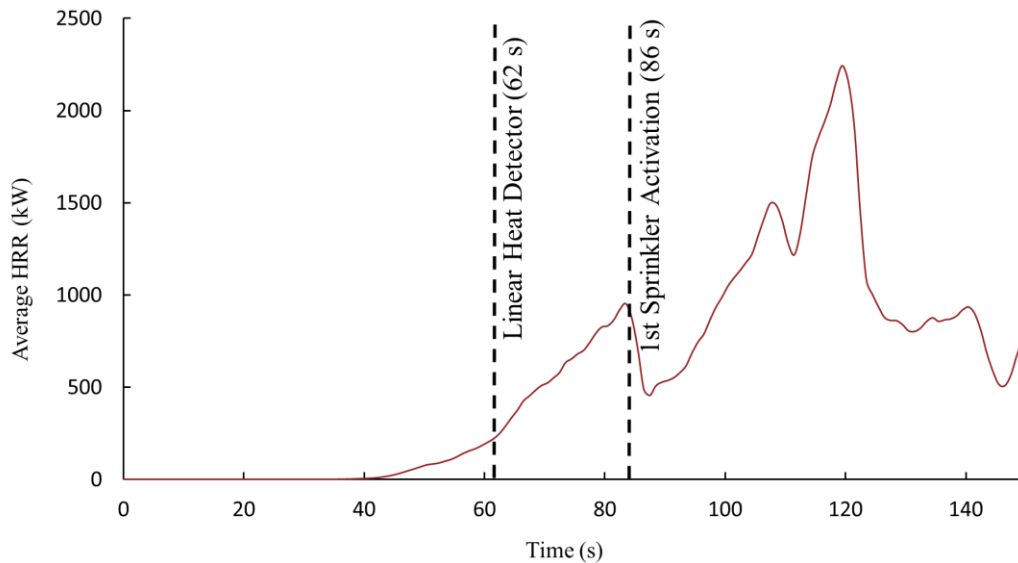
Figure   3-6:   Heat release rate during a sample CUP test under a 13.7 m (45 ft) ceiling comparing fire size at LHD activation and first sprinkler activation.

3.2   Results

Test 1 was conducted using eight tiers of CUP storage under a 13.7 m (45 ft) ceiling protected with a density of 33 mm/min (0.8 gpm/ft^2). Following ignition, the fire size continued to grow until the first LHD activated at 62 s as expected based on the previous LHD testing. The water was turned on and delivered to the six open sprinklers within 10 s of the LHD signal. Figure 3-7 shows the fire development through the early phase of the test. The flame height had grown to just above the fourth tier when it was detected by the LHD. The flame height increased an additional tier prior to water delivery. Following water delivery, the fire size began to drop and after 2 min the fire stabilized with flames in the first four tiers of the main array. Figure 3-8 shows a time history of the estimated convective heat release rate (HRR), calculated using flame plume correlations and the ceiling thermocouple data. The estimated convective HRR was between 300 and 400 kW for a period of 7 min. Following sprinkler activation, these values are only estimates as the cooling from the sprinklers can cause significant distortion of the calculated HRR. However, as additional sprinklers operated during that period, the trend of the curve demonstrates stabilization. Visually, the size of the fire plume in the array was also consistent over this period. The flame did not spread further, and the contributing commodity was depleted resulting in the flame height receding and ultimately subsiding.

The Test 1 results showed that the reduced water flow provided adequate protection of the commodity stored under a 13.7 m (45 ft) ceiling. Activation of the LHD occurred earlier than the first sprinkler activation in a traditional ceiling-only test under the same conditions. The fire reached the sixth tier during the test, but never reached the ceiling as it had in tests using traditional ceiling-only sprinklers. It appears that the pre-wetting of the surrounding commodity after activation limited the fire growth during the test. The lack of spread caused the fire duration to be driven by the ignited commodity, which led to a reduced fire size as the commodity was consumed.

| 0 s | 58 s |
| Ignition | 4 s before sprinkler activation |

| 68 s | 132 s |
| Water applied | Fire size stabilized |

Figure   3-7:   Smart Sprinkler Protection Test 1 fire development with eight tiers of rack storage using a density of 33 mm/min (0.8 gpm/ft^2).

Activation of the LHDs was as expected from previous results. The thermocouples at the ceiling were used to compare the LHD activation to the SMART algorithm for detection. Figure 3-9 shows the estimated temperatures of thermocouples placed 0.3 m (1 ft) below the ceiling just before water delivery. Following sprinkler operation, the ceiling temperatures dropped and resulted in delayed temperature rise. When using the SMART algorithm, a temperature rise of 5°C (9°F) over one minute occurred at one location at 62 s, and nine locations by 69 s. This is just 7 s after the LHD activated and is

consistent with the earlier findings that in-rack detectors would activate at similar times to the FM Global SMART system.
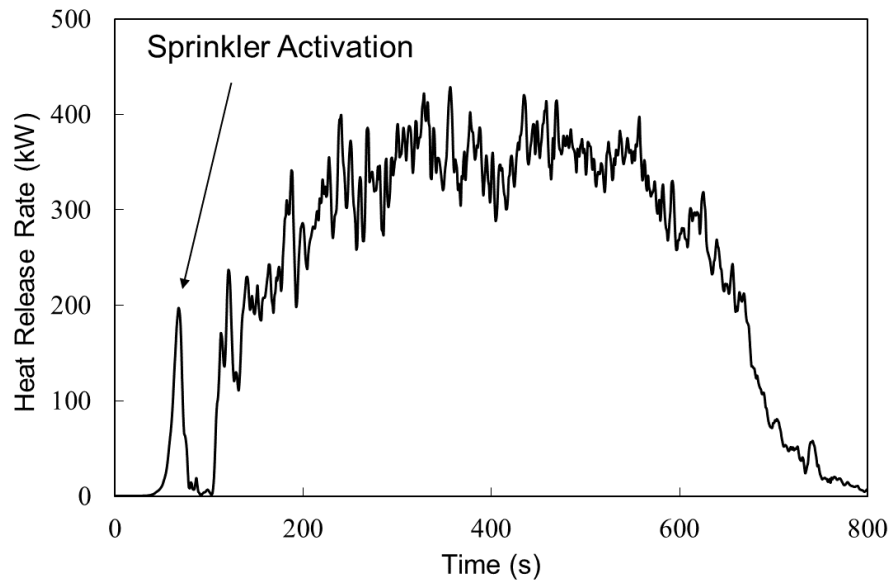
Figure   3-8:   SMART sprinkler high-bay rack-storage Test 1 estimated convective HRR with sprinkler activation at 62 s.
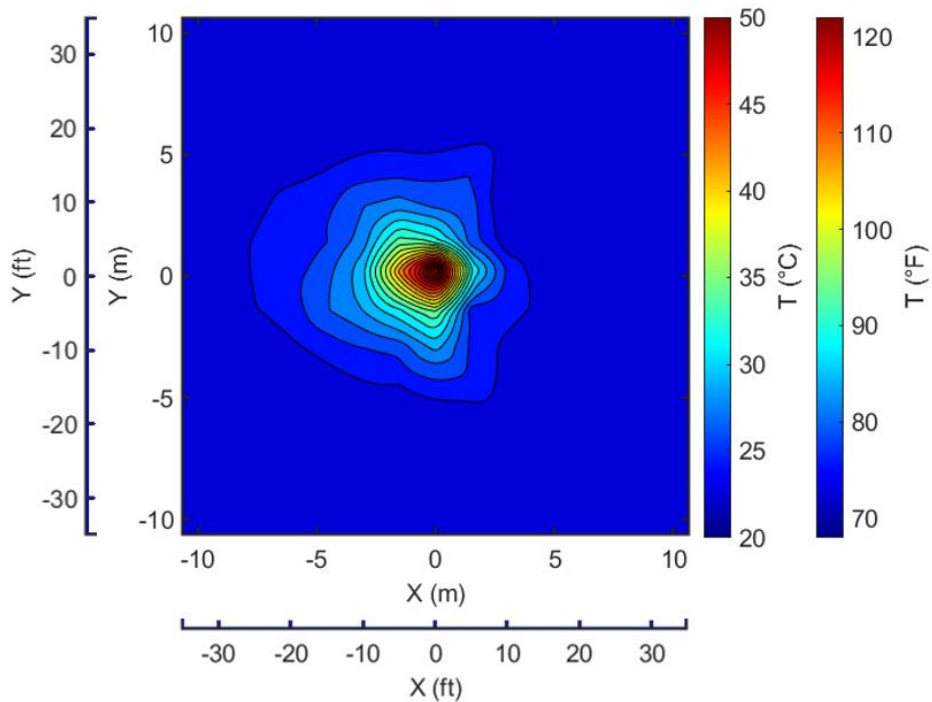
Figure   3-9:   SMART sprinkler high-bay rack-storage temperature profile of virtual thermocouples placed 0.3 m (1 ft) from ceiling at sprinkler activation (62 s after ignition).

Figure   3-10: SMART sprinkler high-bay rack-storage Test 1 fire damage to east side of main array represented by red hatch marks.

From Figure 3-9, the fire plume location was also at the center of the ceiling with its centroid between the six sprinklers which were selected for activation. The damage to the commodity was limited to the

main array between the six operating sprinklers. Figure 3-10 shows the damage to the east side of the main array. Damage from the west side was similar but did not extend to the sixth tier. There was no fire damage to the target arrays.

Ultimately, Test 1 showed adequate protection with the combination of SMART sprinklers and linear heat detectors within the racks for early detection of the fire. Test 1 under the 13.7 m (45 ft) ceiling showed that scaling the water flow down by 20% relative to results from the previous SMART testing was successful. Additional damage to the main array did result as expected relative to the previous SMART testing; however, the fire did not spread to either target arrays or the ends of the main array.

Fire control in Test 1 was achieved with early activation at 62 s. The early activation ensured that the fire size was small allowing the non-participating commodity to be prewetted by the sprinklers, which helped to minimize fire spread. With adequate water density, the fire was contained within the main array and burned until the fuel supply was depleted.

The fire size in Test 1 remained constant for a duration of approximately 7 min while the commodity burned out. During this time, flames were also in the aisle space. These observations indicate that the water density used in Test 1 is close to the threshold of fire control. Therefore, a slightly higher water density or additional sprinkler activation may be recommended to further ensure that the target arrays do not ignite. Test 1 showed successful activation using the in-rack LHD and provided early application of water to the fire for control, while ensuring practical temperature limits for detection. Since the fire was detected early, the water provided pre-wetting of surfaces before the fire could grow and spread when the fire size was estimated to be 400 kW. Finally, the delivered water density when using the six simultaneously operated sprinklers provided a reduction of water by 77% when compared to the recommendations found in DS 8-9 for ceiling-only protection of CUP at 13.7 m (45 ft). No factor of safety has been applied to the results of these tests and the imposition of additional safety factor would lower the water reduction benefit.

4.   Open-Top Container (OTCC) Storage

OTCCs are used in warehouses and manufacturing plants to facilitate storage and transport of commodities. However, they introduce challenges for the fire protection system as they can collect the water discharged from sprinklers preventing it from reaching the fire in a timely manner [11]. The water collection allows the fire to grow larger reducing the effectiveness of the protection system. The resulting hazard of OTCCs has been clearly demonstrated, though the proper sprinkler protection requirements have not.

The hazard of OTCC was examined with respect to standard commodities and the results were used to determine the feasibility of ceiling-only protection using either traditional sprinklers or SMART sprinklers. The main challenge with open-top containers is the potential for water loss and transport delay greatly impacting the water demand required to adequately protect the hazard. The effect of the increased hazard of water collection on sprinkler protection requirements needs to be understood; however, little experimental data exist showing effective protection to draw from as a baseline for comparison. Six fire tests were conducted to determine the hazard posed by one type of plastic OTCC with respect to standard commodities. The results showed that the CDF when using standard the WAA activation protocol is higher than 73 mm/min (1.8 gpm/ft^2), while that for a simulated SMART sprinkler is approximately 32 mm/min (0.79 gpm/ft^2). Both CDFs are higher than those of all FM Global standard commodities, limiting the potential for ceiling-only protection solutions following existing guidance. The simulated SMART system did provide more than 50% water reduction in the CDF. Therefore, potential ceiling-only options might be available at limited storage heights with the support of large-scale tests using a SMART system. Even though reduction in the CDF was observed, fire protection for OTCCs with a SMART system would still likely require water demands in excess of any current protection guidance for standard commodities.

4.1   Experimental Setup

All testing was conducted under the 20-MW Fire Products Collector. The commodity classification setup used is shown in Figures 4-1 and 4-2 using OTCC. The array configuration consisted of a 3-tier rack-storage arrangement with a nominal tier height of 1.5 m (5 ft). The dimensions of the array were approximately 2.7 × 5.5 × 4.3 m (9 × 18 × 14 ft) utilizing a 2.7 m (9 ft) wide central bay with 1.2 m (4 ft) wide bays on each side. The containers placed in the 1.2 m (4 ft) wide bays were rotated so that the 1.1 m (45 in.) side of the container was on the face of the array to easily fit the commodity between the rack uprights. The flue spaces throughout the storage array were nominally 150 mm (6 in.).

The test array was positioned under the Water Application Apparatus (WAA), which consists of 48 full cone nozzles installed on six suppression pipes on 0.6 × 0.6 m (2.0 × 2.0 ft) spacing located 203 mm (8 in.) above the commodity. Tests 1 and 5 utilized a water flux of 73 mm/min (1.8 gpm/ft^2), the maximum water flux that can be provided by the WAA. This water flux was selected as a starting point based on the assumption that the portion of the discharged water entering the flue space needs to be at least equivalent to the flow expected for the same type of commodity when the top is closed. This required at least five times the CDF for UUP, or 63 mm/min (1.6 gpm/ft^2) for a 3-tier storage

arrangement. The water flux was decreased in Tests 2, 3 and 4 to 17 mm/min (0.42 gpm/ft^2) to compare the hazard of open-top containers to the highest hazard standard commodity CDF, that of UEP. The last test, Test 6, used a water flux of 41 mm/min (1.0 gpm/ft^2).

The water was applied when a hypothetical sprinkler link, assumed to be 3.0 m (10 ft) above the fire, activated based on set sprinkler parameters [10]. Tests 1 and 2 utilized the standard hypothetical sprinkler parameters for commodity classification tests, a response time index (RTI) of 276 (m·s)$^{1/2}$ (500 [ft·s]$^{1/2}$) and an activation temperature of 141°C (286°F). A SMART system was simulated in Tests 3 to 6 by changing the theoretical sprinkler properties to an RTI of 28 (m·s)$^{1/2}$ (50 [ft·s]$^{1/2}$) and an activation temperature of 57°C (135°F). These parameters were selected for consistency with the other SMART sprinkler work presented.
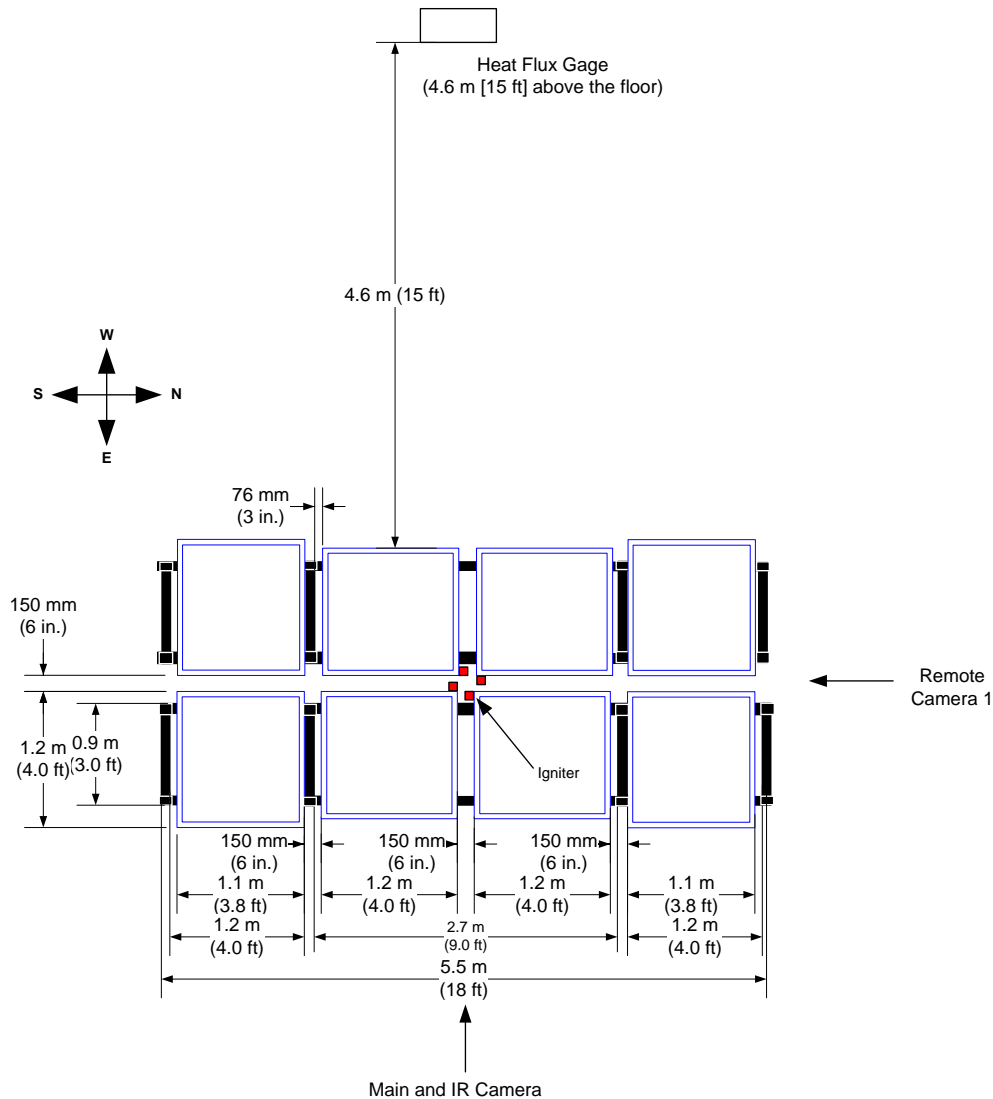
Figure 4-1: Plan view of 3-tier commodity classification test with open-top combustible containers.

Suppression water pipe

200 mm
(8 in.)

Nozzle

Commodity

Rack

4.3 m
(14 ft)

0.5 m
(1.5 ft)

1.5 m
(5.0 ft)

1.1 m   Floor
(3.5 ft)

1.1 m
(3.8 ft)

1.2 m
(4.0 ft)

1.2 m
(4.0 ft)

1.1 m
(3.8 ft)

1.2 m
(4.0 ft)

2.7 m
(9.0 ft)

1.2 m
(4.0 ft)
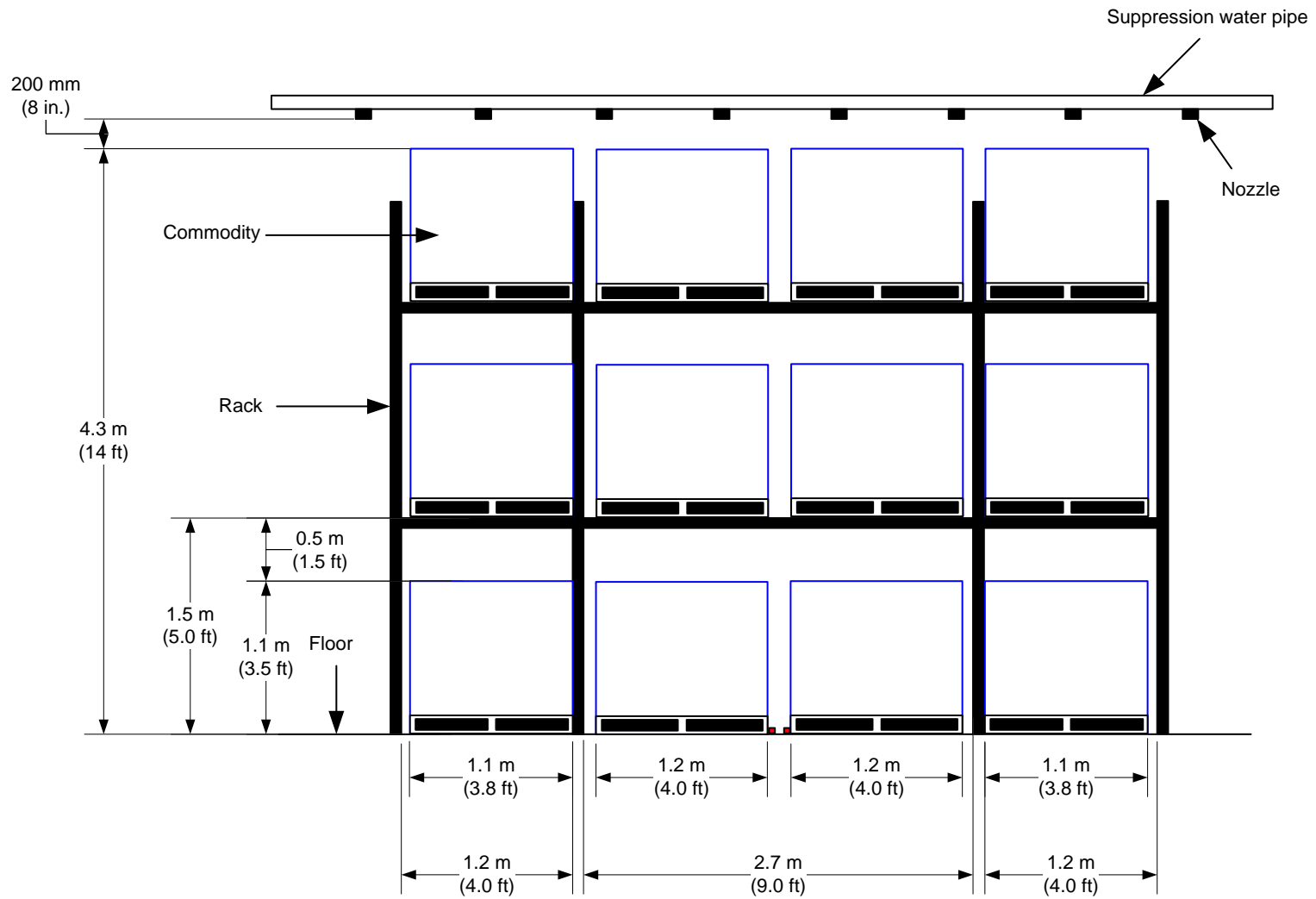
Figure 4-2:   Elevation view of 3-tier commodity classification test with open-top combustible containers.

Ignition was achieved with four standard half ignitors centered in the test array. Figure 4-3 shows the ignitor placement.

Figure   4-3:   Ignitor placement for open-top container tests.

Evaluation of commodity classification tests is based on control of the fire. The requirements for a controlled and uncontrolled fire are provided below.

Controlled Fire: This scenario is represented by a delivered water flux that prevents the chemical heat release rate (HRR) from continuously increasing after water application and prevents the fire from spreading to the extent of the array along the longitudinal direction.

Uncontrolled Fire: This scenario is represented by a delivered water flux that allows the chemical heat release rate (HRR) to increase over time or the fire to spread to the extent of the array along the longitudinal direction.

For the commodity classification test results to be conclusive, the commodity must maintain ideal behavior, meaning the basic geometry cannot change during the test. For example, commodity that breaches its container and spills creating a pool fire would not provide conclusive results in the test due to the changed geometry of storage containers to a liquid pool, and the lack of repeatability of that event in a real scenario.

4.2   Results and Discussion

A summary of the fire test results is presented in Table 4-1 with the fire development for each test presented in Figures 4-4 to 4-6.

The fire behaved in a similar manner in all tests except for Test 3. During Test 3, the fire development was much slower due to only two of the four ignitors being lit at the start of the test. This delayed the fire development by about 2 min 30 s when compared to Test 4 which was a repeat of Test 3. For all other tests, the fire steadily propagated upwards impinging on the bottom of the second-tier commodity by 2 min after ignition. At around 3 min, flames reached the top of the second tier and were extending out the top of the array by 3 min 30 s. In Tests 1 and 2 with standard WAA response water activation, the water was applied at 4 min 5 s and 3 min 50 s respectively. In Test 3, with the two-ignitor ignition scenario and simulated SMART sprinkler response water activation, water was applied at 4 min

34 s. The remaining tests, Tests 4 to 6, all used simulated SMART sprinkler response for water activation and had water applied between 2 and 2 ½ min: in Test 4 water was applied at 2 min 7 s, Test 5 at 2 min 27 s and Test 6 at 2 min 1 s.

Table   4-1:   Summary of open-top container fire test results.

Test Result	Test 1	Test 2	Test 3[a]	Test 4	Test 5	Test 6
Test Date	9/13/18	9/17/18	9/20/18	10/02/18	10/05/18	10/31/18
Theoretical Sprinkler Response	Commodity Classification	Commodity Classification	SMART	SMART	SMART	SMART
Theoretical Sprinkler Activation Temperature, °C (°F)	141 (286)	141 (286)	57 (135)	57 (135)	57 (135)	57 (135)
Response Time Index (RTI), $(m \cdot s)^{1/2}$ $[(ft \cdot s)^{1/2}]$	276 (500)	276 (500)	28 (50)	28 (50)	28 (50)	28 (50)
Plastic Liner Present	Yes	Yes	Yes	Yes	No	No
Length of Test, min:s	30:00	6:15	7:20	6:00	8:00	13:00
Delivered Water Flux, mm/min (gpm/ft^2)	73 (1.8)	17 (0.42)	17 (0.42)	17 (0.42)	73 (1.8)	41 (1.0)
Water Applied, min:s	4:05	3:50	4:34	2:07	2:27	2:01
Fire Travel to Array Extent	No	Yes	Yes	Yes	No	No
Fire Controlled	Inconclusive[b]	No	No	No	Yes	Yes
Fire Growth Rate (before water application), kW/s	97	111	16	15	6	8
HRR at Beginning of Extinguishment ($\dot{q}_{be}$), kW	3,332	3,250	337	445	244	350

[a] Ignition was achieved with only two of the four ignitors at the start of the test leading to slower fire development.
[b] Control achieved through container failure and subsequent release of collected water and not necessarily because of the water flux applied.

Tests 1, 5, and 6 resulted in controlled fires. However, Test 1 likely controlled the fire through container failure and the subsequent release of the large quantity of collected water and not by the water flux applied; this is not the standard control mechanism for commodity classification tests. In Test 1, the fire was growing and was very quickly extinguished. In Tests 5 and 6 a slower progression towards extinguishment was observed in which the fire gradually decreased in size until it was extinguished. Tests 2, 3, and 4 resulted in uncontrolled fires where the fire continued to grow until the test was terminated due to the fire product collector limitations. Chemical heat release rates (HRR) are presented in Figure 4-7 for Tests 1 to 4, where plastic bag liners were placed in the containers to collect water, and

Figure 4-8 for Tests 5 and 6, without plastic bag liners. Note that time in the figures is shifted to align water application at 167 s for the simulated quick-response and 230 s for standard-response scenarios.

Figure 4-7 illustrates the consistent fire development observed in all tests along with the time of water application for both the standard WAA activation protocol response and the simulated SMART response. The standard WAA activation protocol response applied water when the fire size was about 3,000 kW and as expected the simulated SMART response applied water sooner when the fire size was less than 400 kW. In Test 1, using the standard-response water application, the HRR decreases initially after water application, but soon starts to increase again. At 5 min 54 s the HRR abruptly decreases again. This change was believed to be caused by failure of the container bottom and the subsequent release of the collected water. Due to the higher water flux used during the test, enough water was released to lead to the extinguishment of the fire. Test 4 also appeared to exhibit the same phenomenon. However, in Test 4 with the lower water flux the HRR never decreased after initial water application, but at 5 min 31 s it dropped abruptly only to increase out of control again. The drop in HRR was again believed to be caused by container failure and the release of the collected water. However, with the lower water flux, an insufficient amount was collected and released to control the fire as had been seen in Test 1. This phenomenon, although seen in Test 4, was not observed in Test 3. Post-test observations of Test 3 showed that the plastic bag liners still held water and had not failed on the top tier as they had in Test 4. The standard-response results for Test 1 indicate a controlled fire as the fire was extinguished. However, for the purpose of calculating the CDF the fire was considered uncontrolled due to the method in which control was achieved. Protection cannot rely on the failure of containers in order to achieve control. Thus, the results of Tests 1 and 2 indicate that the CDF would be greater than 73 mm/min (1.8 gpm/ft^2) for the open-top containers tested using the standard commodity classification protocol.

Test ID	Density mm/min (gpm/ft²)	Fire Size for SMART System Response Activation at 57°C (135°F)	Water Applied Activation at 141°C (286°F)	1 min after Water Applied	2 min after Water Applied
1	73 (1.8)		4 min 5 s		
2	17 (0.42)		3 min 50		
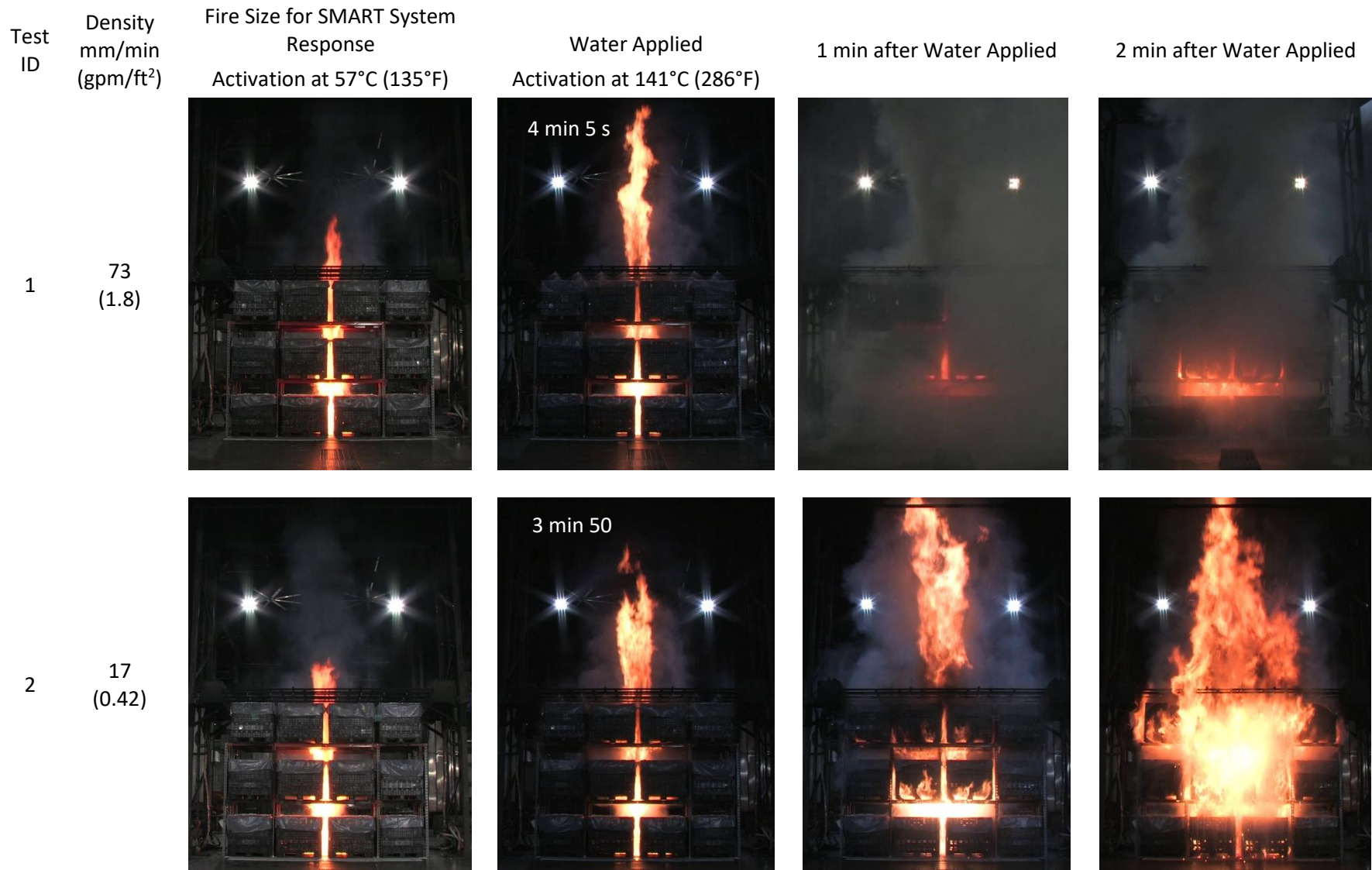
Figure   4-4:   Open-top container fire development for Tests 1 and 2 using the standard WAA activation protocol theoretical sprinkler and plastic liners.

Test ID	Density mm/min (gpm/ft²)	Water Applied Activation at 57°C (135°F)	1 min after Water Applied	2 min after Water Applied
3	17 (0.42)	4 min 34 s		
4	17 (0.42)	2 min 7 s		
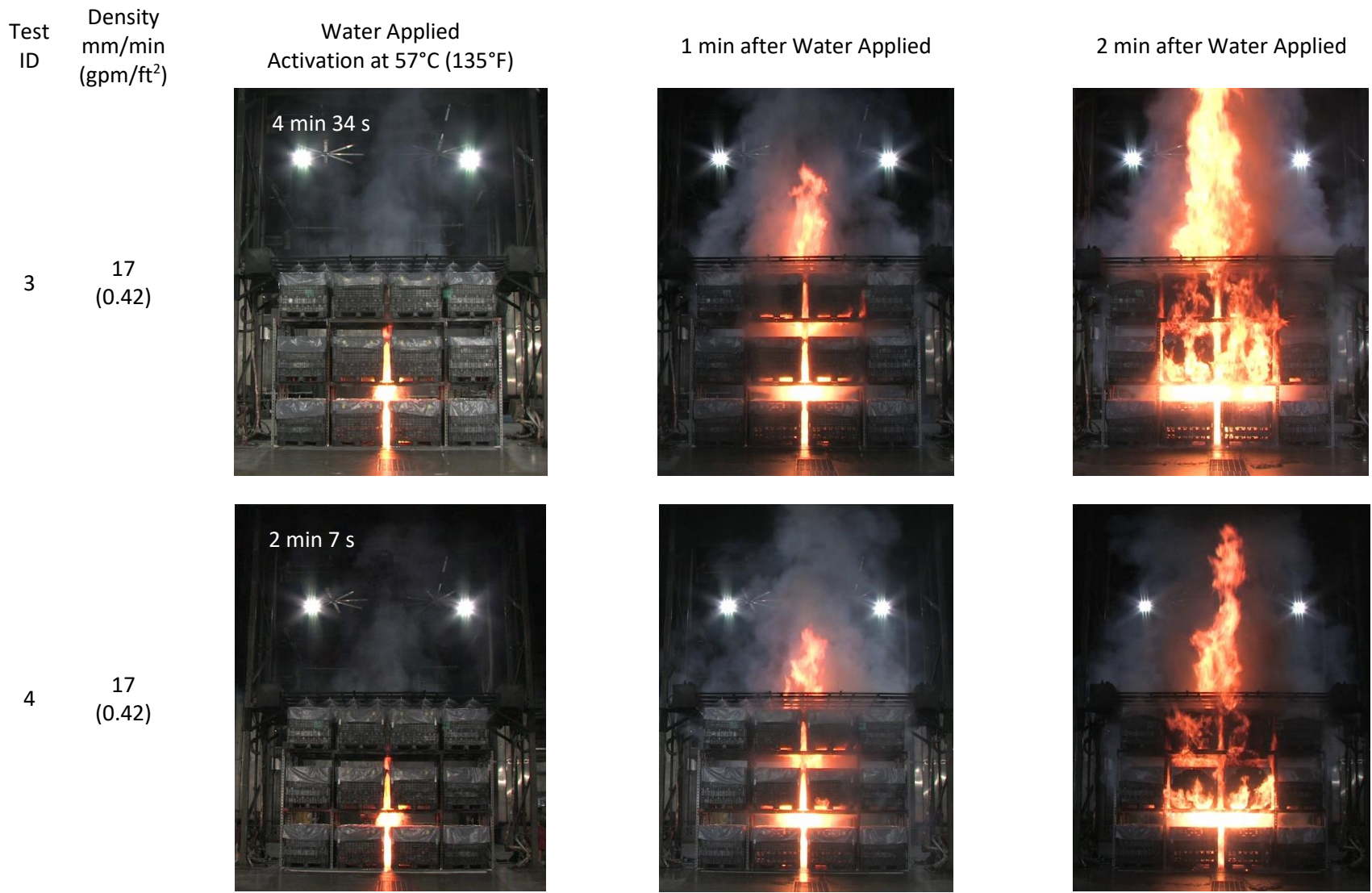
Figure   4-5:   Open-top container fire development for Tests 3 and 4 using a simulated SMART theoretical sprinkler and plastic liners.

Test ID	Density mm/min (gpm/ft^2)	Water Applied Activation at 57°C (135°F)	1 min after Water Applied	2 min after Water Applied
5	73 (1.8)	2 min 27 s		
6	41 (1.0)	2 min 1 s		
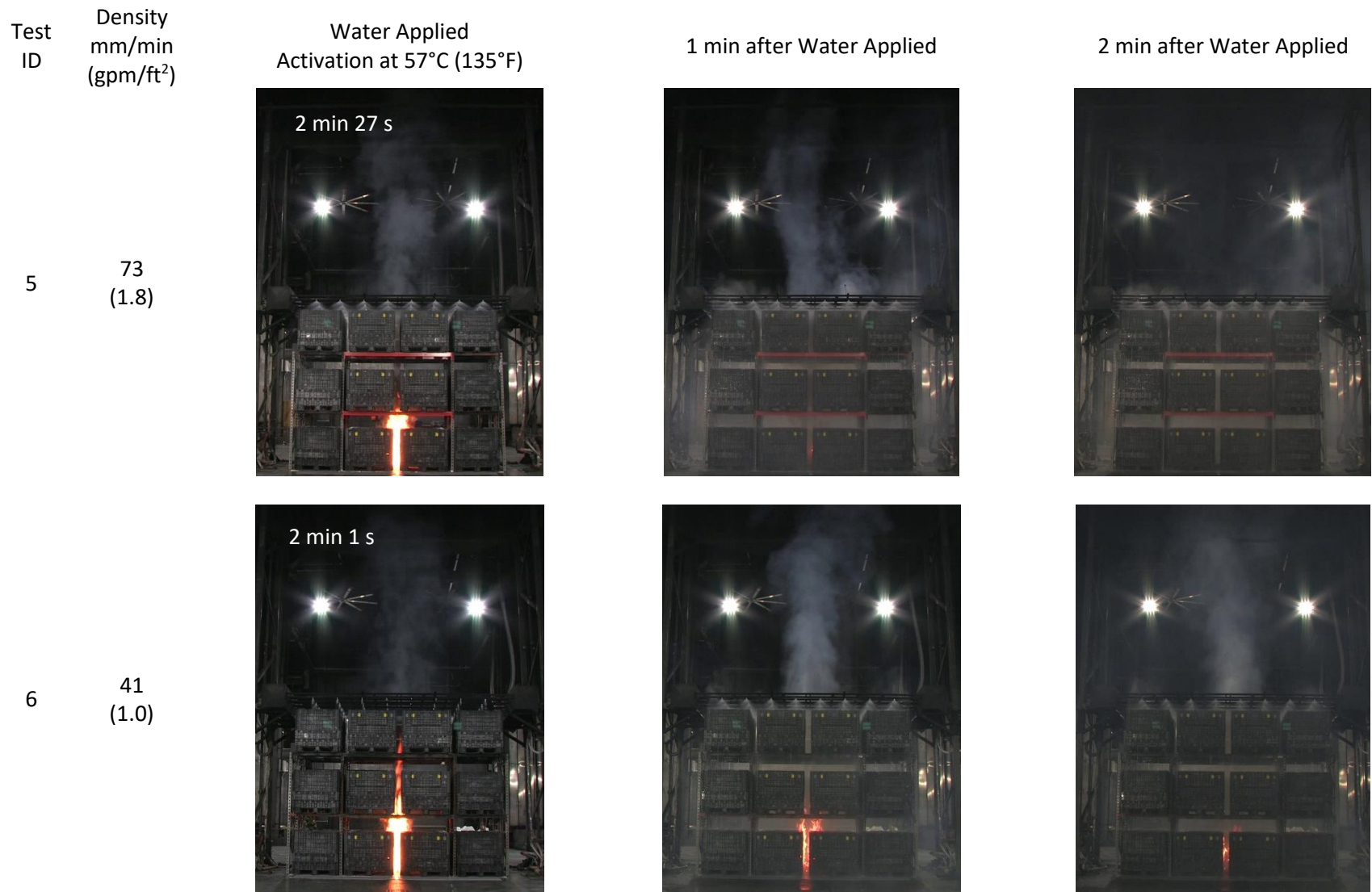
Figure   4-6:   Open-top container fire development for Tests 5 and 6 using a simulated SMART theoretical sprinkler and no plastic liners.
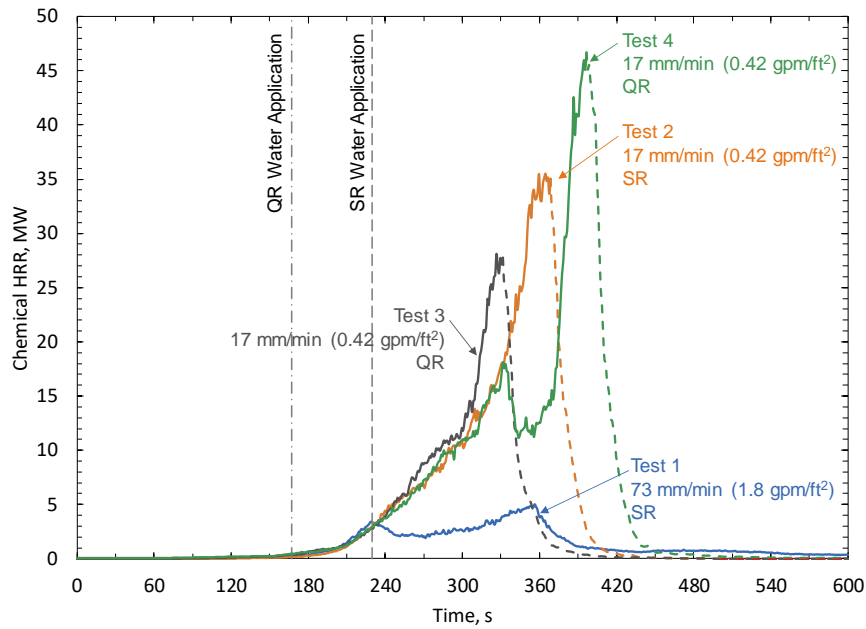
Figure   4-7:   Open-top container heat release rate curves for Tests 1 to 4 with liners.
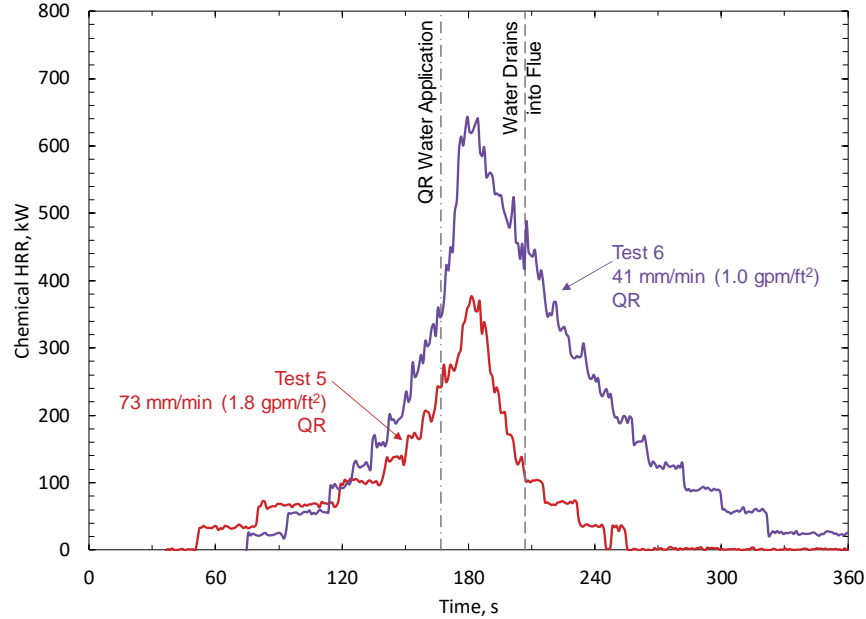
Figure   4-8:   Open-top container heat release rate curves for Tests 5 and 6 without liners (Note: The HRR values are at the low end of the measurement range, which may result in a higher level of uncertainty).

Figure 4-8 presents the HRR data for Tests 5 and 6. Both tests used the SMART response and higher water fluxes, which limited the fire size and extinguishment was achieved. These tests also did not use the plastic bag liner which introduced the question as to which factor played more of a role in the successful fire control, the simulated SMART response or the allowed water drainage. These two test parameters were changed at the same time to provide the best chance for a positive result. However, changing two parameters complicates determining which factor played the dominant role in the positive result. The vertical lines in Figure 4-8 indicate when the water was applied and the earliest time at which water was expected to have started to drain into the flue spaces. The timing of this occurrence was expected no sooner than 40 s after the water was applied, as was shown in cold flow tests. During the time between the water application and the start of water drainage into the flue spaces, the HRR for both tests is declining due to the initial water application. This observation leads to the conclusion that the faster response was likely the determining factor in the successful control rather than the allowed water drainage. Using the data available, a CDF for the simulated SMART sprinkler results can be calculated using Test 4 and 6, yielding a QR critical delivered flux of 32 mm/min (0.79 gpm/ft^2). This suggests that a reduction of at least 50% in the CDF may be achieved using a faster responding system when it is assumed that the CDF is greater than 73 mm/min (1.8 gpm/ft^2) using the standard WAA water activation protocol. It is noted that water drainage is expected to occur after the peak HRR and may impose a secondary effect on the HRR curve. This could result in a larger uncertainty in the calculated QR CDF.

The fire in all cases spread from the ignition location in the center of the array up the longitudinal flue and laterally to the commodity in the columns to either side of ignition. Photographs of the fire damage are presented in Figure 4-9. In Test 1, more damage occurred in the second tier but was limited to the central columns of commodity. In Test 2, damage occurred mainly on the second and third tiers. The damage on the second tier was limited to the central columns of commodity, while damage on the third tier extended out to the end of the array. Damage in Tests 3 and 4 occurred mainly on the second and third tiers and extended out to the end of the array on each tier. In Tests 5 and 6, damage was observed mainly at the ignition location and up the intersection of the longitudinal and central transverse flues.

In summary, the results identified two methods to achieve protection of open-top containers: faster response and drainage (for this specific drainage geometry). Regardless of which method was used, a higher water flux was still needed to control the fire than that required for any standard commodity protection.

Test 1

Test 2

Test 3

Test 4

Test 5

Test 6

Figure   4-9:   Open-top container fire damage for Tests 1 to 6.

5. **Conclusions**

A key element to success in controlling any fire is through early detection. This is particularly important if less water is available for fire protection. FM Global conducted a number of tests using the concept of a SMART sprinkler system and an AWC system to offer options for areas where water resources are insufficient or to reduce overall associated system cost. In all cases, early detection was vital to limiting the amount of water needed for adequate protection.

Both SMART sprinklers and the AWC system were examined for low-piled storage solutions to reduce the water demand requirements for adequate protection. SMART systems provide very early and simultaneous activation of multiple sprinklers that surround the fire and by design, avoid sprinkler skipping. The AWCs are designed to take advantage of fast image-based flame detection to provide early detection and targeted water delivery. As an example, for protection of CUP in a solid-piled arrangement up to 1.5 m (5 ft) high under a 9.1 m (30 ft) ceiling, the recent testing results were very positive with the SMART sprinklers showing water demand reductions up to 87% and AWCs up to 92% compared to a traditional ceiling-only sprinkler system. The SMART sprinkler water demand reductions are presented in Table 5-1 for both CUP and UUP under 9.1 m (30 ft) and 18.3 m (60 ft) ceilings. The AWC was able to achieve a greater water reduction protecting the CUP commodity compared to the SMART sprinkler due to the targeted water delivery and required flow of 230 lpm (60 gpm) resulting in a 92% reduction when compared to a traditional sprinkler system. This suggests that the AWC system with targeted water delivery can be more efficient than SMART sprinklers in terms of water demand.

The SMART sprinkler activation criterion used was very conservative. Most SMART sprinkler systems to be available in the future will likely be designed to yield much earlier activation times. Earlier activation can further reduce the required density and therefore offer greater reductions in water demand compared to what was achieved during this project. On the other hand, negative factors like crossflowing air over the storage, if not properly arranged in accordance with Data Sheet 2-0, *Installation Guidelines for Automatic Sprinklers* (DS 2-0), may need to be compensated by allowing for a larger number of sprinkler activations.

High-bay rack storage was another application investigated to explore the reduction in water demand that SMART sprinklers could provide. The testing showed successful activation using the in-rack LHDs and provided early application of water to the fire for control, while ensuring practical temperature limits for detection. The delivered water density when using the six simultaneously operated sprinklers provided a reduction of water by 77% when compared to the guidance found in DS 8-9 for ceiling-only protection of CUP at 13.7 m (45 ft). No factor of safety has been applied to the results of these tests and the inclusion of additional safety factor would lower the water reduction benefit.

The feasibility of using a ceiling-only SMART fire protection system to protect open-top containers was also examined. Six tests were conducted not only to evaluate the performance of a ceiling-only SMART fire protection system, but also to determine the hazard of plastic open-top containers with respect to FM Global standard commodities. The test results showed that the critical delivered flux (CDF) using the standard WAA activation protocol is higher than 73 mm/min (1.8 gpm/ft^2), while the CDF using a

simulated SMART sprinkler response is about 32 mm/min (0.79 gpm/ft^2). Even though the results indicate water reduction is feasible for rack storage of open-top containers using a SMART system, the overall water requirement would still be greater than that of standard commodities due to the inherent challenges of water collection. Despite an observed reduction in the CDF, fire protection for OTCCs with a SMART system would still likely require water demands in excess of any current protection guidance for standard commodities.

Table   5-1:   Reduction in water demand for SMART sprinklers compared to traditional ceiling sprinkler protection.

Commodity	Ceiling Height m (ft)	DS 3-26 Design* mm/min over m^2 (gpm/ft^2 over ft^2)	SMART Sprinkler System Density mm/min (gpm/ft^2)	Reduction in Water Demand	
				5-Sprinklers	9-Sprinklers
Single-Activation					
CUP	9.1 (30)	12/232 (0.3/2,500)	8 (0.2)	87 %	76 %
	18.3 (60)	20/280 (0.5/3,000)	15 (0.37)	88 %	78 %
UUP†	9.1 (30)	45/93 (1.1/1,000)	24 (0.6)	73 %	51 %
	18.3 (60)	65/93 (1.6/1,000)	41 (1.0)	69 %	44 %
Dual-Activation					
CUP	9.1 (30)	12/232 (0.3/2,500)	8 (0.3)	80 %	64 %
	18.3 (60)	20/280 (0.5/3,000)	15 (0.37)	88 %	78 %
UUP†	9.1 (30)	45/93 (1.1/1,000)	33 (0.8)	63 %	35 %
	18.3 (60)	65/93 (1.6/1,000)	41 (1.0)	69 %	44 %
* Assuming 9.3 m^2 (100 ft^2) coverage area per sprinkler. † UUP sprinkler design listed in DS 3-26 (Table 3) [6] as number of K360 (K25.2) sprinklers at a specified pressure.					

Future explorations are expected to continue investigating commercial systems using these innovative technologies for water demand reductions. In addition to protection effectiveness, the system reliability is another area that deserves additional studies. The present work shows promise and offers potential protection solutions for those facilities that exist in areas where water is scarce.

References

1. Y. Xin, K. Burchesky, J. de Vries, H. Magistrale, X. Zhou, and S. D'Aniello, "SMART Sprinkler Protection for Highly Challenging Fires - Part 1: System Design and Function Evaluation," *Fire Technology*, vol. 53, no. 3, pp. 1847-1884, September 2017.

2. Y. Xin, K. Burchesky, J. de Vries, H. Magistrale, X.Y. Zhou, and S. D/Aniello, "SMART Sprinkler Protection for Highly Challenging Fires - Part 2: Full-Scale Fire Tests in Rack Storage," *Fire Technology*, vol. 53, no. 5, pp. 1885-1906, September 2017.

3. Y. Xin, S. Thumuluru, J. Fenghui, R. Yin, B. Yao, K. Zhang, and B. Liu, "An Experimental Study of Automatic Water Cannon Systems for Fire Protection of Large Open Spaces," *Fire Technology*, vol. 50, pp. 233-248, 2014.

4. FM Approvals, FM Approvals Standard 1421, Fire Protection Monitor Assemblies, May 2018.

5. M. Khan, J. de Ris, and S. Ogden, "Effect of Moisture on Ignition Time of Cellulosic Materials," in *Fire Safety Science - Proceedings of the Ninth International Symposium, International Association for Fire Safety Science*, 2008, pp. 167-178.

6. FM Global, Property Loss Prevention Data Sheet 3-26, Fire Protection for Nonstorage Occupancies, April 2019.

7. National Fire Protection Association, NFPA 13, Standard for the Installation of Sprinkler Systems, 2016.

8. Y. Xin, "Estimation of Chemical Heat Relase Rate in Rack Storage Fires based on Flame Volume," *Fire Safety Journal*, vol. 63, pp. 29-36, 2014.

9. M. A. Vasiliev, L. M. Meshman, A. Yu. Snegirev, A. S. Tsoi and L. T. Tanklevskiy, "A Novel Methodology of Electrically Controlled Sprinkler Activation," in *Interflam 2013*, London UK, June 2013.

10. Y. Xin, "Effects of Storage Height on Critical Delivered Flux of Representative Fuels," *Fire Safety Journal*, vol. 91, pp. 624-632, April 2017.

11. FM Global, Property Loss Prevention Data Sheet 8-9, Storage of Class 1, 2, 3, 4 and Plastic Commodities, July 2018.